Structure-Activity Studies on the Simplified Analog of Aplysiatoxin and Identification of the PKC Isozymes Involved in Its Anti-Proliferative Activity

Yusuke Hanaki

2018

Contents

General Introduction 1

Chapter 1 Structure-Activity Studies at Position 27 of Aplog-1 11

Chapter 2 Structure-Activity Studies on the Phenolic Group of 10-Methyl-Aplog-1 37

Chapter 3 Identification of the PKC Isozymes Involved in the Anti-Proliferative and Pro-Apoptotic Activities of 10-Methyl-Aplog-1 53

Summary and Conclusion 63

Acknowledgements 65

References 67

List of Publications 75

Abbreviations

ATP	adenosine-5'-triphosphate
ATX	aplysiatoxin
Bn	benzyl
Bryo-1	bryostatin 1
CDK	cyclin-dependent kinase
CSA	10-camphorsulfonic acid
DAG	1,2-*sn*-diacylglycerol
DAT	debromoaplysiatoxin
DCM	dichloromethane
DDQ	2,3-dichloro-5,6-dicyano-*p*-benzoquinone
DGK	diacylglycerol kinase
DIBAL	diisobutylaluminium hydride
DMAP	*N*,*N*-dimethyl-4-aminopyridine
DMF	*N*,*N*-dimethylformamide
DMSO	dimethyl sulfoxide
DPP	12-deoxyphorbol 13-phenylacetate
EBV-EA	Epstein-Barr virus early antigen
Et	ethyl
GFP	green fluorescent protein
IP_3	inositol-1,4,5-triphosphate
LDS	lithium dodecyl sulfate
MAPK	mitogen activated protein kinase
Me	methyl
MPM	*p*-methoxyphenylmethyl
MTT	3-(4,5-di-methylthiazol-2-yl)-2,5-diphenyltetrazolium bromide
NHS	*N*-hydroxysuccinimide
PDBu	phorbol 12,13-dibutyrate
PIP_2	phosphatidylinositol-4,5-bisphosphate
PKC	protein kinase C
PKD	protein kinase D
PLC	phospholipase C
Pr	propyl
PVDF	polyvinylidene difluoride
RasGRP	guanyl nucleotide-releasing protein
SDS	sodium dodecyl sulfate
TES	triethylsilyl
TFA	trifluoroacetic acid
THF	tetrahydrofuran
TPA	12-*O*-tetradecanoylphorbol 13-acetate

General Introduction

Protein Kinase C

Protein kinase C (PKC) is a member of a family of serine/threonine kinases whose members play a pivotal role in diverse cellular functions such as proliferation, differentiation, migration, and apoptosis.[1] When Nishizuka and coworkers first discovered PKC in 1977 as a proenzyme that is proteolytically activated by Ca^{2+}-dependent protease.[2,3] Soon after, they discovered that Ca^{2+} and phospholipids also activated PKC without proteolysis. Additionally, 1,2-*sn*-diacylglycerol (DAG), which is produced transiently by phospholipase C (PLC)-mediated hydrolysis of phosphatidylinositol-4,5-bisphosphate (PIP_2), dramatically decreased the requirement of Ca^{2+} and phospholipids for its full activation (Figure 1).[4,5] These findings uncovered the physiological significance of inositol phosphate breakdown induced by various extracellular stimuli.[6,7] Thereafter, the DAG/PKC pathway was recognized as a key mediator between extracellular and intracellular signaling, and has since been studied intensively all over the world.

Today, at least ten PKC isozymes are recognized. These are subdivided into three groups based on their structures and cofactor requirement (Figure 2).[8] Catalytic domains are conserved among all the isozymes, while their regulatory domains differ from one another. Conventional or classical PKCs (α, βI, βII, and γ) depend on both Ca^{2+} and DAG for their activation, while novel PKCs (δ, ε, η, and θ) are independent of Ca^{2+} but require DAG. The C2 domain of conventional PKCs is a Ca^{2+} sensor required for their localization to the plasma membrane. On the other hand, the C2-like domain of novel PKCs lacks the key asparagine residue that coordinates Ca^{2+}. Both conventional and novel PKCs have tandem C1 domains (C1A and C1B), the binding site for DAG. Since the C1 domains of novel PKCs show a stronger affinity for DAG than those of conventional PKCs, novel PKCs are fully activated without Ca^{2+}.[9] Atypical PKCs (ζ, λ and ι) only require phospholipid but neither Ca^{2+} nor DAG for their activation. They also have one C1 domain, but it lacks the affinity for DAG. Instead, they have a Phox and Bem1p (PB1) domain that interacts with other PB1 domains of protein scaffolds.[10]

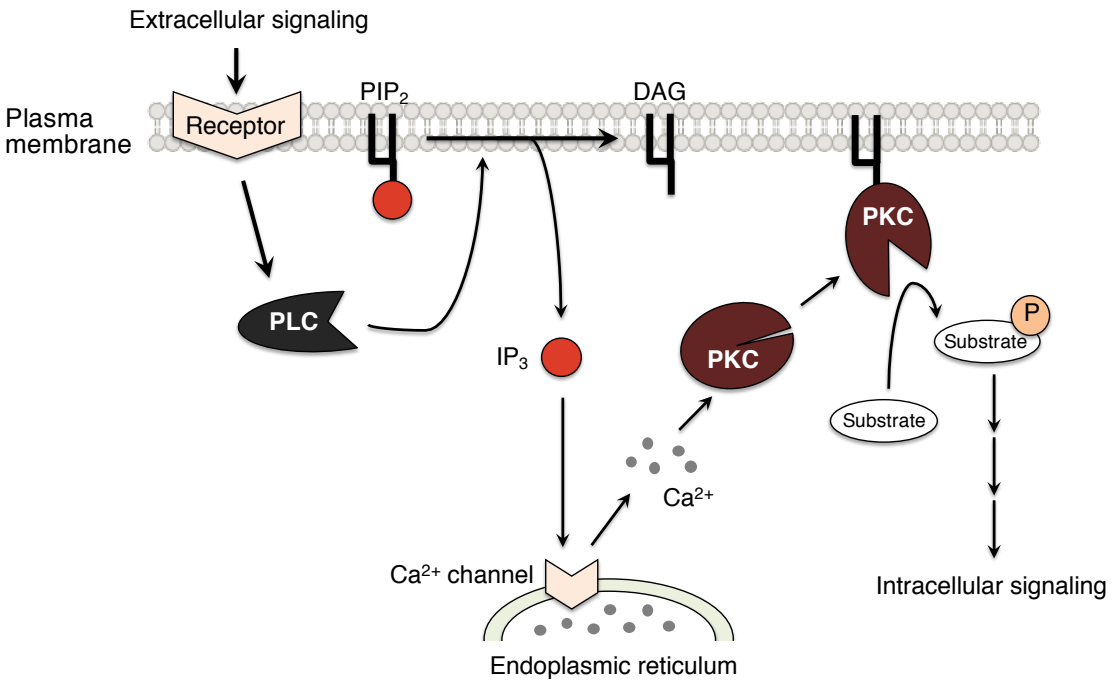

Figure 1. PLC and PKC as mediators between extracellular and intracellular signaling.

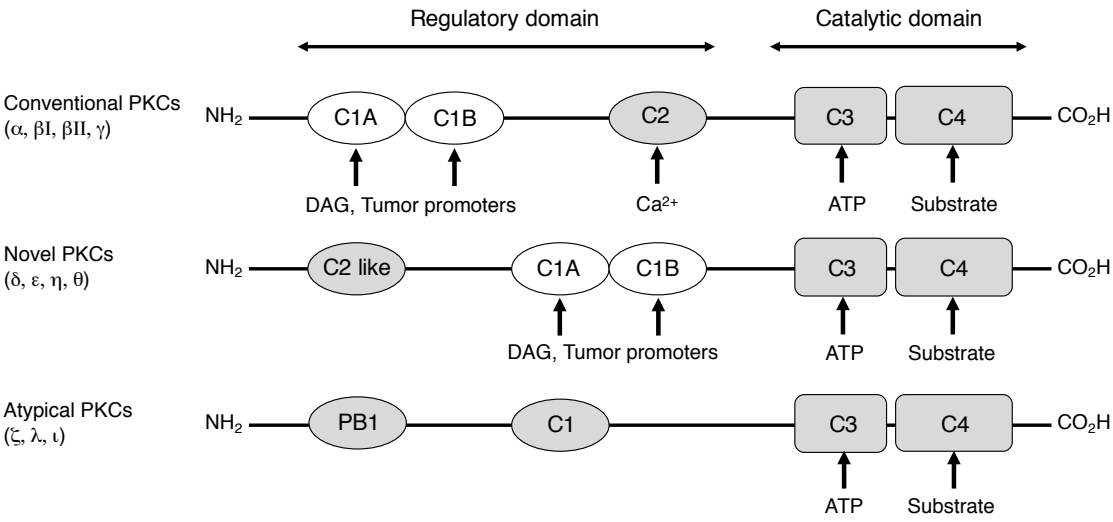

Figure 2. Domain organization of PKC isozymes

PKC as a Target of Cancer Therapy

Castagna and Nishizuka reported that tumor-promoting phorbol esters such as 12-*O*-tetradecanoylphorbol 13-acetate (TPA) activate PKC directly even in the absence of DAG.[11] Moreover, other class tumor-promoters, including teleocidins and apysiatoxins, have also been shown to be PKC activators (Figure 3).[12] These compounds bind to the DAG-responsive C1 domains of conventional and novel PKCs and recruit them to the cellular membrane, causing their abnormal activation. These facts led to the dogma that PKC activation promotes tumorigenesis, and that PKC inhibitors are potential medicinal seeds. Staurosporine is a typical adenosine-5'-triphosphate (ATP)-competitive PKC inhibitor, but ATP-binding domains are widely conserved among other kinases.[13,14] Thus, many derivatives of staurosporine have been developed to improve the selectivity to the PKC family or specificity among PKC isozymes (Figure 4).[15-19] In addition, an antisense oligonucleotide (ISIS3521) to PKCα was also considered as a potential anti-cancer agent.[20] However, the clinical trials using PKC inhibitors have not succeeded.[21]

On the other hand, there are unique PKC activators that exhibit anti-cancer activity albeit with little tumor-promoting activity. A key representative of such activators is bryostatin 1 (bryo-1, Figure 3), which was isolated from the marine bryozoan *Bugula neritina*.[22] Bryo-1 has been in phase I and II clinical trials for the treatment of solid tumors, leukemia, and lymphoma, though with little success.[23,24] The most successful example of an activator as a medicine is ingenol 3-angelate (PEP005, Figure 3) isolated from *Euphorbia peplus*. PEP005 was approved by the U.S. Food and Drug Administration (FDA) for topical treatment of precancerous actinic keratosis.[25] However, side effects such as pain, pruritus, erythema, crusting, swelling, and ulceration at the application site have been observed.[26] Therefore, structural optimization of these compounds based on structure-activity studies is indispensable to enhance anti-cancer activity and reduce side effects, but synthetic difficulty has hampered such studies. To overcome this problem, several organic chemists developed practical synthetic routes of bryo-1 and its analogs.[27-30] Wender's group synthesized a simplified analog of bryo-1 that showed stronger anti-cancer activity than bryo-1 itself,[31] and recently achieved the total synthesis of bryo-1 in a small number of steps.[32] Excellent synthetic methods for ingenol and its derivatives have also been developed by several groups.[33-35]

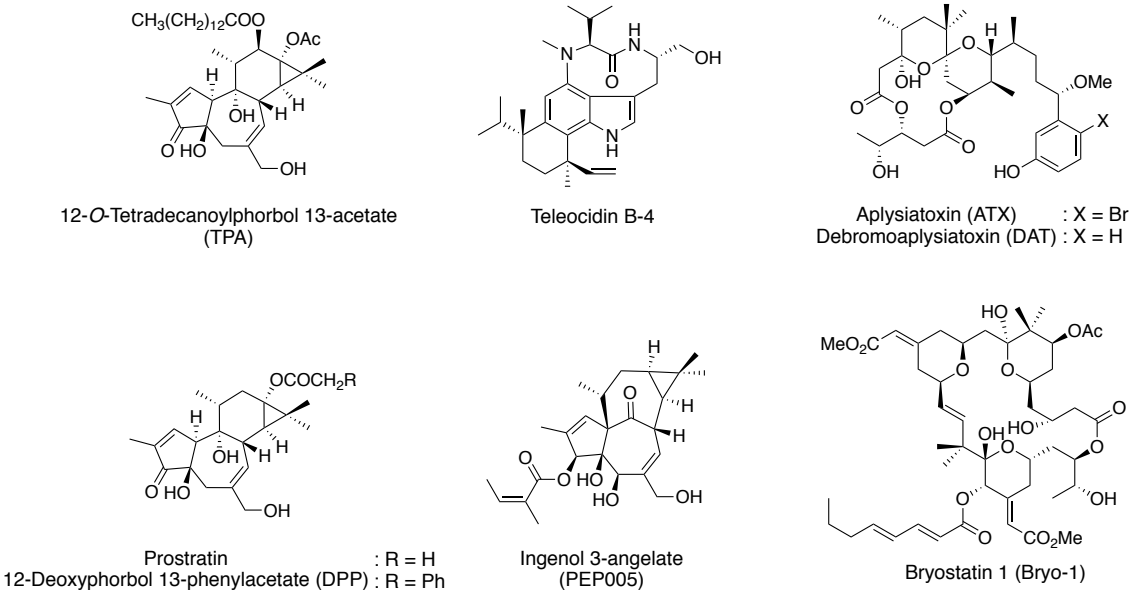

Figure 3. Structures of PKC activators.

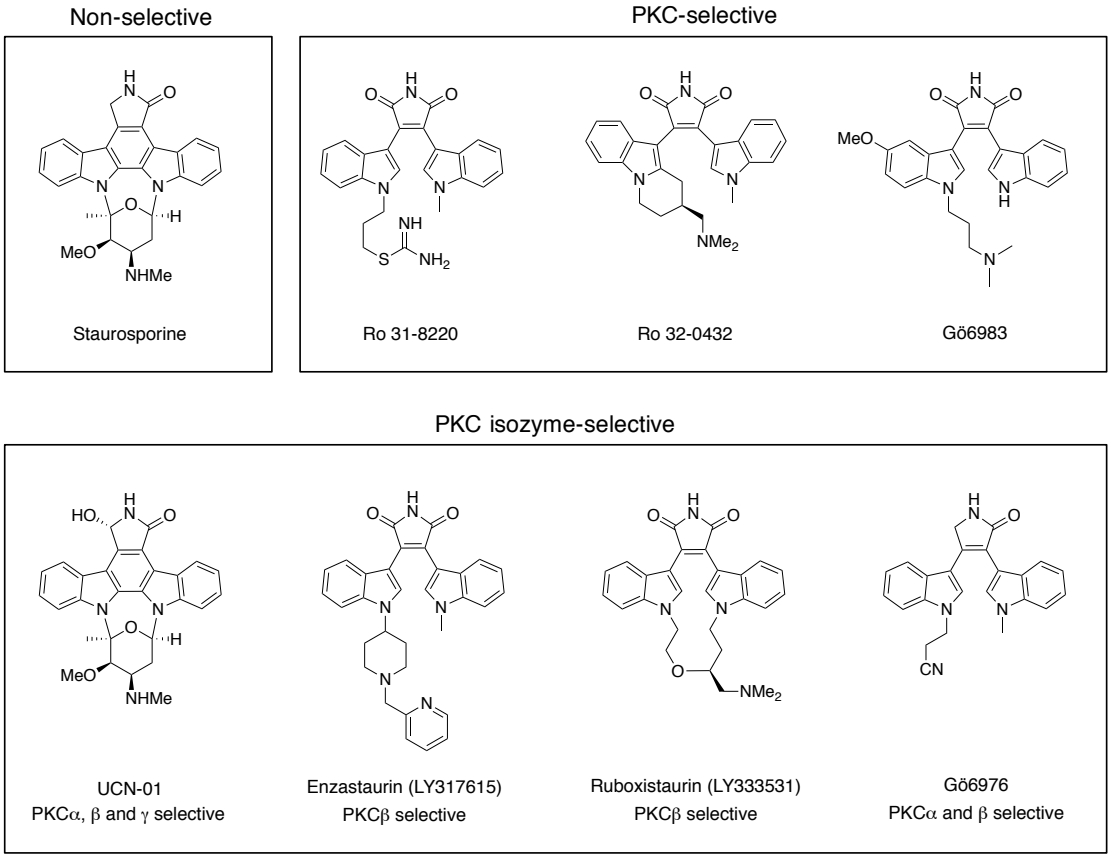

Figure 4. Structures of PKC inhibitors.

The Simplified Analogs of Aplysiatoxin as Anti-Cancer Leads

The tumor-promoting activities of PKC ligands usually depend on their molecular hydrophobicity. For example, prostratin and 12-deoxyphorbol 13-phenyl acetate (DPP, Figure 3), which are less hydrophobic analogs of TPA, did not show potent tumor-promoting activity,[36] because the affinity of phorbol class compounds for PKC isozymes was correlated with their hydrophobicity. On the other hand, aplysiatoxin (ATX) was reported to show a characteristic difference from other tumor-promoters. Debromoaplysiatoxin (DAT), a less hydrophobic analog of ATX, showed weaker tumor-promoting activity than ATX, but retains an affinity for PKC isozymes comparable to that of ATX.[37] This observation led Nakagawa and colleagues to synthesize aplog-1 (Figure 5), which lacks the hemiacetal hydroxyl group, the methoxy group, and the chiral methyl groups of DAT. Aplog-1 therefore features decreased hydrophobicity, along with increased synthetic accessibility and chemical stability.[38] Fortunately, aplog-1 exhibits little tumor-promoting activity like bryo-1. Moreover, aplog-1 retains significant anti-proliferative activity and binding affinity for PKC isozymes, although the affinity for PKC is one order of magnitude weaker than that of DAT. Subsequent structure-activity studies on the spiroketal moiety of aplog-1 identified 10-methyl-aplog-1 (**1**) as an optimized anti-cancer seed.[39] Compound **1** surpasses DAT in anti-proliferative activity against several cancer cell lines, but exhibits negligible tumor-promoting and proinflammatory activities, unlike DAT. More recently, a scalable synthetic method to supply several hundred milligrams of **1** has also been developed.[40] Therefore, **1** is a possible medicinal lead for anti-cancer therapy.

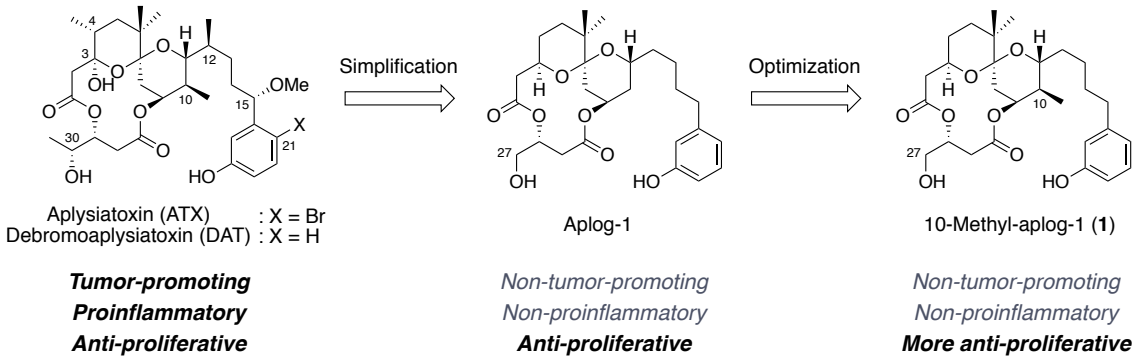

Figure 5. Structural simplification and optimization of aplysiatoxin

Possible Anti-Cancer Mechanisms of PKC Ligands

As mentioned above, PKC isozymes were believed to be oncoproteins because tumor-promoters can activate them with high potency. However, PKCδ, in particular, has been thought to be involved in anti-cancer signaling. PKCδ is the first PKC isozyme identified as a caspase substrate and is therefore proteolytically activated in apoptotic cells.[41] Thus, there are many reports that have linked PKCδ to pro-apoptotic signaling,[42] resulting in the assumption that it is the particular isozyme responsible for cancer suppression although other isozymes have also been found to be activated by caspases.[43,44] The anti-cancer activity of bryo-1 was also explained according to PKCδ-dependent mechanisms, namely that tumor-promoting TPA significantly downregulates PKCδ levels while bryo-1 protects PKCδ from degradation by TPA.[45] This difference was considered to be attributed to the localization profiles of PKCδ. TPA induces translocation of PKCδ to the plasma membrane while bryo-1 causes its translocation to the nuclear membrane and perinuclear region.[46] PEP005 was also reported to increase the activity of PKCδ while repressing that of PKCα in Colo-205 cells, resulting in apoptosis mediated by ERK1/2 activation.[47] In addition, 10-methyl-aplog-1 (**1**) showed some binding selectivity for PKCδ, η, and θ, while tumor-promoting DAT binds with equal affinity to all conventional and novel PKC isozymes.[39] Therefore, the anti-proliferative activity of these compounds as well as their lack of tumor-promoting activity may be attributed to their preference for PKCδ.

However, the actual functions of each PKC isozyme remain unclear. Indeed, PKCδ has been reported to induce apoptosis via activation of p53, c-Abl, and lamin,[48-50] and to inhibit cell-cycle progression via induction of cyclin-dependent kinase (CDK) inhibitors such as p21 and p27, or suppression of cyclin D1.[51-53] In contrast, some studies have indicated that PKCδ activates survival pathways such as cyclin D1 and Akt.[54,55] In addition, other isozymes are also involved in both proliferative and anti-proliferative signaling similar to PKCδ.[56,57] Therefore, despite the number of studies done on PKC signalings, the exact roles of each PKC isozyme in cancer have not fully been identified. Such complexities are associated with the fact that the functions of PKC isozymes are altered depending on cell type and cellular context. For example, PEP005 showed cell line-selective growth inhibitory activity, but the sensitivity of each cell line appeared to not be correlated with the expression levels of PKC isozymes.[47] The anti-proliferative activity of **1** was also highly selective for specific cancer cell lines, although the expression levels of PKC isozymes in each cell line were not determined.[39,40] Thus, PKC could act differently according to the cell type. Moreover, each PKC isozyme may play

different roles even in the same cell depending on the cell-cycle phase. In H358 non-small cell lung cancer cells, PKCδ was found to induce the up-regulation of p21 during G1 phase and thereby inhibit the entry into S phase. During S phase in the same cell line, PKCα was involved in p21 mediated-inhibition of progression into G2 phase (Figure 6A).[58,59] Thus, functional PKC isozymes could be altered by the timing of activation stimuli. In rat thyroid cells, PKCδ reportedly promotes G1 phase cell-cycle progression, but blocks G2 phase entry, resulting in S phase accumulation followed by apoptosis.[60] Similar effects were also observed in rat 3Y1 fibroblasts.[61] In such cases, PKCδ appears to be oncogenic in G1 phase, but behaves solely as a tumor-suppressor as shown by its ability to promote apoptosis.

Another difficulty in analyzing the modes of action of PKC ligands is associated with the instability of activated PKC isozymes. Mechanisms of degradation of activated PKC isozymes were examined extensively by Newton's group (Figure 7).[62-64] Newly synthesized PKC isozymes are processed post-translationally by phosphorylation of at least three residues, and adopts an autoinhibited conformation before activation. The sensitivity of its active conformation to phosphatases (PHLPP, PP2A) is much greater than that of the auto-inhibited conformation, and dephosphorylation is followed by ubiquitination and proteasomal degradation. Therefore, PKC activators can be regarded as PKC suppressors, and it is always controversial whether activation or degradation of PKC triggers each cellular response. It is indisputable that tumor-promoting TPA shows anti-proliferative activity against cancer cell lines although it induces tumorigenesis *in vivo*. Recently, Newton *et al*. reported that most mutations of all PKC isozymes in human cancers are loss-of-function rather than gain-of-function.[65] Based on their results, they postulated that degradation rather than activation of PKC may cause phorbol ester-induced tumor-formation.[64] Moreover, repeated application of staurosporine, a potent inhibitor of PKC and other kinases, significantly enhanced tumor-formation on the mouse skin like TPA.[66] Considering these results, activation of all PKC isozymes may be involved in the cancer cell growth inhibition induced by PKC ligands.

Regarding **1**, there may be another anti-proliferative mechanism independent of PKC isozymes. DAT and **1** exhibited stronger anti-proliferative activity against several cancer cell lines than that of bryo-1.[38,39] On the other hand, their affinity for PKC isozymes was equal to that of bryo-1.[38,39] Therefore, the skeleton of DAT may bind to target proteins other than PKC isozymes. In order to understand the anti-proliferative mechanisms of **1**, it is essential to identify PKC isozymes or other proteins responsible for its anti-proliferative activity against each cell line.

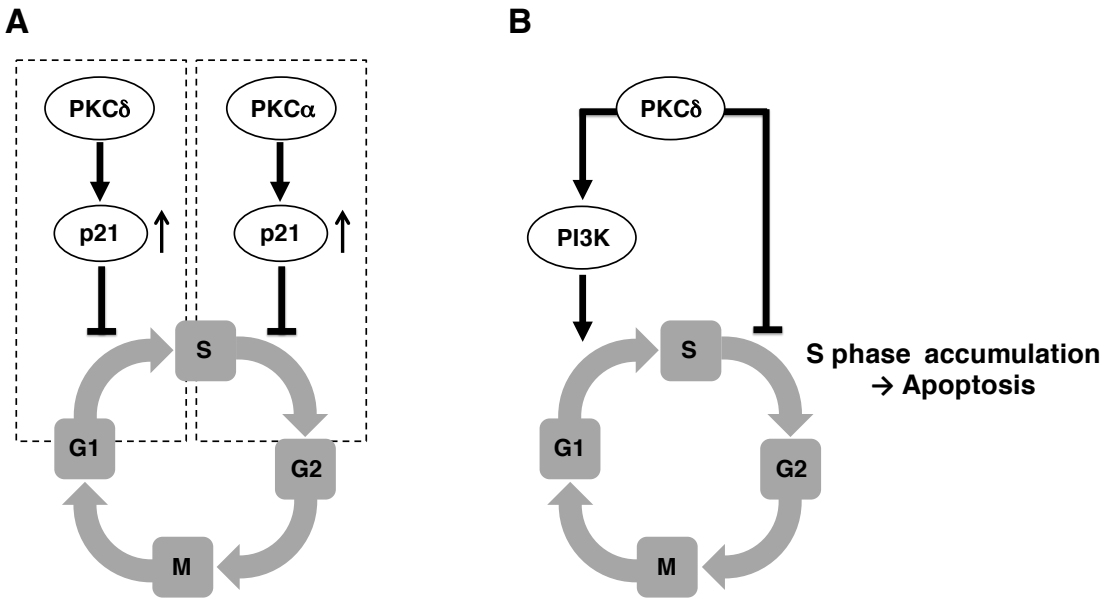

Figure 6. Cell-cycle phase-specific roles of PKC isozymes in (A) H358 and (B) rat thyroid cells

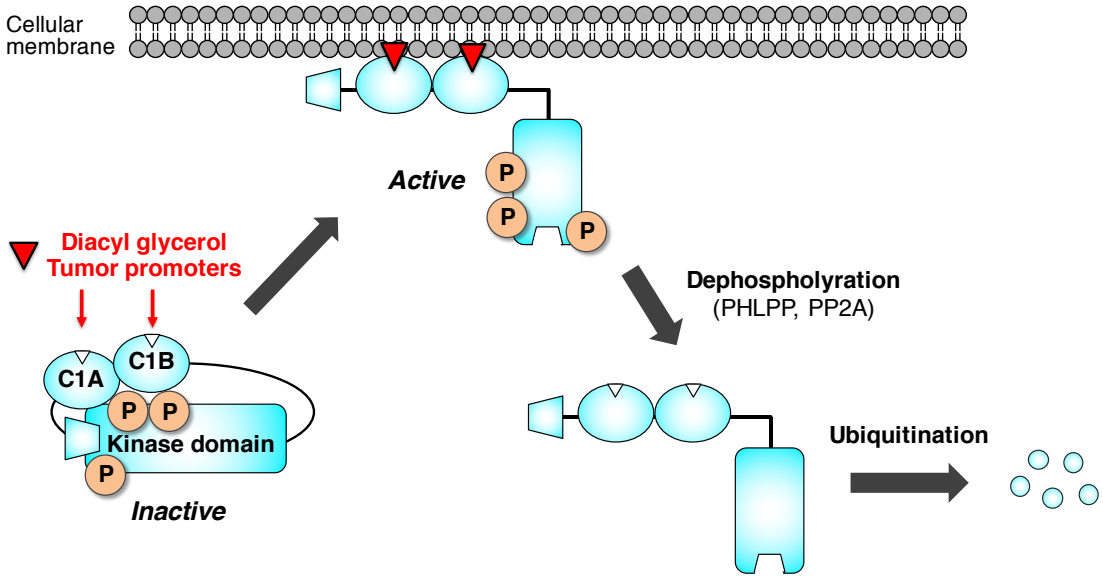

Figure 7. The proposed mechanism of PKC degradation

Objective and Outline of This Study

Although aplog-1 (Figure 5) and its derivatives are promising anti-cancer leads, their mode of action remains unknown. To uncovered their mode of action, the precise functions of PKC isozymes and their growth inhibitory activity must be elucidated. At first, the author tried to address this problem with the structure-activity studies. Kishi and colleagues reported that the hydroxyl group at position 30 of DAT can form hydrogen bonds with the amino acid residues of PKC C1 domains.[67,68] Furthermore, the aromatic side chain of DAT can be inserted into the cellular membrane, similar to the ester side chain of TPA, and was expected to be a driving force for PKC translocation from the cytosol to the cellular membrane.[67,68] These insights led the author to synthesize new derivatives of aplog-1 and **1**, whose structures were modified around the position 27 and the aromatic ring, respectively (Figure 8). In the structure-activity studies of position 27 on aplog-1, a good correlation was observed between the ability to bind to and activate PKCδ, and the anti-proliferative activity against several cancer cell lines (Chapter 1), suggesting the involvement of PKC isozymes in the cell line-selective anti-proliferative activity of aplogs. In Chapter 2, the roles of the phenolic group in the side chain of **1** were investigated. The phenolic moiety could interact with not only the cellular membrane but also the PKC C1 domain through either a hydrogen bond or a CH/π interaction. Moreover, since **16** showed significant tumor-promoting and proinflammatory activities, the phenolic group was proposed to suppress these adverse effects.

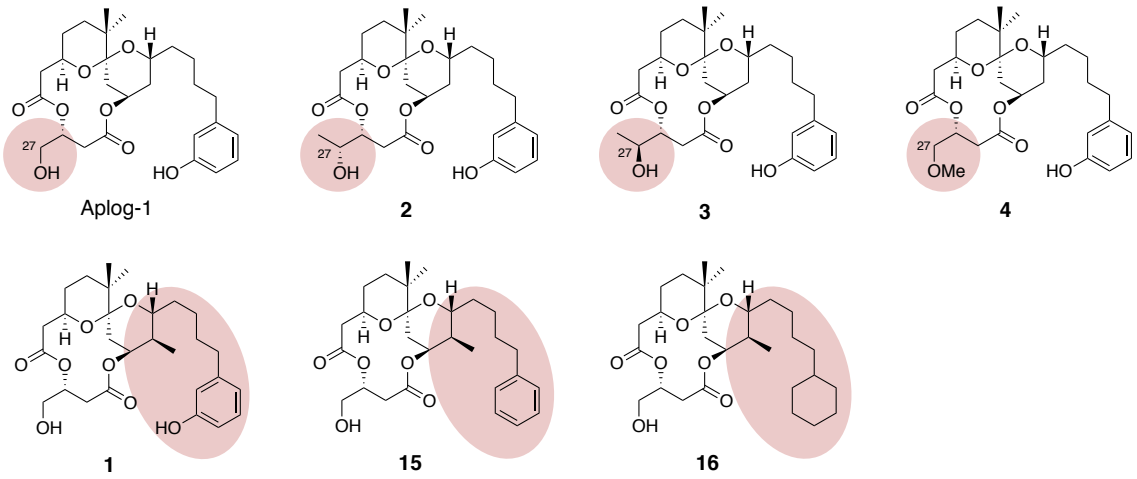

Figure 8. Structures of aplog-1 and its derivatives.

Finally, the author identified the PKC isozymes involved in the anti-proliferative activities of **1** (Chapter 3). The expression levels of all novel and conventional PKC isozymes were precisely quantified in nine cancer cell lines. Subsequently, the effects of knocking down of predominant isozymes, PKCα and δ, on the anti-proliferative activity of **1**, DAT and TPA against aplog-sensitive cell lines were evaluated. Since PKC ligands induced the activation and degradation of PKC isozymes, the roles of PKC isozymes in cellular responses to them was highly controversial. On the other hand, knockdown experiments performed in this study indicated that activation, but not degradation of PKCα and δ was involved in the cell line-selective anti-proliferative activity. This indication was supported by the failure of the knockdown to influence cell proliferation, and by significant attenuation of the growth inhibitory effects of PKC ligands.

Chapter 1

Structure-Activity Studies at Position 27 of Aplog-1*

Introduction

Kishi and Rando's study on the pharmaphocore of DAT suggested that the hydroxyl group of position 30 is necessary to bind to PKC C1 domains.[67,68] They also revealed that the epimer of DAT at position 30 showed only a marginal ability to activate PKC.[67,68] According to this study, 27-(*R*)-methyl-aplog-1 (**2**), whose absolute configuration was the same as that of DAT at position 30, should activate PKC isozymes, while 27-(*S*)-methyl-aplog-1 (**3**), an epimer of **2** at position 27, and 27-*O*-methyl-aplog-1 (**4**) should not. Thus, **3** and **4** could be inactive controls for investigating the contribution of PKC isozymes towards the anti-proliferative activity of aplog-1.

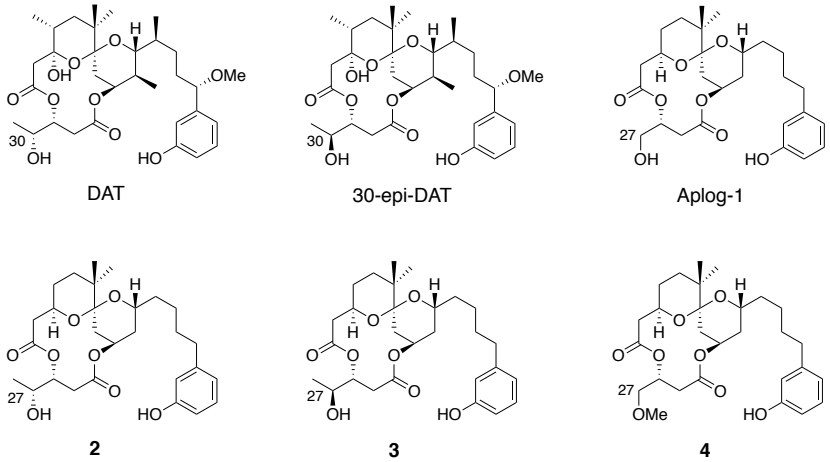

Figure 9. Structures of DAT, 30-epi-DAT, aplog-1, and its derivatives.

---

*The content described in this Chapter was originally published in Tetrahedron. Yusuke Hanaki, Masayuki Kikumori, Sayo Ueno, Harukuni Tokuda, Nobutaka Suzuki, and Kazuhiro Irie (2013) Structure-activity studies at position 27 of aplog-1, a simplified analog of debromoaplysiatoxin with anti-proliferative activity. *Tetrahedron* **69**, 7636-7645. doi: 10.1016/j.tet.2013.02.008 © 2013 Elsevier Ltd.

Results and Discussion

The synthesis of **2**-**4** is outlined in Scheme 1. They were synthesized from a previously reported spiroketal (**11**)[38] and each carboxylic acid unit (**10a**-**c**). Coupling of (*S*)-glycidol (**5**) with 1,3-dithiane gave a diol. Transacetalization of the diol with *p*-anisaldehyde dimethyl acetal afforded the cyclic acetal, which was reductively cleaved by DIBAL; the result was a 3:1 mixture of regioisomers in which the desired primary alcohol (**6**) predominated. Subsequently, oxidation of **6**, and a stereoselective Grignard reaction generated an alcohol (**7a**) in 97% ee. Protection by a benzyl group, deprotection of dithioacetal, and oxidation gave a carboxylic acid (**10a**). The Mitsunobu reaction[69] of **7a** was employed to generate an epimer alcohol (**7b**) in 92% ee. The synthesis of **10b** from **7b** was achieved in a similar manner to the synthesis of **10a**. Compound **10c** was provided by oxidation of the known aldehyde (**9c**).[70] Yamaguchi's esterification[71] of **11** with the carboxylic acid (**10a**), followed by switching of the protecting group from a 4-methoxyphenylmethyl (MPM) group to a triethylsilyl (TES) group, and oxidative cleavage of the olefin group provided a carboxylic acid (**13a**). Deprotection of the TES group, lactonization, and deprotection of the two benzyl groups gave **2**. The synthesis of **3** and **4** was similarly achieved (**2**, 13%; **3**, 15%; **4**, 29% in seven steps from **11**).

As a representative of PKC isozymes, the author evaluated affinity for PKCδ, which is ubiquitously expressed in many types of tissues, using a synthetic PKCδ-C1B peptide[72] and human recombinant PKCδ. The affinity was measured by a competition binding assay with [^{3}H]phorbol 12,13-dibutyrate (PDBu) as described previously by Sharkey and Blumberg.[73,74] Recombinant whole PKCδ has both the C1A and C1B domains, but its instability can diminish accuracy and reproducibility of binding assay. Therefore, a more reliable assay using synthetic δ-C1B peptide, which is stable and inexpensive, was simultaneously performed. The main binding site of tumor-promoters was found to be the C1B domain of PKCδ rather than the C1A domain, and the binding constants of some PKC ligands were almost equal to those of whole PKCδ.[39,75,76] As shown in Table 1, the affinity of **2** was several times weaker than that of aplog-1, while **3** and **4** hardly bound to PKCδ and δ-C1B at all. Their abilities to activate PKCδ were also evaluated by measuring phosphorylation levels with a fluorescence-labeled peptide substrate (Figure 10). Both aplog-1 and **2** activated PKCδ in a concentration-dependent manner, while **3** and **4** did not activate PKCδ even at 10 μM. Since PKC activation requires higher concentration than PKC binding as shown in many PKC ligands,[77] these activation profiles correlated well with the results of the binding assay.

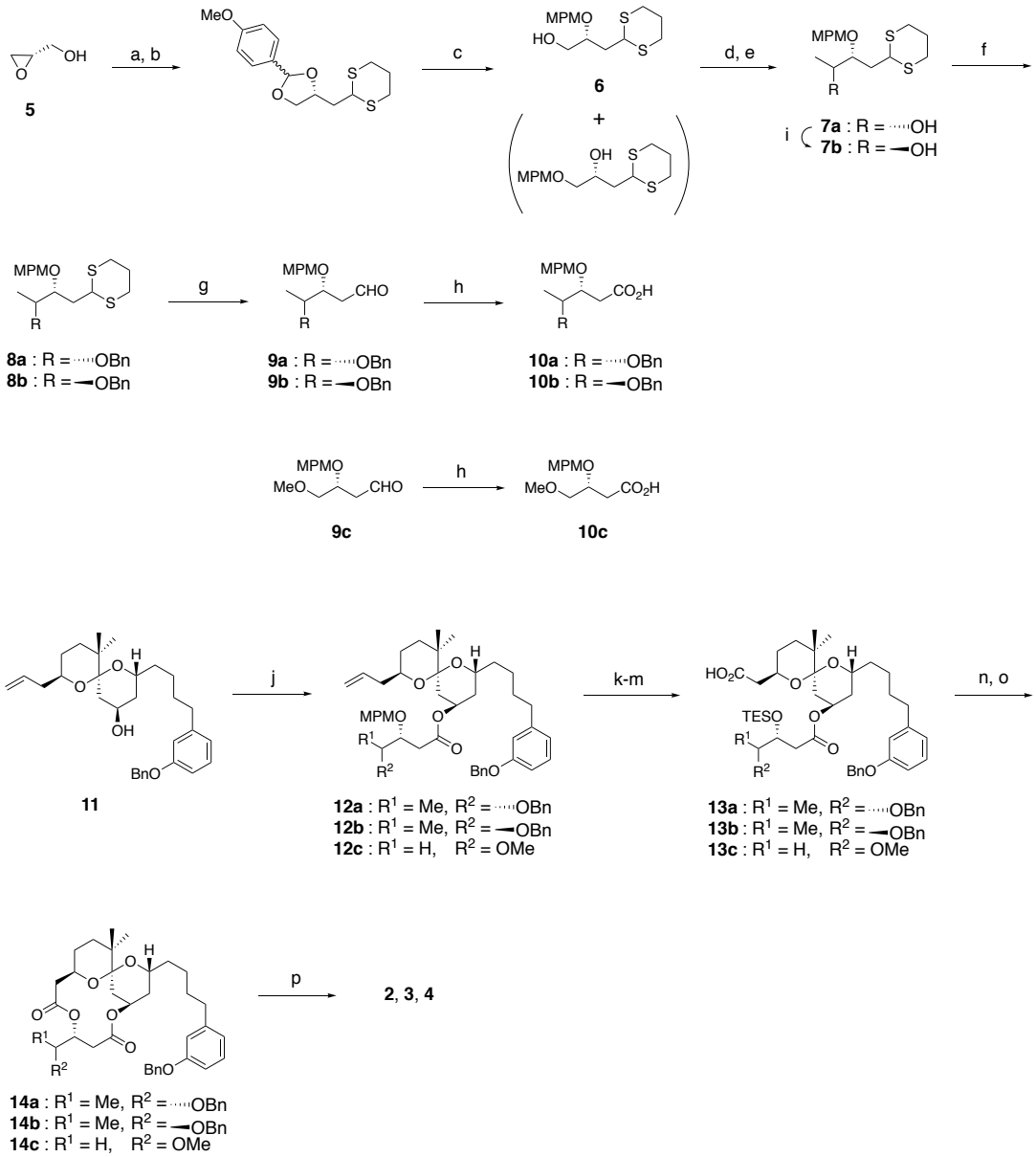

Scheme 1. (a) 1,3-dithiane, *n*-BuLi, THF; (b) *p*-MeO(C_6H_4)CH($OMe)_2$, CSA, DMF; (c) DIBAL, DCM (70% in three steps); (d) SO_3·pyridine, DMSO, Et_3N, DCM (82%); (e) MeMgBr, $MgBr_2$·Et_2O, DCM (83%); (f) BnBr, NaH, THF (**a**, 37%; **b**, 49%); (g) MeI, $NaHCO_3$, MeCN, H_2O (**a**, 73%; **b**, 87%); (h) $NaClO_2$, 2-methyl-2-butene, *t*-BuOH, sat. NaH_2PO_4 aq. (**a**, 77%; **b**, 88%; **c**, 95%); (i) 1) *p*-nitrobenzoic acid, diisopropyl azodicarboxylate, PPh_3, THF (73%); 2) NaOH, H_2O, THF, MeOH (93%); (j) **7a**-**c**, 2,4,6-trichlorobenzoyl chloride, Et_3N, DMAP, toluene (**a**, 97%; **b**, quant.; **c**, quant.); (k) DDQ, H_2O, DCM (**a**, 79%; **b**, 75%; **c**, 91%); (l) TES-Cl, imidazole, THF (**a**, 84%; **b**, quant.; **c**, 90%); (m) $KMnO_4$, $NaIO_4$, *t*-BuOH, pH 7 buffer (**a**, 45%; **b**, 43%; **c**, 66%); (n) HF·pyridine (**a**, 83%; **b**, 74%; **c**, 96%); (o) 2,4,6-trichlorobenzoyl chloride, Et_3N, DMAP, toluene (**a**, 65%; **b**, 79%; **c**, 76%); (p) 10% Pd-C, EtOH or MeOH (**a**, 83%; **b**, 77%; **c**, 74%).

Table 1. Values of K_i for the inhibition of [^{3}H]PDBu binding by aplog-1, **2**, **3**, and **4**.

	K_i (nM)			
	Aplog-1[a]	**2**	**3**	**4**
δ–C1B peptide	7.4	24 (2.6)[b]	> 2,500	> 2,500
whole PKCδ	15	31 (1.9)	> 5,000	> 5,000

[a]Cited from 38.

[b]Values in parentheses represent the standard deviation from triplicate experiments.

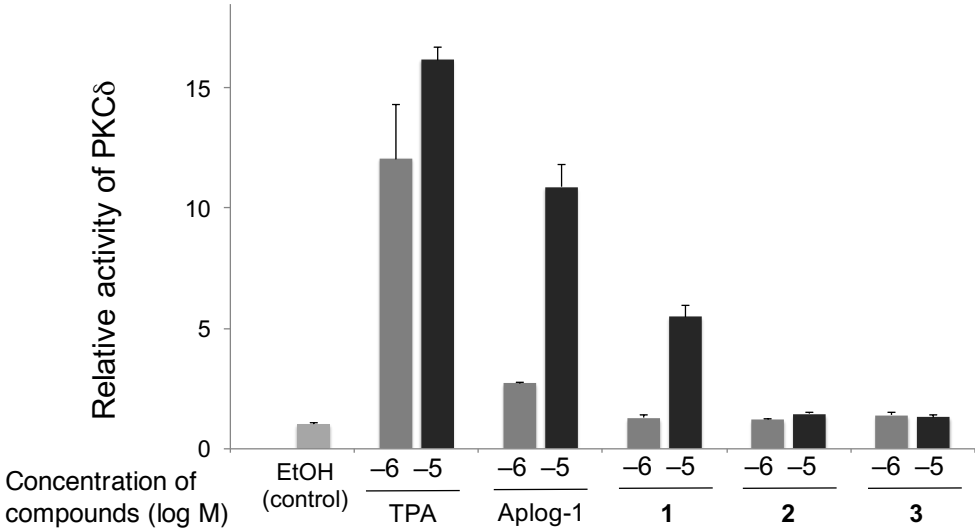

Figure 10. Kinase activity of PKCδ stimulated by TPA, aplog-1, **2**, **3**, and **4**. The values were expressed as a percentage relative to the control (EtOH). The final concentration of EtOH was 2.0%. The results were presented as the average of duplicated points when all compounds were simultaneously tested. Error bars represent the standard error of the mean (n = 2). Another experiment gave a similar result.

The tumor-promoting activities of **2**-**4** was estimated by testing the induction of Epstain-Barr virus early antigen (EBV-EA) production *in vitro* (Figure 11).[78,79] EBVs under the strict control of host human B lymphoblastoid Raji cells, are activated by treatment with tumor-promoters to produce early antigen (EA), which can be detected by an indirect immunofluorescence technique. Compared with tumor-promoting TPA, **2**-**4** induced only weak EA production even at 1 μM like aplog-1. This result suggests that the methyl group at position 27 does not enhance the tumor-promoting activity. However, it might enhance the tumor-promoting activity in combination with other substituents eliminated when DAT was simplified, since DAT's tumor-promoting activity was stronger than that of oscilatoxin A, that lacks the methyl group at position 30.[80]

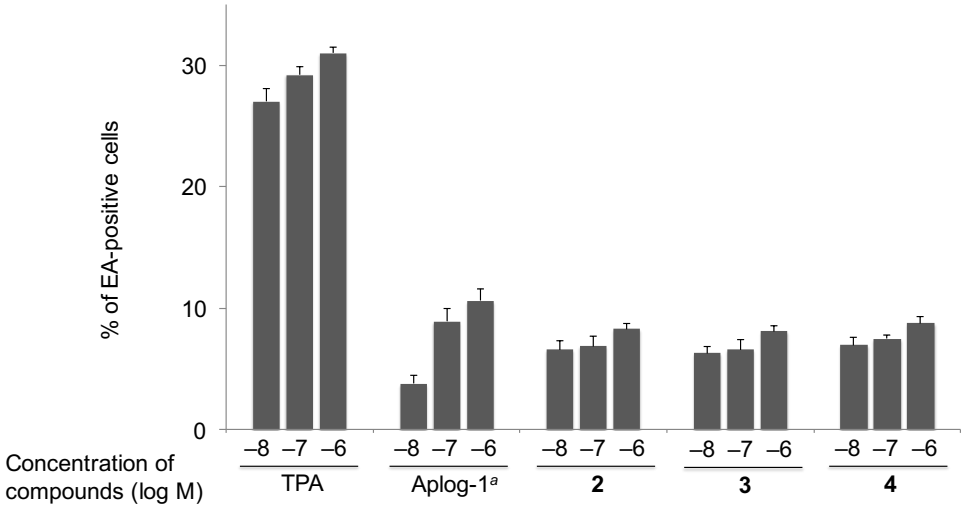

Figure 11. EBV-EA production induced by TPA, aplog-1, **2**, **3**, and **4**. Percentages of EA-positive cells are shown. Sodium *n*-butyrate (4 mM) was added to all samples to enhance the sensitivity of Raji cells. Only 0.1% of the cells were positive for EA at 4 mM sodium *n*-butyrate. The final concentration of DMSO was 0.4%. Cell viability exceeded 60% in all experiments except for that with TPA at 10^{-6} M (>50%). Error bars present the standard error of the mean (n = 3). [a]Cited from ref. 38

Finally, the anti-proliferative activities of **2**-**4** were evaluated using a panel of 39 human cancer cell lines (JFCR39) established by Yamori and colleagues.[81] The growth inhibitory activity was expressed as the concentration required to inhibit cell growth by 50% as compared to an untreated control, GI_{50} (M). The results for the cell lines where aplog-1 showed activity with log GI_{50} values of less than –5.30, are listed in Table 2 (the rest of the data are provided in Supporting Information). Although the growth inhibitory activity of **2** was slightly weaker than that of aplog-1, **2** showed substantial activity like aplog-1 especially in the cell lines listed in Table 2, while **3** and **4** exhibited only weak activity. On the other hand, there was no correlation between the anti-proliferative activity and the ability to bind to and activate PKCδ in aplog-insensitive cell lines (Table 3). All derivatives significantly inhibited the growth of all cell lines at high concentration ($10^{-5} \sim 10^{-4}$ M). These effects were estimated to be caused by non-specific interaction rather than specific targets, because almost all compounds tested in JFCR39 exhibited significant cytotoxicity at the concentration.[82] These results indirectly suggest that aplog-1 and its analogs could inhibit the growth of aplog-sensitive cell lines through PKC-dependent mechanisms.

In summary, aplog-1 and **2** exhibited cell line-selective anti-proliferative activity, while **3** and **4**, without ability to bind to PKCδ, showed only weak growth inhibition in all cancer cell lines. Since conventional and novel PKC isozymes has C1 domains, their activation could be involved in the anti-proliferative activity against aplog-sensitive cancer cell lines. Besides, protein kinase D (PKD), diacylglycerol kinases (DGK), Ras guanyl nucleotide-releasing protein (RasGRP), and chimerin, that contain PKC C1 homology domains,[83] should be considered as possible targets responsible for aplogs' activity.

Table 2. Growth inhibition of aplog-1, **2**, **3**, and **4** against aplog-sensitive cancer cell lines

		log GI_{50} (log M)			
cancer type	cell line	Aplog-1[a]	**2**	**3**	**4**
Breast	HBC-4	–6.33	–6.15	–4.78	–4.71
	MDA-MB-231	–5.61	–5.03	–4.80	–4.50
Colon	HCC2998	–5.43	–5.08	–4.79	–4.70
Lung	NCI-H460	–5.60	–5.66	–4.78	–4.70
	A549	–5.32	–5.09	–4.80	–4.76
Melanoma	LOX-IMVI	–5.74	–5.18	–4.76	–4.80
Stomach	St-4	–5.55	–5.17	–4.71	–4.70
	MKN45	–5.33	–4.99	–4.77	–4.75

[a]Cited from ref. 38

Table 3. Growth inhibition of aplog-1, **2**, **3**, and **4** against aplog-insensitive cancer cell lines

		log GI_{50} (log M)			
cancer type	cell line	Aplog-1[a]	**2**	**3**	**4**
Breast	MCF-7	–4.72	–4.73	–4.79	–4.88
Colon	HT-29	–4.77	–4.77	–4.75	–4.71
Lung	DMS114	–4.79	–4.82	–4.82	–4.88
Ovarian	OVCAR-3	–4.78	–4.77	–4.78	–4.83
Stomach	MKN74	–4.76	–4.80	–4.76	–4.80
Prostate	DU-145	–4.85	–4.80	–4.73	–4.67

[a]Cited from ref. 38

Experimental

General remarks

The following spectroscopic and analytical instruments were used: digital polarimeter, DIP-1000 (Jasco, Tokyo, Japan); ^{1}H and ^{13}C NMR, Avance III 400 and Avance III 500 (reference TMS, Brucker, Germany); HPLC, model 600E with a model 2487 UV detector (Waters, Tokyo, Japan); and HR-FAB-MS, JMS-600H (JEOL, Tokyo, Japan) and JMS-700 (JEOL, Tokyo, Japan). HPLC was carried out on YMC packed ODS-A AA12S05-1520WT and SIL SL12S05-2510WT (Yamamura Chemical Laboratory, Kyoto, Japan) and CHIRALCEL OJ-RH (Daicel Corporation, Osaka, Japan). Wakogel C-200 (silica gel, Wako Pure Chemical Laboratory, Osaka, Japan) was used for column chromatography. [^{3}H]PDBu (18.7 Ci/mmol) was custom synthesized by Perkin-Elmer Life Sciences Research Products (Boston, MA). The human recombinant PKCδ was purchased from Life Technologies (Carlsbad, CA). PKCδ C1B peptide was synthesized as reported previously.[72] All other chemicals and reagents were purchased from chemical companies and used without further purification. The purity of **2**-**4** was greater than 95% as judged by HPLC (Appendix).

Synthesis of 27-(*R*)-methyl-aplog-1 (2)

To a solution of 1,3-dithiane (2.18 g, 18.2 mmol, 4 equiv.) in THF (50 mL) was added 1.6 M *n*-BuLi in hexane (11.3 mL, 18.2 mmol, 4 equiv.) at 4 ºC. After stirring for 1 h at 4 ºC, a solution of (*S*)-glycidol (**5**) (336 mg, 4.54 mmol) in THF (1 mL) was added at 4 ºC. The reaction mixture was stirred for 2 h at 4 ºC, and the reaction was quenched with saturated aq. NH_4Cl (40 mL). The mixture was extracted with EtOAc (70 mL x 3). The combined organic layers were washed with brine, dried over Na_2SO_4, filtered, and concentrated *in vacuo*. The residue was purified by column chromatography (silica gel, 60% EtOAc/hexane) to afford a crude diol.

After the diol was dissolved in DMF (12 mL), *p*-anisaldehyde dimethyl acetal (1.24 g, 6.81 mmol, 1.5 equiv.) and (±)-CSA (70.0 mg, 0.302 mmol, 0.07 equiv.) were added to the mixture at room temperature, which was stirred at room temperature for 1.5 h. The reaction was quenched with saturated aq. $NaHCO_3$ (12 mL), and the mixture was extracted with EtOAc (15 mL x 3). The combined organic layers were washed with brine, dried over Na_2SO_4, filtered, and concentrated *in vacuo*. The residue was purified by column chromatography (silica gel, 15% EtOAc/hexane) to afford an acetal.

The acetal was dissolved in DCM (20 mL), and 1 M DIBAL in toluene (9.00 mL, 9.00 mmol, 2 equiv.) was added at –78 ºC. The reaction mixture was stirred at –78 ºC for 1 h, and then 1 M DIBAL in toluene (4.00 mL, 4.00 mmol, 0.9 equiv.) was added at –78 ºC. After an additional 1 h of stirring at –78 ºC, the reaction was quenched with MeOH (6 mL). The mixture was warmed

to room temperature, and saturated aq. Rochelle salt (20 mL) was added. The mixture was poured into EtOAc (30 mL). After the organic layer was separated, the aqueous layer was extracted with EtOAc (30 mL x 3). The combined organic layers were washed with brine, dried over Na_2SO_4, filtered, and concentrated *in vacuo*. The residue was purified by column chromatography (silica gel, 10% → 20% EtOAc/hexane) to afford **6** (991 mg, 3.16 mmol, 70% in three steps) as a clear oil, in which the two regioisomers existed in a ratio of 3:1. ^{1}H NMR (400 MHz, $CDCl_3$, 0.017 M) ppm: δ 1.82 (1H, m), 1.84-1.93 (2H, m), 2.06-2.14 (2H, m), 2.78-2.91 (4H, m), 3.52 (1H, m), 3.76 (1H, m), 3.81 (3H, s), 3.83 (1H, m), 4.12 (1H, dd, *J* = 8.7, 5.8 Hz), 4.54 (1H, d, *J* = 11.1 Hz), 4.58 (1H, d, *J* = 11.1 Hz), 6.88-6.91 (2H, m), 7.28-7.31 (2H, m); ^{13}C NMR (100 MHz, $CDCl_3$, 0.017 M) ppm: δ 25.9, 30.1, 30.4, 37.2, 43.8, 55.3, 64.1, 71.9, 76.0, 113.9 (2C), 129.6 (2C), 130.4, 159.4; IR (KBr) cm^{-1}: 3452, 2933, 1645, 1516, 1247, 1040, 821; HR-FAB-MS (matrix, glycerol) *m/z*: 315.1085 ([M+H]$^+$ Calcd. for $C_{15}H_{23}O_3S_2$ 315.1089); $[\alpha]_D$ –3.5º (*c* = 0.27, $CHCl_3$, 28.9 ºC).

To a solution of **6** (538 mg, 1,71 mmol) in DCM (6.8 mL) and DMSO (1.8 mL) were added Et_3N (1.67 mL, 12.0 mmol, 7equiv.) and SO_3·pyridine (1.09 g, 6.86 mmol, 4 equiv.) at 0 ºC. After stirring at room temperature for 2.5 h, the reaction was quenched with saturated aq. NH_4Cl (10 mL). The organic layer was separated, and the aqueous layer was extracted with DCM (10 mL x 3). The combined organic layer was washed with brine, dried over Na_2SO_4, filtered, and concentrated *in vacuo*. The residue was purified by column chromatography (silica gel, 10% → 15% EtOAc/hexane) to afford an aldehyde (438 mg, 1.40 mmol, 82%) as a clear oil.

To a solution of the aldehyde (438 mg, 1.40 mmol) in DCM (6.5 mL) was added $MgBr_2$·Et_2O (433 mg, 1.68 mmol, 1.2 equiv.) at –78 ºC. After stirring for 1 h, 3 M MeMgBr in Et_2O (0.70 mL, 2.10 mmol, 1.5 equiv.) was added at –78 ºC. The reaction mixture was stirred at –78 ºC for 1.5 h, and the reaction was quenched with saturated aq. NH_4Cl (10 mL). After the organic layer was separated, the aqueous layer was extracted with DCM (10 mL x 3). The combined organic layer was washed with brine, dried over Na_2SO_4, filtered, and concentrated *in vacuo*. The residue was purified by column chromatography (silica gel, 20% EtOAc/hexane) to give **7a** (381 mg, 1.16 mmol, 83%) as a clear oil. ^{1}H NMR (400 MHz, $CDCl_3$, 0.019 M) ppm: δ 1.20 (3H, d, *J* = 6.4 Hz), 1.87 (1H, m), 1.97 (2H, dd, *J* = 7.1, 6.1 Hz), 2.08-2.16 (2H, m), 2.77-2.91 (4H, m), 3.56 (1H, dd, *J* = 11.6, 5.8 Hz), 3.74 (1H, m), 3.81 (3H, s), 4.10 (1H, t, *J* = 7.2 Hz), 4.56 (1H, d, *J* = 11.0 Hz), 4.67 (1H, d, *J* = 11.0 Hz), 6.88-6.91 (2H, m), 7.28-7.32 (2H, m); ^{13}C NMR (100 MHz, $CDCl_3$, 0.019 M) ppm: δ 19.3, 25.9, 30.2, 30.5, 37.1, 43.9, 55.3, 69.5, 73.4, 80.0, 113.9 (2C), 129.7 (2C), 130.5, 159.4; IR (KBr) cm^{-1}: 3451, 2900, 1613, 1513, 1247, 1067, 820; HR-FAB-MS (matrix, *m*-nitrobenzyl alcohol) *m/z*: 329.1247 ([M+H]$^+$ Calcd. for $C_{16}H_{25}O_3S_2$ 329.1245); $[\alpha]_D$ +4.7º (*c* = 0.30, $CHCl_3$, 26.6 ºC).

To a solution of 60% NaH in oil (23.5 mg, 0.588 mmol, 1.1 equiv.) in THF (5.9 mL) was

added a solution of **7a** (175 mg, 0.534 mmol) in THF (0.5 mL). After stirring for 30 min at 0 ºC, BnBr (67 μL, 0.564 mmol, 1.05 equiv.) was added at 0 ºC. The reaction mixture was stirred at room temperature for 21.5 h, and the reaction was quenched with saturated aq. NH_4Cl (6 mL). After the organic layer was separated, the aqueous layer was extracted with EtOAc (10 mL x 3). The combined organic layer was washed with brine, dried over Na_2SO_4, filtered, and concentrated *in vacuo*. The residue was purified by column chromatography (silica gel, 5% EtOAc/hexane) to afford **8a** (82.7 mg, 0.198 mmol, 37%) as a clear oil. ^{1}H NMR (500 MHz, $CDCl_3$, 0.012 M) ppm: δ 1.16 (3H, d, *J* = 6.4 Hz), 1.82-1.93 (2H, m), 2.01-2.11 (2H, m), 2.72 (1H, m), 2.79-2.83 (3H, m), 3.65 (1H, m), 3.81 (3H, s), 3.82 (1H, m), 4.02 (1H, dd, *J* = 9.9, 4.9 Hz), 4.50-4.60 (4H, m), 6.86-6.89 (2H, m), 7.25-7.36 (7H, m); ^{13}C NMR (125 MHz, $CDCl_3$, 0.012 M) ppm: δ 14.8, 26.1, 29.8, 30.2, 35.7, 44.1, 55.3, 71.1, 72.8, 75.1, 77.0, 113.8 (2C), 127.5, 127.7 (2C), 128.4 (2C), 129.7 (2C), 131.0, 138.8, 159.3; IR (KBr) cm^{-1}: 2898, 1612, 1513, 1460, 1246, 1087, 818; HR-FAB-MS (matrix, glycerol); *m/z*: 419.1716 ([M+H]$^+$ Calcd. for $C_{23}H_{31}O_3S_2$ 419.1715); $[\alpha]_D$ +20.4º (*c* = 0.50, $CHCl_3$, 11.4 ºC).

To a solution of **8a** (78.0 mg, 0.187 mmol) and $NaHCO_3$ (47.0 mg, 0.560 mmol, 3 equiv.) in MeCN (1.8 mL) and H_2O (0.52 mL) was added MeI (0.58 mL, 9.31 mmol, 50 equiv.) at room temperature. The reaction mixture was stirred at room temperature for 19 h, then diluted with H_2O (3 mL). The mixture was extracted with EtOAc (5 mL x 3), and the combined organic layer was washed with brine, dried over Na_2SO_4, filtered, and concentrated *in vacuo*. The residue was purified by column chromatography (silica gel, 15% EtOAc/hexane) to afford the known aldehyde **9a**[84] (44.7 mg, 0.136 mmol, 73%) as a clear oil.

To a solution of **9a**[84] (2.6 mg, 7.9 μmol) in *t*-BuOH (44 μL) and saturated aq. NaH_2PO_4 (44 μL) were added 2 M 2-mehyl-2-butene in THF (22 μL, 44.0 μmol, 5.6 equiv.) and $NaClO_2$ (0.8 mg, 8.8 μmol, 1.1 equiv.) at 4 ºC. The mixture was stirred at 4 ºC for 30 min, and the reaction was quenched with 5% aq. H_3PO_4 (0.5 mL). The resulting mixture was extracted with EtOAc (2 mL x 3). The combined organic layers were washed with brine, dried over Na_2SO_4, filtered, and concentrated *in vacuo*. The residue was purified by column chromatography (silica gel, 30% EtOAc/hexane containing 0.1% AcOH) to afford **10a** (2.1 mg, 6.1 μmol, 77%) as a pale yellow oil. This procedure was repeated several times. ^{1}H NMR (400 MHz, $CDCl_3$, 0.010 M) ppm : δ 1.18 (3H, d, *J* = 6.4 Hz), 2.54 (1H, dd, *J* = 16.0, 8.4 Hz), 2.72 (1H, dd, *J* = 16.0, 4.2 Hz), 3.69 (1H, m), 3.79 (3H, s), 3.98 (1H, m), 4.48-4.60 (4H, m), 6.83-6.87 (2H, m), 7.20-7.36 (7H, m); ^{13}C NMR (100 MHz, $CDCl_3$, 0.010 M) ppm: δ 14.5, 35.1, 55.3, 71.2, 72.6, 74.8, 76.8, 113.8 (2C), 127.7, 127.7 (2C), 128.4 (2C), 129.6 (2C), 130.0, 138.2, 159.4, 175.2; IR (KBr) cm^{-1}: 3452, 2934, 1709, 1645, 1516, 1249, 1084, 822; HR-FAB-MS (matrix, glycerol) *m/z* : 345.1714 ([M+H]$^+$ Calcd. for $C_{20}H_{25}O_5$ 345.1702); $[\alpha]_D$ –15.2º (*c* = 0.19, $CHCl_3$, 25.0 ºC).

To a solution of **10a** (28.6 mg, 83.1 μmol, 1.5 equiv.) and Et_3N (12.9 μL, 92.7 μmol, 1.7

equiv.) in toluene (580 μL) was added 2,4,6-trichlorobenzoyl chloride (14.5 μL, 92.7 μmol, 1.7 equiv.) at room temperature. After 3 h of stirring at room temperature, the supernatant of the suspension was added to a solution of **11** prepared as reported previously[36] (26.1 mg, 54.6 μmol) and DMAP (14.0 mg, 115 μmol, 2.1 equiv.) in toluene (580 μL) at room temperature. The mixture was stirred at 50 ºC for 1.5 h, and then poured into H_2O (2.0 mL). The mixture was extracted with EtOAc (2 mL x 3). The combined organic layers were washed with brine, dried over Na_2SO_4, filtered, and concentrated *in vacuo*. The residue was purified by column chromatography (silica gel, 2.5% → 7.5% EtOAc/hexane) to afford **12a** (42.7 mg, 53.1 μmol, 97%) as a clear oil. ^{1}H NMR (400 MHz, $CDCl_3$, 0.0027 M) ppm: δ 0.87 (3H, s), 0.96 (3H, s), 1.15 (3H, d, *J* = 6.4 Hz), 1.23-1.67 (13H, m), 2.19-2.26 (2H, m), 2.34 (1H, m), 2.53 (1H, dd, *J* = 15.9, 9.0 Hz), 2.57 (2H, t, *J* = 7.8 Hz), 2.63 (1H, dd, *J* = 15.9, 3.7 Hz), 3.46 (1H, m), 3.67 (1H, m), 3.78 (3H, s), 4.07 (1H, m), 4.21 (1H, m), 4.48-4.57 (4H, m), 4.95-5.04 (2H, m), 5.04 (2H, s), 5.11 (1H, m), 5.83 (1H, m), 6.77-6.85 (5H, m), 7.16-7.45 (13H, m); ^{13}C NMR (100 MHz, $CDCl_3$, 0.0020 M) ppm: δ 14.6, 21.6, 24.8, 25.6, 26.5, 26.8, 31.3, 34.2, 34.7, 35.6, 35.8, 36.0, 36.9, 41.1, 55.3, 63.9, 68.2, 70.0, 71.1, 71.7, 72.7, 75.0, 77.6, 100.1, 111.8, 113.8(2C), 115.2, 116.6, 121.2, 127.5, 127.5 (2C), 127.6 (2C), 127.9, 128.3 (2C), 128.6 (2C), 129.2, 129.4 (2C), 130.8, 135.2, 137.3, 138.7, 144.7, 158.9, 159.2, 172.3; IR (KBr) cm^{-1}: 2935, 1724, 1514, 1449, 1249, 1070; HR-FAB-MS (matrix, *m*-nitrobenzyl alcohol) *m/z*: 827.4497 ([M+Na]$^+$ Calcd. for $C_{51}H_{64}O_8Na$ 827.4499); $[\alpha]_D$: +5.2º (*c* = 0.12, $CHCl_3$, 28.6 ºC).

To a vigorously stirred solution of **12a** (40.4 mg, 50.2 μmol) in DCM (2.6 mL) and H_2O (0.47 mL) was added DDQ (22.7 mg, 100 μmol, 2 equiv.) at room temperature. The mixture turned brown. After stirring at room temperature for 1 h, the color gradually changed to yellow-orange with precipitation. The mixture was poured into saturated aq. $NaHCO_3$ (8 mL), and extracted with DCM (10 mL x 3). The combined organic layers were washed with brine, dried over Na_2SO_4, filtered, and concentrated *in vacuo*. The residue was purified by column chromatography (silica gel, 5% → 20% EtOAc/hexane) to afford an alcohol (27.1 mg, 39.6 mmol, 79%) as a clear oil.

To a solution of the alcohol (26.2 mg, 38.3 μmol) in THF (380 μL) were added imidazole (7.8 mg, 115 μmol, 3 equiv.) and TES-Cl (7.7 μL, 45.9 μmol, 1.2 equiv.) at room temperature. After stirring at room temperature for 4 h, the reaction was quenched with brine (2 mL). The resulting mixture was extracted with EtOAc (3 mL x 3). The combined organic layers were washed with brine, dried over Na_2SO_4, filtered, and concentrated *in vacuo*. The residue was purified by column chromatography (silica gel, 2% EtOAc/hexane) to afford a silyl ether (25.6 mg, 32.0 μmol, 84%) as a clear oil.

To a suspension of $NaIO_4$ (15.6 mg, 72.9 μmol, 8 equiv.) in pH 7.2 phosphate buffer (750 μL) was added $KMnO_4$ (1.4 mg, 8.9 μmol, 1 equiv.) in one portion. After 3 min of vortexing at room

temperture under an Ar atmosphere, the mixture was added to a solution of the silyl ether (7.1 mg, 8.9 μmol) in *t*-BuOH (750 μL). The reaction mixture was vortexed at room temperature for 8 min, and the reaction was quenched with $Na_2S_2O_3$ (4.3 mg). The resulting mixture was poured into EtOAc (3 mL) and H_2O (5 mL). The organic layer was separated, and the aqueous layer was extracted with EtOAc (5 mL x 3). This procedure was repeated three times and a total of 25.0 mg (31.3 μmol) of the silyl ether was reacted. The combined organic layers were washed with brine, dried over Na_2SO_4, filtered, and concentrated *in vacuo*. The residue was purified by column chromatography (silica gel, 10% → 20% EtOAc/hexane containing 0.1% AcOH) to afford **13a** (11.6 mg, 14.2 μmol, 45%) as a clear oil. ^{1}H NMR (400 MHz, $CDCl_3$, 0.0025 M) ppm: δ 0.55 (6H, q, *J* = 7.9 Hz), 0.90 (3H, s), 0.90 (9H, t, *J* = 7.9 Hz), 0.98 (3H, s), 1.15 (3H, d, *J* = 6.4 Hz), 1.34-1.87 (13H, m), 2.18 (1H, br. d, *J* = 15.9 Hz), 2.44 (1H, dd, *J* = 15.6, 8.6 Hz), 2.55-2.64 (5H, m), 3.56 (1H, m), 3.90 (1H, m), 4.11 (1H, m), 4.36 (1H, m), 4.50 (1H, d, *J* = 11.8 Hz), 4.58 (1H, d, *J* = 11.8 Hz), 5.05 (2H, s), 5.10 (1H, m), 6.78-6.82 (3H, m), 7.18 (1H, t, *J* = 7.8 Hz), 7.26-7.45 (10H, m); ^{13}C NMR (125 MHz, $CDCl_3$, 0.014 M) ppm: δ 4.9 (3C), 6.8 (3C), 13.3, 21.9, 24.9, 25.6, 26.6, 27.1, 31.3, 33.5, 34.4, 35.6, 36.0, 37.1, 37.1, 41.0, 64.8, 67.5, 69.2, 70.0, 70.2, 70.9, 77.6, 101.6, 111.9, 115.2, 121.2, 127.5 (2C), 127.6, 127.8 (2C), 127.9, 128.4 (2C), 128.6 (2C), 129.2, 137.3, 138.5, 144.5, 158.9, 171.7, 172.3; IR (KBr) cm^{-1}: 3424, 2928, 1712, 1647, 1449, 1163, 1085; HR-FAB-MS (matrix, *m*-nitrobenzyl alcohol) *m/z*: 839.4537 ([M+Na]$^+$ Calcd. for $C_{48}H_{68}O_9SiNa$ 839.4530); $[\alpha]_D$ +23.4° (*c* = 0.10, $CHCl_3$, 28.5 °C).

To a solution of **13a** (19.7 mg, 24.1 μmol) in THF (2 mL) was added a freshly prepared solution of buffered HF·pyridine (500 μL : prepared by adding 75 μL of HF·pyridine to 150 μL of pyridine in 600 μL of THF) at 4 °C. The reaction mixture was stood in a refrigerator for 22 h, then diluted with H_2O (4 mL) and warmed at room temperature. The mixture was extracted with $CHCl_3$ (6 mL x 3). The combined organic layers were washed with brine, dried over Na_2SO_4, filtered, and concentrated *in vacuo*. The residue was purified by column chromatography (silica gel, 10% → 50% EtOAc/hexane containing 0.1% AcOH) to afford a *seco*-acid (14.1 mg, 20.1 μmol, 83%) as a clear oil.

To a solution of the *seco*-acid (12.7 mg, 18.1 μmol) and Et_3N (7.6 μL, 54.6 μmol, 3 equiv.) in toluene (1.7 mL) was added 2,4,6-trichlorobenzoyl chloride (5.6 μL, 39.0 μmol, 2.2 equiv.) at room temperature. The mixture was stirred at room temperature for 3 h, and then diluted with toluene (11 mL). The supernatant of the mixture was added dropwise to a solution of DMAP (33.3 mg, 273 μmol, 15 equiv.) in toluene (19 mL) over 2.5 h. The anhydride flask was rinsed twice with toluene (4.3 mL) (each rinse was added in one portion to the reaction mixture). After an additional 1 h of stirring at room temperature, H_2O (15 mL) was added and the resulting biphasic mixture was poured into EtOAc (20 mL). The organic layer was separated, and aqueous layer was extracted with EtOAc (20 mL x 3). The combined organic layers were

washed with brine, dried over Na_2SO_4, filtered, and concentrated *in vacuo*. The residue was purified by column chromatography (silica gel, 7.5% EtOAc/hexane) to afford **14a** (8.1 mg, 11.8 μmol, 65%) as a clear oil. ^{1}H NMR (500 MHz, $CDCl_3$, 0.011 M) ppm: δ 0.86 (3H, s), 0.98 (3H, s), 1.14 (3H, d, *J* = 6.4 Hz), 1.33-1.69 (13H, m), 2.34 (1H, dd, *J* = 12.5, 10.9 Hz), 2.43 (1H, br. d, *J* = 15.5 Hz), 2.47 (1H, dd, *J* = 12.5, 2.7 Hz), 2.60 (2H, t, *J* = 7.8 Hz), 2.70 (1H, dd, *J* = 16.9, 3.0 Hz), 2.80 (1H, dd, *J* = 16.9, 11.6 Hz), 3.82-3.88 (2H, m), 4.16 (1H, m), 4.52 (1H, d, *J* = 11.8 Hz), 4.65 (1H, d, *J* = 11.8 Hz), 5.05 (2H, s), 5.17 (1H, m), 5.25 (1H, m), 6.77-6.85 (3H, m), 7.18 (1H, t, *J* = 7.8 Hz), 7.27-7.44 (10H, m); ^{13}C NMR (125 MHz, $CDCl_3$, 0.011 M) ppm: δ 14.2, 21.2, 24.9, 25.4, 25.9, 27.3, 31.2, 34.6, 34.7 34.8, 35.6, 36.0, 36.8, 42.7, 63.7, 68.6, 69.9, 70.5, 70.6, 71.4, 73.8, 100.0, 111.8, 115.2, 121.2, 127.5 (2C), 127.7, 127.7 (2C), 127.8, 128.4 (2C), 128.5 (2C), 129.1, 137.4, 138.4, 144.7, 158.9, 170.1, 170.6; IR (KBr) cm^{-1}: 2937, 1725, 1448, 1264, 1067; HR-FAB-MS (matrix, *m*-nitrobenzyl alcohol) *m/z*: 685.3716 ([M+H]$^+$ Calcd. for $C_{42}H_{53}O_8$ 685.3740); $[\alpha]_D$ +16.4 º (*c* = 0.39, $CHCl_3$, 15.6ºC).

To 10% Pd-C (wet support, Degussa type E101 NE/W, Aldrich) (4.0 mg) in a flask was added a solution of **14a** (8.0 mg, 11.7 μmol) in EtOH (1.2 mL) at room temperature. The mixture was vigorously stirred under a H_2 atmosphere at room temperature for 2 h. The mixture was filtered, and the filtrate was concentrated *in vacuo*. The residue was purified by HPLC (column, YMC-Pack SIL SL12S05-2510WT; solvent, *i*-PrOH/$CHCl_3$/hexane = 5:15:80, flow rate, 3.0 mL/min; pressure, 420 psi; UV detector, 254 nm; retention time, 17.2 min) to afford **2** (4.9 mg, 9.7 μmol, 83 %) as a clear oil. ^{1}H NMR (500 MHz, $CDCl_3$, 0.0040 M) ppm: δ 0.87 (3H, s, H_3-22 or 23), 0.98 (3H, s, H_3-22 or 23), 1.21 (3H, d, *J* = 6.5 Hz, H_3-28), 1.26-1.71 (13H, m, H_2-4, H_2-5, H-8a, H_2-10, H_2-12, H_2-13, H_2-14), 2.44 (1H, dd, *J* = 13.0, 10.8 Hz, H-2a), 2.49-2.53 (2H, m, H-8b, OH), 2.56-2.59 (3H, m, H-2b, H_2-15), 2.73 (1H, dd, *J* = 16.5, 10.3 Hz, H-25a), 2.79 (1H, dd, *J* = 16.5, 4.0 Hz, H-25b), 3.90 (1H, m, H-3), 4.01 (1H, m, H-27), 4.25 (1H, m, H-11), 5.08 (1H, ddd, *J* = 10.3, 5.2, 4.0 Hz, H-26), 5.17 (1H, m, H-9), 6.35 (1H, br. s, Ph-OH), 6.68 (1H, dd, *J* = 8.1, 1.9 Hz, H-19), 6.73 (1H, d, *J* = 7.6 Hz, H-21), 6.83 (1H, t, *J* = 1.8 Hz, H-17), 7.14 (1H, t, *J* = 7.8 Hz, H-20); ^{13}C NMR (125 MHz, $CDCl_3$, 0.0040 M) ppm: δ 18.5 (C-28), 21.2 (C-22 or 23), 24.0 (C-13), 25.3 (C-8), 25.9 (C-22 or 23), 27.4 (C-4), 29.6 (C-14), 34.4 (C-5 or 12), 34.7 (C-5 or 12), 34.9 (C-10 or 15), 35.1 (C-10 or 15), 36.0 (C-25), 36.9 (C-6), 42.8 (C-2), 63.0 (C-11), 68.5 (C-27), 69.1 (C-9), 70.6 (C-3), 74.5 (C-26), 100.4 (C-7), 112.6 (C-19), 115.1 (C-17), 120.7 (C-21), 129.4 (C-20), 144.6 (C-16), 156.2 (C-18), 170.0 (C-24), 172.5 (C-1); IR (KBr) cm^{-1}: 3439, 2933, 1716, 1629, 1449, 1291, 1068; HR-FAB-MS (matrix, glycerol) *m/z*: 505.2806 ([M+H]$^+$ Calcd. for $C_{28}H_{41}O_8$ 505.2801); $[\alpha]_D$ +44.0º (*c* = 0.085, $CHCl_3$, 24.5 ºC).

Synthesis of 27-(*S*)-methyl-aplog-1 (3)

To a solution of **7a** (381 mg, 1.16 mmol), *p*-nitrobenzoic acid (581 mg, 3.48 mmol, 3 equiv.),

and Ph_3P (911 mg, 3.48 mmol, 3 equiv.) in THF (6 mL) was added 1.9 M diisopropyl azodicarboxylate in toluene (1.83 mL, 3.48 mmol, 3 equiv.) at 0 ºC. The reaction mixture was stirred at room temperature for 21 h, and the reaction was quenched with saturated aq. $NaHCO_3$ (6 mL). After the organic layer was separated, the aqueous layer was extracted with EtOAc (10 mL x 3). The combined organic layer was washed with brine, dried over Na_2SO_4, filtered, and concentrated *in vacuo*. The residue was purified by column chromatography (silica gel, 2% → 5% → 7% → 10% EtOAc/hexane) to afford an ester (403 mg, 0.845 mmol, 73%) as a clear oil.

To a solution of the ester (435 mg, 0.912 mmol) in THF (4.0 mL), MeOH (1.8 mL) and H_2O (2.4 mL) was added NaOH (91.0 mg, 2.28 mmol, 2.5 equiv.) at 0 ºC. The reaction mixture was stirred at room temperature for 12 h, and then diluted with H_2O (10 mL). The mixture was extracted with EtOAc (20 mL x 3). The combined organic layer was washed with brine, dried over Na_2SO_4, filtered, and concentrated *in vacuo*. The residue was purified by column chromatography (silica gel, 20% EtOAc/hexane) to afford **7b** (279 mg, 0.851 mmol, 93%) as a clear oil. ^{1}H NMR (400 MHz, $CDCl_3$, 0.046 M) ppm: δ 1.15 (3H, d, *J* = 6.5 Hz), 1.83-1.92 (2H, m), 1.98-2.14 (3H, m), 2.73-2.91 (4H, m), 3.66 (1H, dt, *J* = 9.5, 3.2 Hz), 3.81 (3H, s), 4.03 (1H, m), 4.13 (1H, dd, *J* = 10.1 4.4 Hz), 4.53 (1H, d, *J* = 11.0 Hz), 4.60 (1H, d, *J* = 11.0 Hz), 6.88-6.92 (2H, m), 7.28-7.31 (2H, m); ^{13}C NMR (100 MHz, $CDCl_3$, 0.046 M) ppm: δ 17.7, 26.0, 30.0, 30.5, 34.7, 44.0, 55.3, 67.6, 72.2, 79.2, 113.9 (2C), 129.6 (2C), 130.5, 159.4; IR (KBr) cm^{-1}: 3435, 2921, 1626, 1513, 1247, 1065, 817; HR-FAB-MS (matrix, *m*-nitrobenzyl alcohol) *m/z*: 329.1255 ([M+H]$^+$ Calcd. for $C_{16}H_{25}O_3S_2$ 329.1245); $[\alpha]_D$ +28.9º (*c* = 0.74, $CHCl_3$, 25.1 ºC).

Compound **7b** was treated in a manner similar to that described for the synthesis of **8a** to give **8b** (49%). ^{1}H NMR (500 MHz, $CDCl_3$, 0.0043 M) ppm: δ 1.21 (3H, d, *J* = 6.4 Hz), 1.85-1.93 (2H, m), 2.03 (1H, m), 2.10 (1H, m), 2.72-2.87 (4H, m), 3.64 (1H, m), 3.79 (1H, m), 3.81 (3H, s), 4.14 (1H, dd, *J* = 10.0, 4.6 Hz), 4.50 (1H, d, *J* = 11.0 Hz), 4.58 (1H, d, *J* = 12.0 Hz), 4.62 (1H, d, *J* = 12.0 Hz), 4.66 (1H, d, *J* = 11.0 Hz), 6.86-6.89 (2H, m), 7.25-7.37 (7H, m); ^{13}C NMR (125 MHz, $CDCl_3$, 0.0043 M) ppm: δ 15.7, 26.1, 30.0, 30.4, 37.1, 44.3, 55.3, 71.1, 72.6, 76.7, 78.3, 113.8 (2C), 127.5, 127.6 (2C), 128.3 (2C), 129.6 (2C), 131.1, 138.9, 159.2; IR (KBr) cm^{-1}: 2899, 1614, 1515, 1463, 1246, 1039, 819; HR-FAB-MS (matrix, glycerol); *m/z*: 419.1734 ([M+H]$^+$ Calcd. for $C_{23}H_{31}O_3S_2$ 419.1715); $[\alpha]_D$ = +8.8º (*c* = 0.19, $CHCl_3$, 9.8 ºC).

Compound **8b** was treated in a manner similar to that described for the synthesis of **9a** to give **9b** (87%). ^{1}H NMR (500 MHz, $CDCl_3$, 0.013 M) ppm: δ 1.23 (3H, d, *J* = 5.5 Hz), 2.60 (1H, ddd, *J* = 16.5, 4.8, 2.1 Hz), 2.74 (1H, ddd, *J* = 16.5, 7.1, 2.2 Hz), 3.65 (1H, m), 3.80 (3H, s), 3.91 (1H, dt, *J* = 7.1, 4.8 Hz), 4.52 (1H, d, *J* = 11.0 Hz), 4.53 (1H, d, *J* = 11.9 Hz), 4.56 (1H, d, *J* = 11.0 Hz), 4.62 (1H, d, *J* = 11.9 Hz), 6.85-6.88 (2H, m), 7.22-7.36 (7H, m), 9.75 (1H, t, *J* = 2.2 Hz); ^{13}C NMR (125 Hz, $CDCl_3$, 0.013 M) ppm: δ 16.2, 45.3, 55.3, 71.2, 72.0, 76.1, 77.6, 113.9 (2C), 127.6, 127.7 (2C), 128.4 (2C), 129.5 (2C), 130.2, 138.4, 159.4, 201.1; IR (KBr) cm^{-1}: 2871,

1723, 1615, 1515, 1463, 1247, 1173, 821; HR-FAB-MS (matrix, glycerol); *m/z*: 329.1761 ($[M+H]^+$ Calcd. for $C_{20}H_{25}O_4$ 329.1753); $[a]_D$ +31.6º (*c* = 0.21, $CHCl_3$, 10.9 ºC).

Compound **9b** was treated in a manner similar to that described for the synthesis of **10a** to give **10b** (88%). ^1H NMR (400 MHz, $CDCl_3$, 0.074 M) ppm: δ 1.23 (3H, d, *J* = 6.3 Hz), 2.64 (1H, dd, *J* = 15.9, 5.2 Hz), 2.69 (1H, dd, *J* = 15.9, 6.8 Hz), 3.64 (1H, m), 3.78 (3H, s), 3.85 (1H, m), 4.54 (1H, d, *J* = 11.8 Hz), 4.57 (2H, s), 4.62 (1H, d, *J* = 11.8 Hz), 6.83-6.86 (2H, m), 7.22-7.33 (7H, m); ^{13}C NMR (100 MHz, $CDCl_3$, 0.074 M) ppm: δ 16.1, 36.4, 55.3, 71.2, 72.4, 76.0, 78.6, 113.8 (2C), 127.6, 127.7 (2C), 128.4 (2C), 129.6 (2C), 130.1, 138.3, 159.3, 176.7; IR (KBr) cm^{-1}: 3430, 2929, 1710, 1647, 1518, 1249, 1068, 820; HR-FAB-MS (matrix, glycerol) *m/z*: 345.1708 ($[M+H]^+$ Calcd. for $C_{20}H_{25}O_5$ 345.1702); $[\alpha]_D$ +14.5º (*c* = 1.27, $CHCl_3$, 25.3 ºC).

Compound **11**[38] and **10** were treated in a manner similar to that described for the synthesis of **12a** to give **12b** quantitatively. ^1H NMR (400 MHz, $CDCl_3$, 0.0037 M) ppm: δ 0.86 (3H, s), 0.96 (3H, s), 1.22 (3H, d, *J* = 6.3 Hz), 1.35-1.67 (13H, m), 2.17-2.27 (2H, m), 2.35, (1H, m), 2.56 (2H, t, *J* = 7.8 Hz), 2.55-2.67 (2H, m), 3.45 (1H, m), 3.60 (1H, m), 3.78 (3H, s), 3.95 (1H, m), 4.21 (1H, m), 4.51-4.62 (4H, m), 4.96-4.99 (2H, m), 5.04 (2H, s), 5.09 (1H, m), 5.82 (1H, m), 6.78-6.85 (5H, m), 7.16-7.45 (13H, m); ^{13}C NMR (100 MHz, $CDCl_3$, 0.0037 M) ppm: δ 16.0, 21.6, 24.8, 25.5, 26.4, 26.7, 31.3, 34.1, 34.6, 35.6, 36.0, 36.9, 37.2, 41.0, 55.3, 63.9, 68.2, 69.9, 71.0, 71.7, 72.6, 76.4, 79.1, 100.0, 111.7, 113.7 (2C), 115.1, 116.6, 121.2, 127.4, 127.5 (2C), 127.5 (2C), 127.9, 128.3 (2C), 128.5 (2C), 129.2, 129.4 (2C), 130.7, 135.2, 137.2, 138.7, 144.6, 158.9, 159.2, 172.1; IR (KBr) cm^{-1}: 2936, 1725, 1515, 1455, 1250, 1068; HR-FAB-MS (matrix, *m*-nitrobenzyl alcohol) *m/z*: 827.4497 ($[M+Na]^+$ Calcd. for $C_{51}H_{64}O_8Na$ 827.4499); $[\alpha]_D$ +11.7º (*c* = 0.12, $CHCl_3$, 28.1 ºC).

Compound **12b** was treated in a manner similar to that described for the synthesis of **13a** to give **13b** (32% in three steps). ^1H NMR (400 MHz, $CDCl_3$, 0.0042 M) ppm: δ 0.61 (6H, q, *J* = 7.9 Hz), 0.89 (3H, s), 0.93 (9H, t, *J* = 7.9 Hz), 0.97 (3H, s), 1.18 (3H, d, *J* = 6.3 Hz), 1.31-1.75 (13H, m), 2.12 (1H, br. d, *J* =14.2 Hz), 2.48-2.63 (6H, m), 3.47 (1H, m), 3.91 (1H, m), 4.09 (1H, m), 4.17 (1H, dt, *J* = 7.8, 4.5 Hz), 4.54 (1H, d, *J* = 11.9 Hz), 4.62 (1H, d, *J* = 11.9 Hz), 5.05 (2H, s), 5.08 (1H, m), 6.78-6.82 (3H, m), 7.18 (1H, t, *J* = 7.8 Hz), 7.26-7.45 (10H, m); ^{13}C NMR (125 MHz, $CDCl_3$, 0.017 M) ppm: δ 5.1 (3C), 6.9 (3C), 15.7, 22.1, 24.9, 25.5, 26.6, 27.3, 31.3, 33.3, 34.4, 35.6, 36.0, 37.0, 39.7, 41.1, 64.8, 67.5, 69.2, 70.0, 71.1, 72.7, 78.6, 101.6, 111.9, 115.2, 121.2, 127.5, 127.5 (2C), 127.6 (2C), 127.9, 128.3 (2C), 128.5 (2C), 129.2, 137.3, 138.7, 144.5, 158.9, 171.9 (2C); IR (KBr) cm^{-1}: 3440, 2939, 1713, 1646, 1449, 1158, 1091; HR-FAB-MS (matrix, *m*-nitrobenzyl alcohol) *m/z*: 839.4537 ($[M+Na]^+$) Calcd. for $C_{48}H_{68}O_9SiNa$ 839.4530); $[\alpha]_D$ +20.1º (*c* = 0.18, $CHCl_3$, 28.4 ºC)

Compound **13b** was treated in a manner similar to that described for the synthesis of **14a** to give **14b** (58% in two steps). ^1H NMR (500 MHz, $CDCl_3$, 0.013 M) ppm: δ 0.86 (3H, s), 0.98

(3H, s), 1.19 (3H, d, *J* = 6.5 Hz), 1.27-1.67 (13H, m), 2.34 (1H, dd, *J* = 12.6, 10.9 Hz), 2.43 (1H, dd, *J* = 12.6, 2.8 Hz), 2.48 (1H, br. d, *J* = 15.5 Hz), 2.59 (2H, t, *J* = 7.8 Hz), 2.72 (1H, dd, *J* = 16.8, 3.0 Hz), 2.95 (1H, dd, *J* = 16.8, 11.6 Hz), 3.82-3.88 (2H, m), 4.16 (1H, m), 4.52 (1H, d, *J* = 11.9 Hz), 4.57 (1H, d, *J* = 11.9 Hz), 5.03 (1H, m), 5.05 (2H, s), 5.16 (1H, br. s), 6.78-6.84 (3H, m), 7.18 (1H, t, *J* = 7.9 Hz), 7.27-7.45 (10H, m); ^{13}C NMR (125 MHz, $CDCl_3$, 0.013 M) ppm: δ 16.5, 21.3, 24.8, 25.3, 25.9, 27.3, 31.2, 34.5, 34.7 (2C), 35.6, 36.0, 36.9, 42.8, 63.7, 68.7, 70.0, 70.6, 71.8, 73.2, 75.2, 100.1, 111.8, 115.2, 121.2, 127.5 (2C), 127.6 (3C), 127.9, 128.3 (2C), 128.5 (2C), 129.1, 137.4, 138.5, 144.7, 158.9, 170.2, 170.6; IR (KBr) cm^{-1}: 2937, 1726, 1447, 1265, 1067; HR-FAB-MS (matrix, *m*-nitrobenzyl alcohol) *m/z*: 685.3737 ([M+H]$^+$ Calcd. for $C_{42}H_{53}O_8$ 685.3740); $[\alpha]^D$ +43.4º (*c* = 0.44, $CHCl_3$, 19.7 ºC)

Compound **14b** was treated in a manner similar to that described for the synthesis of **2** to give **3** (77%). ^{1}H NMR (500 MHz, $CDCl_3$, 0.0079 M) ppm: δ 0.87 (3H, s, H_3-22 or 23), 0.97 (3H, s, H_3-22 or 23), 1.18 (3H, d, *J* = 6.6 Hz, H_3-28), 1.34-1.72 (13H, m, H_2-4, H_2-5, H-8a, H_2-10, H_2-12, H_2-13, H_2-14), 2.44 (1H, dd, *J* = 13.2, 10.9 Hz, H-2a), 2.50-2.54 (2H, m, H-8b, OH), 2.57 (2H, t, *J* = 7.8 Hz, H_2-15), 2.59 (1H, dd, *J* = 13.2, 2.9 Hz, H-2b), 2.68 (1H, dd, *J* = 16.5, 3.0 Hz, H-25a), 2.86 (1H, dd, *J* = 16.5, 11.5 Hz, H-25b), 3.91 (1H, tt, *J* = 11.0, 2.9 Hz, H-3), 4.11 (1H, m, H-27), 4.25 (1H, m, H-11), 5.12 (1H, dt, *J* = 11.5, 3.0 Hz, H-26), 5.17 (1H, m, H-9), 6.29 (1H, br. s, Ph-OH), 6.68 (1H, dd, *J* = 8.1, 2.0 Hz, H-19), 6.72 (1H, d, *J* = 7.6 Hz, H-21), 6.82 (1H, t, *J* = 1.8 Hz, H-17), 7.13 (1H, t, *J* = 7.8 Hz, H-20); ^{13}C NMR (125 MHz, $CDCl_3$, 0.0079 M) ppm: δ 18.1 (C-28), 21.2 (C-22 or 23), 24.3 (C-13), 25.2 (C-8), 25.9 (C-22 or 23), 27.3 (C-4), 29.6 (C-14), 34.6 (C-5 or 12), 34.6 (C-5 or 12), 34.9 (C-10 or 25), 35.0 (C-10 or 25), 35.2 (C-15), 36.9 (C-6), 42.9 (C-2), 62.9 (C-11), 68.4 (C-27), 69.0 (C-9), 70.6 (C-3), 75.4 (C-26), 100.4 (C-7), 112.6 (C-19), 115.0 (C-17), 120.7 (C-21), 129.4 (C-20), 144.6 (C-16), 156.3 (C-18), 169.9 (C-24), 172.4 (C-1); IR (KBr) cm^{-1}: 3430, 2937, 1717, 1539, 1455, 1291, 1068; HR-FAB-MS (matrix, glycerol) *m/z*: 505.2799 ([M+H]$^+$ Calcd. for $C_{28}H_{41}O_8$ 505.2801); $[\alpha]_D$ +49.8º (*c* = 0.18, $CHCl_3$, 24.7 ºC).

Synthesis of 27-*O*-methyl-aplog-1 (4)

Compound **9c** prepared as reported[70] was treated in a manner similar to that described for the synthesis of **10a** to give **10c** (95%). ^{1}H NMR (400 MHz, $CDCl_3$, 0.21 M) ppm: δ 2.61 (1H, dd, *J* = 15.9, 7.1 Hz), 2.66 (1H, dd, *J* = 15.9, 5.6 Hz), 3.37 (3H, s), 3.44 (1H, dd, *J* = 10.1, 5.2 Hz), 3.51 (1H, dd, *J* = 10.1, 5.0 Hz), 3.78 (3H, s), 4.01 (1H, m), 4.56 (1H, d, *J* = 11.2 Hz), 4.60 (1H, d, *J* = 11.2 Hz), 6.84-6.87 (2H, m), 7.24-7.27 (2H, m); ^{13}C NMR (100 MHz, $CDCl_3$, 0.21 M) ppm: δ 37.3, 55.3, 59.3, 72.1, 74.0 (2C), 113.8 (2C), 129.5 (2C), 130.1, 159.3, 176.9; IR (KBr) cm^{-1}: 3440, 2929, 1712, 1617, 1514, 1247, 1035, 824; HR-FAB-MS (matrix, glycerol) *m/z*: 225.1230 ([M+H]$^+$ Calcd. for $C_{13}H_{19}O_5$ 255.1232); $[\alpha]_D$ +14.5º (*c* = 0.48, $CHCl_3$, 7.4 ºC).

Compound **11**[38] and **10c** were treated in a manner similar to that described for the synthesis

of **12a** to give **12c** quantitatively. ^{1}H NMR (400 MHz, $CDCl_3$, 0.011 M) ppm: δ 0.87 (3H, s), 0.97 (3H, s), 1.33-1.68 (13H, m), 2.20-2.27 (2H, m), 2.35 (1H, m), 2.53-2.63 (4H, m), 3.35 (3H, s), 3.41 (1H, dd, *J* = 10.0, 5.0 Hz), 3.45 (1H, m), 3.48 (1H, dd, *J* = 10.0, 5.2 Hz), 3.78 (3H, s), 4.04 (1H, m), 4.21 (1H, m), 4.54 (1H, d, *J* = 11.2 Hz), 4.59 (1H, d, *J* = 11.2 Hz), 4.99-5.06 (2H, m), 5.04 (2H, s), 5.12 (1H, m), 5.84 (1H, m), 6.77-6.87 (5H, m), 7.18 (1H, t, *J* = 7.8 Hz), 7.23-7.45 (7H, m); ^{13}C NMR (100 MHz, $CDCl_3$, 0.011 M) ppm: δ 21.5, 24.8, 25.5, 26.5, 26.7, 31.3, 34.2, 34.6, 35.6, 36.0, 36.9, 38.0, 41.1, 55.3, 59.2, 63.9, 68.2, 69.9, 71.7, 72.0, 74.4, 74.6, 100.0, 111.7, 113.7 (2C), 115.1, 116.6, 121.2, 127.5 (2C), 127.9, 128.5 (2C), 129.2, 129.4 (2C), 130.6, 135.2, 137.2, 144.6, 158.8, 159.2, 171.6; IR (KBr): 2935, 1726, 1515, 1454, 1249, 1072; HR-FAB-MS (matrix, *m*-nitrobenzyl alcohol) *m/z*: 714.4132 ($[M]^+$ Calcd. for $C_{44}H_{58}O_8$ 714.4132); $[\alpha]_D$ +17.6° (*c* = 0.37, $CHCl_3$, 26.8 °C).

Compound **12c** was treated in a manner similar to that described for the synthesis of **13a** to give an alcohol (91%). To a solution of the alcohol (101 mg, 0.170 mmol) in THF (1.7 mL) were added imidazole (34.7 mg, 0.510 mmol, 3 equiv.) and TES-Cl (34 μL, 0.203 mmol, 1.2 equiv.) at room temperature. After stirring at room temperature for 4 h, the reaction was quenched with brine (2.5 mL). The resulting mixture was extracted with EtOAc (4 mL x 3). The combined organic layers were washed with brine, dried over Na_2SO_4, filtered, and concentrated *in vacuo*. The residue was purified by column chromatography (silica gel, 1% → 2% EtOAc/hexane) to afford a silyl ether (108 mg, 0.153 mmol, 90%) as a clear oil.

To a suspension of $NaIO_4$ (41.5 mg, 0.194 mmol, 8 equiv.) in pH 7.2 phosphate buffer (2 mL) was added $KMnO_4$ (3.8 mg 24.1 μmol, 1equiv.) in one portion. After 10 min of stirring at room temperature under an Ar atmosphere, the mixture was added to a solution of the silyl ether (17.2 mg, 24.3 μmol) in *t*-BuOH (2 mL). The reaction mixture was stirred at room temperature for 1 h, and the reaction was quenched with $Na_2S_2O_3$ (11.5 mg). The resulting mixture was poured into EtOAc (10 mL) and water (10 mL). The organic layer was separated, and the aqueous layers were washed with brine, dried over Na_2SO_4, filtered, and concentrated *in vacuo*. The residue was purified by column chromatography (silica gel, 5% → 10% EtOAc/hexane containing 0.5% AcOH) to afford **13c** (11.6 mg, 16.0 μmol, 66%) as a clear oil. ^{1}H NMR (500 MHz, $CDCl_3$, 0.017 M) ppm: δ 0.60 (6H, q, *J* = 7.8 Hz), 0.92 (3H, s), 0.93 (9H, t, *J* = 7.9 Hz), 0.99 (3H, s), 1.36-1.77 (13H, m) 2.23 (1H, br. d, *J* = 15.7 Hz), 2.49 (1H, dd, *J* = 15.3, 8.4 Hz), 2.54 (1H, dd, *J* = 15.3, 4.5 Hz), 2.57-2.65 (4H, m), 3.30 (1H, dd, *J* = 9.5, 6.4 Hz), 3.36 (3H, s), 3.39 (1H, dd, *J* = 9.5, 5.1 Hz), 4.01 (1H, m), 4.13 (1H, m), 4.29 (1H, m), 5.05 (2H, s), 5.13 (1H, m), 6.78-6.83 (3H, m), 7.19 (1H, t, *J* = 7.8 Hz), 7.30-7.45 (5H, m); ^{13}C NMR (125 MHz, $CDCl_3$, 0.032 M) ppm: δ 4.9 (3C), 6.8 (3C), 22.3, 24.9, 25.5, 26.6, 27.5, 31.3, 33.3, 34.4, 35.7, 36.0, 37.0, 40.4, 41.3, 59.1, 64.6, 67.6, 68.3, 69.3, 70.0, 76.6, 101.4, 111.9, 115.2, 121.2, 127.5 (2C), 127.9, 128.5 (2C), 129.2, 137.3, 144.5, 158.9, 171.5, 172.6; IR (KBr) cm^{-1}: 3439, 2939, 1726, 1646, 1449, 1160, 1066; HR-

FAB-MS (matrix, *m*-nitrobenzyl alcohol) *m/z*: 726.4154 ([M]$^+$ Calcd. for $C_{41}H_{62}O_9Si$ 726.4163) $[\alpha]_D$ +16.9º (*c* = 0.18, $CHCl_3$, 28.6 ºC).

Compound **13c** was treated in a manner similar to that described for the synthesis of **2** to give a *seco* acid (96%). To a solution of the *seco*-acid (8.4 mg, 13.7 μmol) and Et_3N (5.7 μL, 41.0 μmol, 3 equiv.) in toluene (1.3 mL) was added 2,4,6-trichlorobenzoyl chloride (3.0 μL, 20.9 μmol, 1.5 equiv.) at room temperature. The mixture was stirred at room temperature for 3.5 h, and then diluted with toluene (8.5 mL). The supernatant of the mixture was added dropwise to a solution of DMAP (25.1 mg, 206 μmol, 15 equiv.) in toluene (15 mL) over 3 h. The anhydride flask was rinsed twice with toluene (2.0 mL) (each rinse was added in one portion to the reaction mixture). After an additional 1 h of stirring at room temperature, H_2O (20 mL) was added and the resulting biphasic mixture was poured into EtOAc (20 mL). The organic layer was separated, and the aqueous layer was extracted with EtOAc (20 mL x 3). The combined organic layers were washed with brine, dried over Na_2SO_4, filtered, and concentrated *in vacuo*. The residue was purified by column chromatography (silica gel, 5% → 20% EtOAc/hexane) to afford **14c** (6.2 mg, 10.4 μmol, 76%) as a clear oil. ^{1}H NMR (500 MHz, $CDCl_3$, 0.021 M) ppm: δ 0.86 (3H, s), 0.97 (3H, s), 1.32-1.68 (13H, m), 2.36 (1H, dd, *J* = 12.7, 10.0 Hz), 2.45 (1H, br. d, *J* = 15.6 Hz), 2.52 (1H, dd, *J* = 12.7, 2.7 Hz), 2.59 (2H, t, *J* = 7.7 Hz), 2.71 (1H, dd, *J* = 16.9, 3.1 Hz), 2.86 (1H, dd, *J* = 16.9, 11.5 Hz), 3.36 (3H, s), 3.52 (2H, m), 3.87 (1H, m), 4.17 (1H, m), 5.05 (2H, s), 5.18-5.22 (2H, m), 6.78-6.82 (3H, m), 7.19 (1H, t, *J* = 7.9 Hz), 7.30-7.45 (5H, m); ^{13}C NMR (125 Hz, $CDCl_3$, 0.021 M) ppm: δ 21.2, 24.8, 25.3, 25.9, 27.3, 31.1, 34.7, 34.8, 35.6, 36.0, 36.9, 37.3, 42.8, 59.4, 63.7, 68.5, 68.9, 70.0, 70.6, 72.9, 100.2, 111.9, 115.2, 121.3, 127.5 (2C), 127.9, 128.5 (2C), 129.1, 137.4, 144.7, 158.9, 170.0, 170.3; IR (KBr) cm^{-1}: 2937, 1726, 1448, 1267, 1065; HR-FAB-MS (matrix, *m*-nitrobenzyl alcohol) *m/z*: 595.3265 ([M+H]$^+$ Calcd. for $C_{35}H_{47}O_8$ 595.3271) [a]^D = +38.3º (*c* = 0.94, $CHCl_3$, 10.0 ºC).

To 10% Pd-C (wet support, Degussa type E101 NE/W, Aldrich) (3.0 mg) in a flask was added a solution of **14c** (6.2 mg, 10.4 μmol) in MeOH (0.6 mL) at room temperature. The mixture was vigorously stirred under a H_2 atmosphere at room temperature for 1 h. The mixture was filtered, and the filtrate was concentrated *in vacuo*. The residue was purified by HPLC (column, YMC-Pack SIL SL12S05-2510WT; solvent, *i*-PrOH/$CHCl_3$/hexane = 1:19:80, flow rate, 3.0 mL/min; pressure, 500 psi; UV detector, 254 nm; retention time, 23.3 min) to afford **4** (3.9 mg, 7.7 μmol, 74%) as a clear oil. ^{1}H NMR (500 MHz, $CDCl_3$, 0.0032 M) ppm: δ 0.86 (3H, s, H_3-22 or 23), 0.96 (3H, s, H_3-22 or 23). 1.33-1.73 (13H, m, H_2-4, H_2-5, H-8a, H_2-10, H_2-12, H_2-13, H_2-14), 2.41 (1H, dd, *J* = 13.2, 10.9 Hz, H-2a), 2.47 (1H, br. d, J = 15.6 Hz, H-8b), 2.56 (2H, t, *J* = 7.8 Hz, H_2-15), 2.58 (1H, dd, *J* = 10.4, 2.7 Hz, H-2b), 2.75 (1H, dd, *J* = 16.8, 3.2 Hz, H-25a), 2.89 (1H, dd, *J* = 16.8, 11.3 Hz, H-25b), 3.38 (3H, s, OMe), 3.56 (2H, d, *J* = 4.5 Hz, H_2-27), 3.92 (1H, dt, *J* = 11.0, 2.8 Hz, H-3), 4.27 (1H, m, H-11), 5.20-5.24 (2H, m, H-9, H-26), 6.39 (1H, s, Ph-OH), 6.68

(1H, dd, J = 8.1, 1.7 Hz, H-19), 6.72 (1H, d, J = 7.7 Hz, H-21), 6.86 (1H, br. s, H-17), 7.13 (1H, t, J = 7.8 Hz, H-20); ^{13}C NMR (125 MHz, $CDCl_3$, 0.099 M); δ 21.2 (C-22 or 23), 24.2 (C-13), 25.3 (C-8), 25.9 (C-22 or 23), 27.3 (C-4), 29.5 (C-14), 34.6 (C-5 or 12), 34.6 (C-5 or 12), 35.0 (C-10 or 15), 35.1 (C-10 or 15), 36.9 (C-6), 37.2 (C-25), 42.9 (C-2), 59.4 (OMe), 62.7 (C-11), 68.6 (C-9), 69.7 (C-26), 70.7 (C-3), 72.7 (C-27), 100.3 (C-7), 112.6 (C-19), 115.0 (C-17), 120.6 (C-21), 129.3 (C-20), 144.6 (C-16), 156.4 (C-18), 169.9 (C-24), 171.8 (C-1); IR (KBr) cm^{-1}: 3431, 2935, 1723, 1597, 1456, 1289, 1067; HR-FAB-MS (matrix, glycerol) m/z: 505.2846 ($[M+H]^+$ Calcd. for $C_{28}H_{41}O_8$ 505.2801); $[\alpha]_D$ +54.0º (c = 0.20, $CHCl_3$, 25.9 ºC).

Inhibition of the specific binding of [^{3}H]PDBu to PKCδ and δ-C1B peptide

The binding of [^{3}H]PDBu to PKCδ and δ-C1B peptide was evaluated by the procedure of Sharkey and Blumberg[73] with modifications as reported previously[74] using 50 mM Tris-maleate buffer (pH 7.4 at 4 ºC), 13.8 nM δ-C1B peptide or 3 nM PKCδ, 20 nM [^{3}H]PDBu (18.7 Ci/mmol), 50 μg/mL 1,2-dioleoyl-*sn*-glycero-3-phospho-L-serine sodium salt (Sigma), 3 mg/mL bovine γ-globulin, and various concentrations of an inhibitor. Binding affinity was evaluated based on the concentration required to cause 50% inhibition of the specific binding of [^{3}H]PDBu, the IC_{50}, which was calculated by a computer program with a probit procedure. The inhibition constant, K_i, was calculated by the method of Sharkey and Blumberg.[73]

Activation of PKCδ

The activation of PKCδ was evaluated with the Pep Tag® non-radioactive protein kinase assay (Promega, Tokyo, Japan) according to the manufacturer's instructions. After the reaction had been stopped by heating at 95ºC for 10 min, the samples were loaded on to a 0.8% agarose gel (Nippon Gene, Toyama, japan) which was then quantified by densitometry software (NIH ImageJ, Bethesda, MD).

EBV-EA induction test

Human B-lymphoblastoid Raji cells (5×10^5/mL) were incubated at 37 °C under a 5% CO_2 atmosphere in 1 mL of RPMI 1640 medium (supplemented with 10% fetal bovine serum) with 4 mM sodium *n*-butyrate (a synergist) and 10, 100, or 1000 nM of each test compound. Each test compound was added as 2 μL of a DMSO solution (5, 50, and 500 μM stock solution) along with 2 μL of DMSO; the final DMSO concentration was 0.4%. After 48 h of incubation, smears were made from the cell suspension, and the EBV-EA-expressing cells were stained by a conventional indirect immunofluorescence technique with an NPC patient's serum (a gift from Kobe University, Japan) and FITC-labeled anti-human IgG (DAKO, Glostrup, Denmark) as reported previously.[61,62] In each assay, at least 500 cells were counted and the proportion of the EA-

positive cells was recorded. Cell viability exceeded 60% in all experiments except for that with TPA at 10^{-6} M (>50%).

Measurements of cell growth inhibition

A panel of 39 human cancer cell lines established by Yamori and colleagues[81] according to the NCI method with modifications was employed, and cell growth inhibitory activity was measured as reported previously.[85] In brief, the cells were plated in 96-well plates in RPMI 1640 medium supplemented with 5% fetal bovine serum and allowed to attach overnight. The cells were incubated with each test compound for 48 h. Cell growth was estimated by the sulforhodamine B assay. The 50% growth inhibition (GI_{50}) parameter was calculated as reported previously.[86] Absorbance for the control well (C) and the test well (T) was measured at 525 nm along with that for the test well at time 0 (T_0). Cell growth inhibition (% growth) by each concentration of drug (10^{-8}, 10^{-7}, 10^{-6}, 10^{-5}, and 10^{-4} M) was calculated as $100[(T - T_0)/(C - T_0)]$ when $T > T_0$, and $100[(T - T_0)/T_0]$ when $T < T_0$, using the average of duplicate points. By processing of these values, each GI_{50} value, defined as $100[(T - T_0)/(C - T_0)] = 50$, was determined.

Supporting Information

I. HPLC analyses of **2**, **3**, and **4**

(i) HPLC analysis of **2**

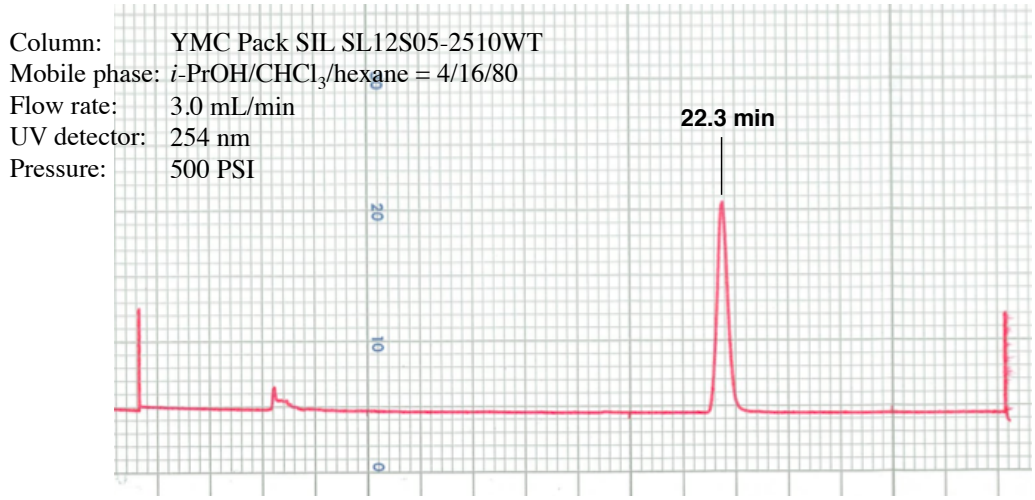

(ii) HPLC analysis of **3**

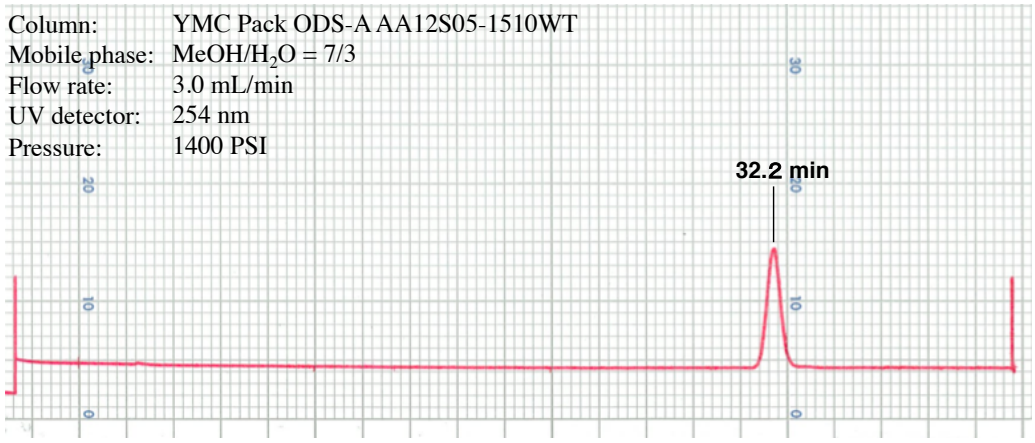

Column: YMC Pack SIL SL12S05-2510WT
Mobile phase: *i*-PrOH/$CHCl_3$/hexane = 4/16/80
Flow rate: 3.0 mL/min
UV detector: 254 nm
Pressure: 500 PSI

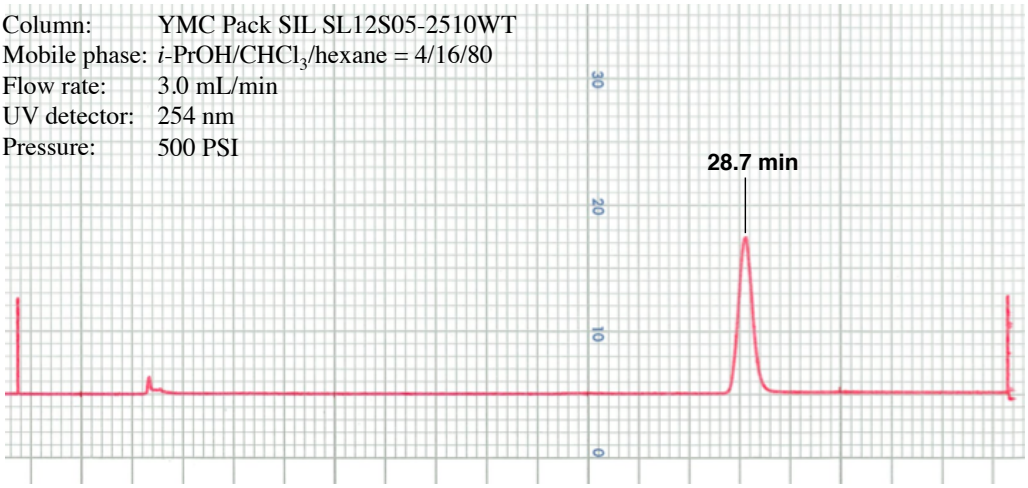

(iii) HPLC analysis of **4**

Column: YMC Pack ODS-A AA12S05-1510WT
Mobile phase: $MeOH/H_2O$ = 7/3
Flow rate: 3.0 mL/min
UV detector: 254 nm
Pressure: 1400 PSI

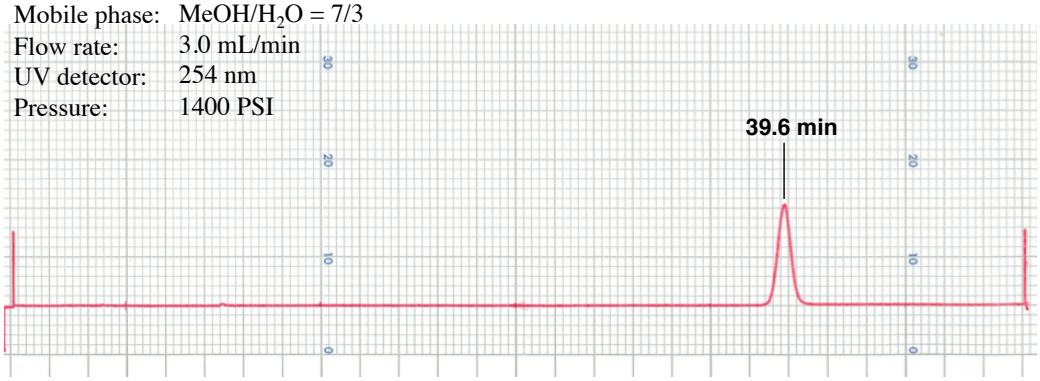

Column: YMC Pack SIL SL12S05-2510WT
Mobile phase: *i*-PrOH/$CHCl_3$/hexane = 1/19/80
Flow rate: 3.0 mL/min
UV detector: 254 nm
Pressure: 500 PSI

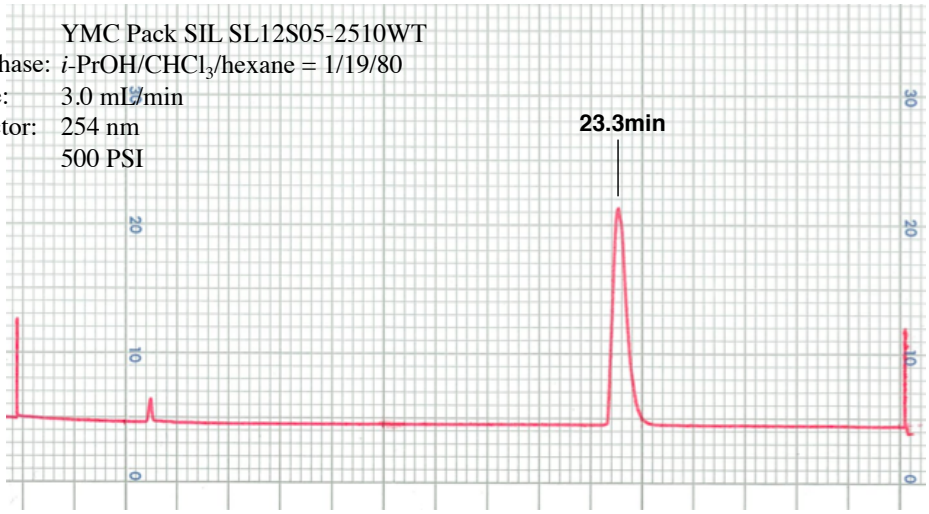

II. NMR spectra of **2**, **3**, and **4**

^{1}H-1D NMR spectrum of **2**
(500 MHz, $CDCl_3$, 0.004 M)

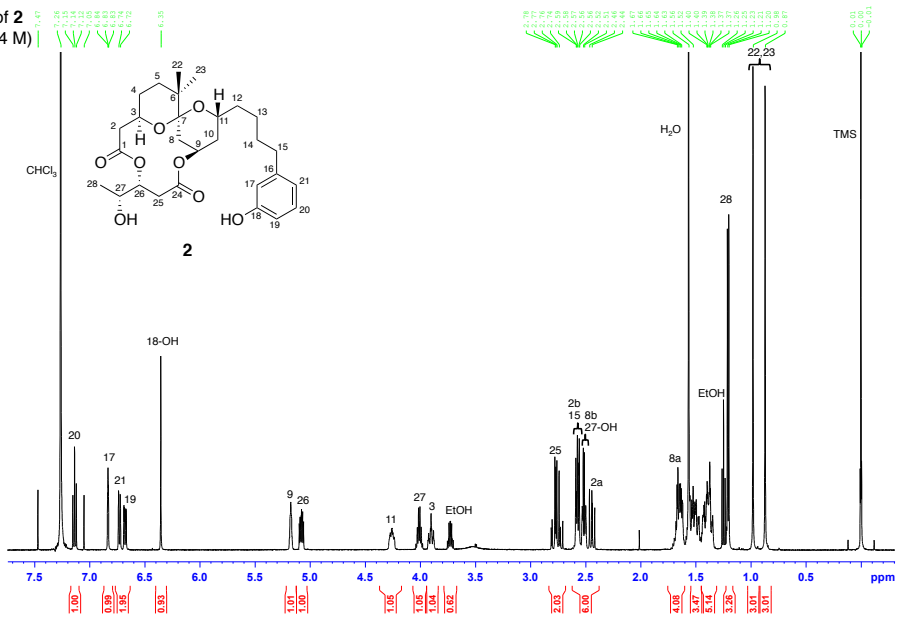

2

^{13}C-1D NMR spectrum of **2**
(125 MHz, $CDCl_3$, 0.004 M)

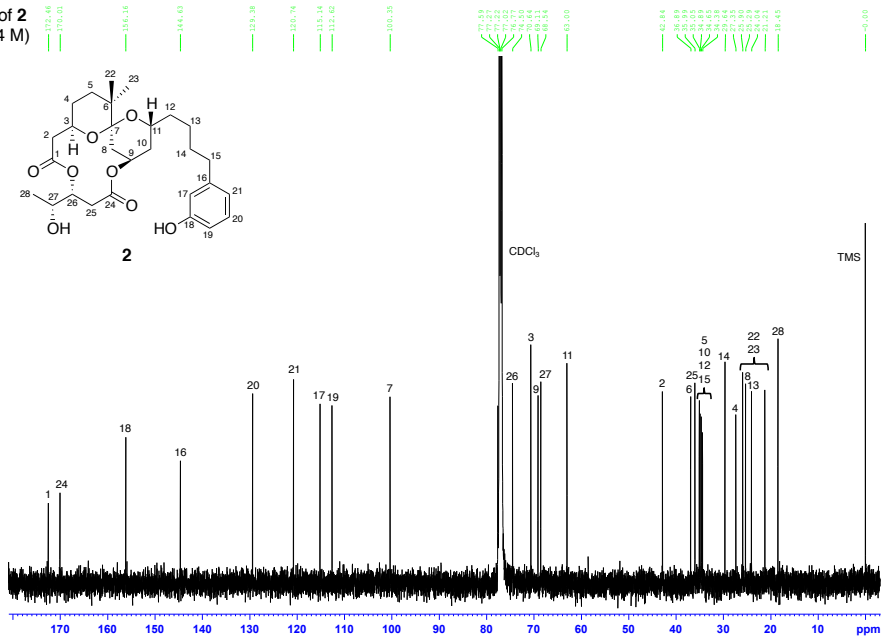

2

^{1}H-1D NMR spectrum of **3**
(500 MHz, $CDCl_3$, 0.008 M)

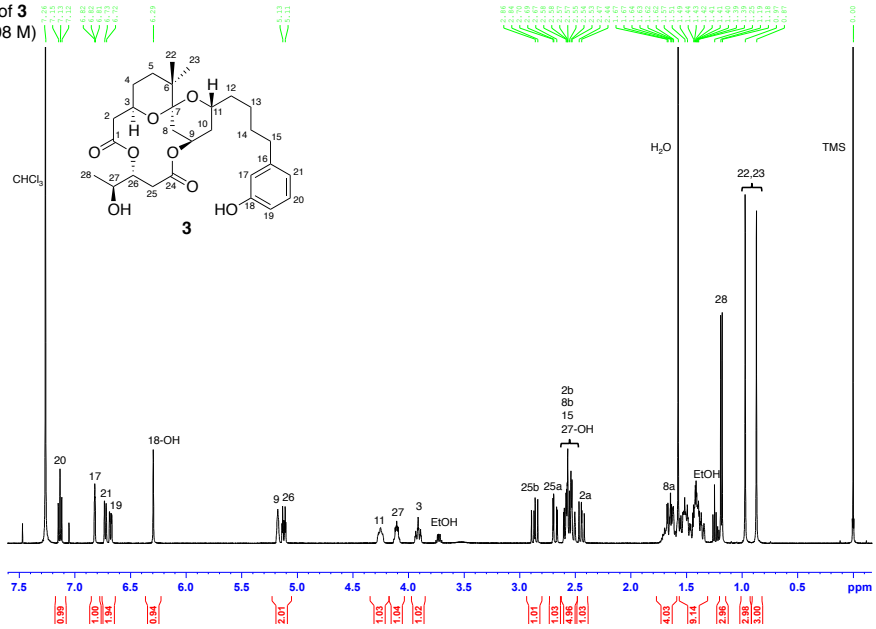

3

^{13}C-1D NMR spectrum of **3**
(125 MHz, $CDCl_3$, 0.008 M)

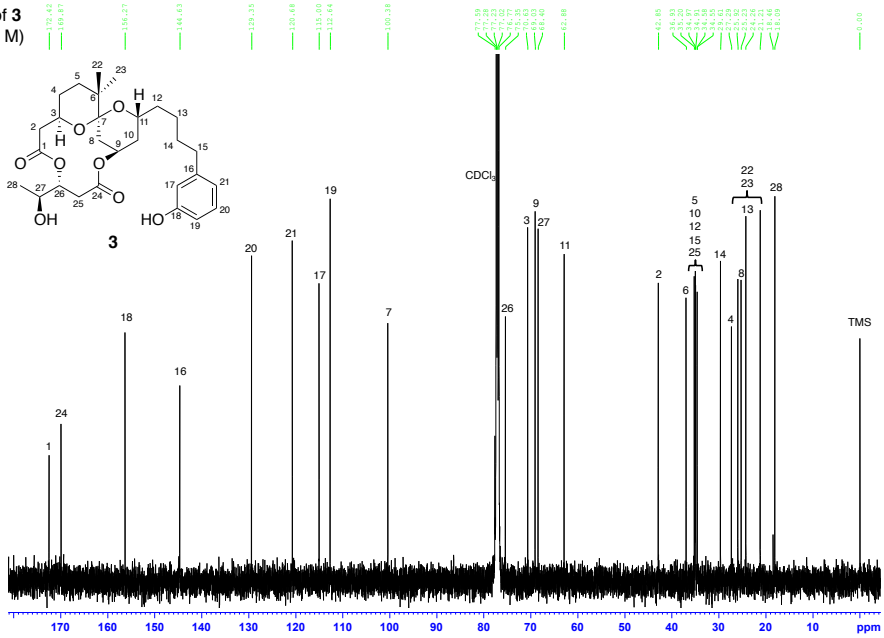

3

^{1}H-1D NMR spectrum of **4**
(500 MHz, $CDCl_3$, 0.003 M)

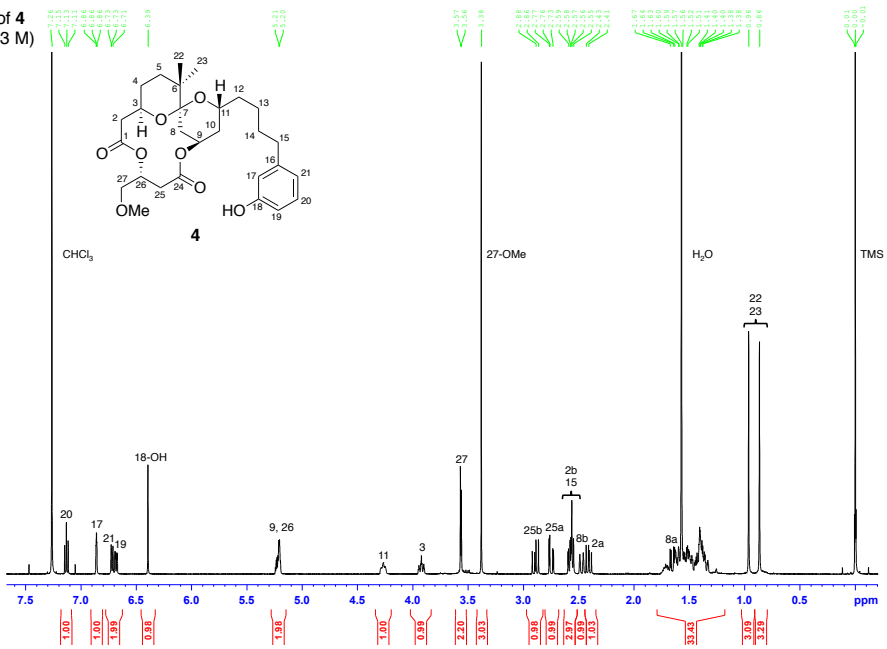

4

^{13}C-1D NMR spectrum of **4**
(125 MHz, $CDCl_3$, 0.099 M)

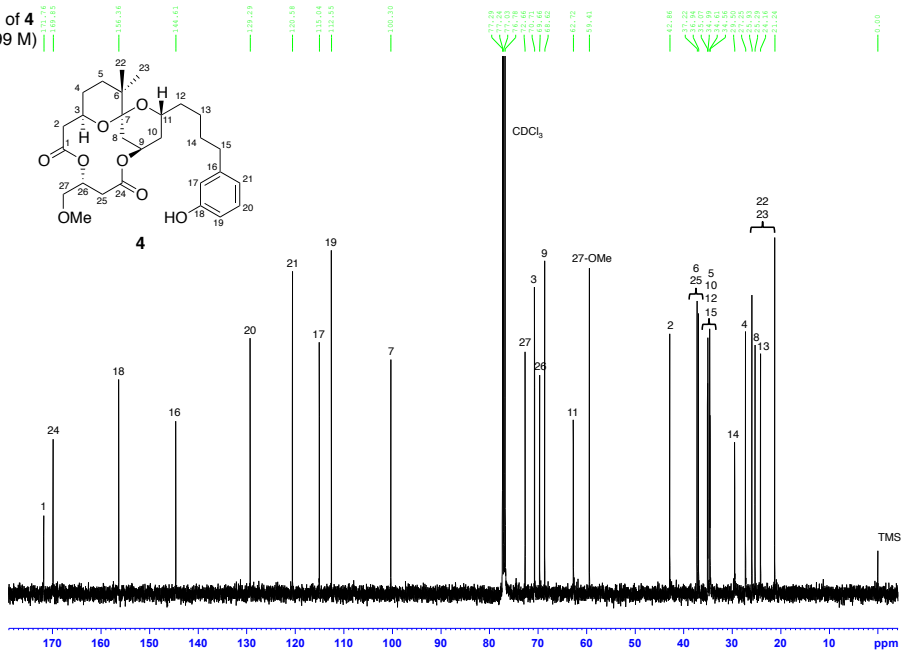

4

III. Growth inhibitory activity of aplog-1, **2**, **3**, and **4** against 39 human cancer cell lines

cancer cell lines		log GI_{50}			
		aplog-1[a]	**2**	**3**	**4**
Breast	HBC-4	–6.33	–6.15	–4.78	–4.71
	BSY-1	–4.87	–4.90	–4.84	–4.86
	HBC-5	–4.76	–4.76	–4.75	–4.76
	MCF-7	–4.72	–4.73	–4.79	–4.88
	MDA-MB-231	–5.61	–5.03	–4.80	–4.50
CNS	U251	–4.83	–5.35	–4.86	–4.78
	SF-268	–4.83	–4.88	–4.94	–4.73
	SF-295	–5.06	–4.72	–4.74	–4.70
	SF-539	–4.97	–4.75	–4.75	–4.69
	SNB-75	–4.80	–4.80	–4.74	–4.74
	SNB-78	–4.72	–5.43	–4.74	–4.69
Colon	HCC2998	–5.43	–5.08	–4.79	–4.70
	KM-12	–4.86	–4.79	–4.74	–4.73
	HT-29	–4.77	–4.77	–4.75	–4.71
	HCT-15	–4.76	–4.80	–4.73	–4.69
	HCT-116	–4.79	–4.82	–4.72	–4.80
Lung	NCI-H23	–4.88	–4.96	–4.67	–4.81
	NCI-H226	–4.81	–4.79	–4.75	–4.79
	NCI-H522	–4.87	–4.76	–4.83	–4.84
	NCI-H460	–5.60	–5.66	–4.78	–4.70
	A549	–5.32	–5.09	–4.80	–4.76
	DMS273	–4.90	–4.79	–4.83	–4.78
	DMS114	–4.79	–4.82	–4.82	–4.88
Melanoma	LOX-IMVI	–5.74	–5.18	–4.76	–4.80
Ovarian	OVCAR-3	–4.78	–4.77	–4.78	–4.83
	OVCAR-4	–4.75	–4.88	–4.82	–4.77
	OVCAR-5	–4.95	–4.94	–4.73	–4.78
	OVCAR-8	–4.71	–4.68	–4.71	–4.80
	SK-OV-3	–4.69	–4.75	–4.70	–4.77
Renal	RXF-631L	–4.79	–4.76	–4.74	–4.79
	ACHN	–4.92	–4.87	–4.73	–4.64
Stomach	St-4	–5.55	–5.17	–4.71	–4.70
	MKN1	–4.86	–4.92	–4.81	–4.79
	MKN7	–4.78	–4.83	–4.79	–4.85
	MKN28	–4.74	–4.83	–4.74	–4.76
	MKN45	–5.33	–4.99	–4.77	–4.75
	MKN74	–4.76	–4.80	–4.76	–4.80
Prostate	DU-145	–4.85	–4.80	–4.73	–4.67
	PC-3	–4.96	–4.88	–4.78	–4.77
MG-MID[b]		–4.98	–4.94	–4.77	–4.76

[a] Nakagawa, Y.; Yanagita, R. C.; Hamada, N.; Murakami, A.; Takahashi, H.; Saito, N.; Nagai, H.; Irie, K. *J. Am. Chem. Soc.* **2009**, *131*, 7573-7579.
[b] MG-MID: average of the log GI_{50} values of each 39 human cancer cell lines

Chapter 2

Structure-Activity Studies on the Phenolic Group of 10-Methyl-Aplog-1*

Introduction

The ester side chain of phorbol esters is indispensable for activating PKC, because its hydrophobicity enhances the interaction between C1 domains of PKC and the cellular membrane. The side chain of DAT has been proposed to play the same role,[67,68] but DAT and 10-methyl-aplog-1 (**1**) are different from phorbol esters in that they have a hydrophilic phenolic group in their side chain. This moiety may play some roles other than the hydrophobic interaction with the cellular membrane. Thus, the author synthesized new derivatives (**15**, **16**) to examine the effects of the loss of the phenolic hydroxyl group and aromaticity on the biological activities of **1**.

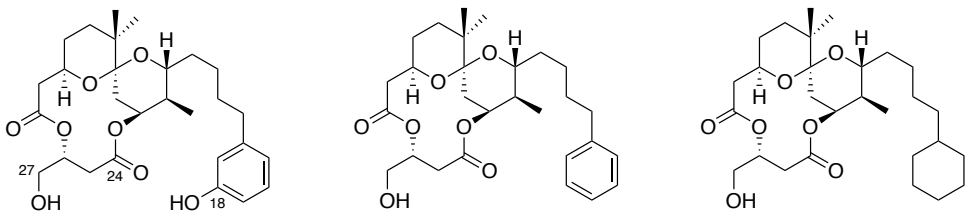

Figure 12. Structures of **1** and its derivatives.

*The content described in this Chapter was originally published in *Molecules*. Yusuke Hanaki, Masayuki Kikumori, Harukuni Tokuda, Mutsumi Okamura, Shingo Dan, Naoko Adachi, Naoaki Saito, Ryo C. Yanagita, and Kazuhiro Irie (2017) Loss of the Phenolic Hydroxyl Group and Aromaticity from the Side Chain of Anti-Proliferative 10-Methyl-aplog-1, a Simplified Analog of Aplysiatoxin, Enhances Its Tumor-Promoting and Proinflammatory Activities. *Molecules* **22**, 631. doi:10.3390/molecules22040631 © 2017 The authors.

Results and Discussion

Compounds **15** and **16** were synthesized from **1** as described in Scheme 2. Selective triflation of the phenolic hydroxyl group followed by hydrogenation produced **15** (65% yield in two steps). Hydrogenation of the aromatic ring of **15** under the conditions reported by Sajiki's group[87] gave **16** with high yield (98%). Since NOE pattern and ^{1}H-NMR coupling constants of **15** and **16** were similar to those of **1** (Supporting Information), these structural modifications did not affect the configuration or the conformation of the spiroketal moiety and the macrolactone ring.

First, the affinity of **15** and **16** for the synthetic δ-C1B peptide was measured as described in chapter 1. The affinity of **15** for δ-C1B was rather weak, but comparable to that of **1** (Table 4). By contrast, **16** showed a binding affinity for δ-C1B lower by one order of magnitude. To predict the binding mode between each derivative and δ-C1B, docking simulation followed by refinement using molecular dynamics (MD) was performed as reported previously.[88] Representative complex structures were shown in Figure 13. Based on previous structure–activity studies of DAT, the hydrophilic moiety at positions 1 and 27–31 was thought to play key roles in the binding to PKC C1 domains.[67,68] In docking models, 24-C=O and 27-OH groups of **1, 15** and **16** could form three hydrogen bonds with Thr-242, Leu-251, and Gly-253 on δ-C1B. In addition, the phenolic hydroxyl group in the side chain of **1** formed another hydrogen bond with the C=O group of Met-239. These results are consistent with a model for binding between ATX and δ-C1B.[88] Instead of this hydrogen bond, the aromatic ring of **15** could be involved in the CH/π interaction with Pro-241, whereas there was no significant interaction between the cyclohexyl moiety of **16** and δ-C1B. These models well explain the differences among **1**, **15**, and **16** in the binding affinity for δ-C1B.

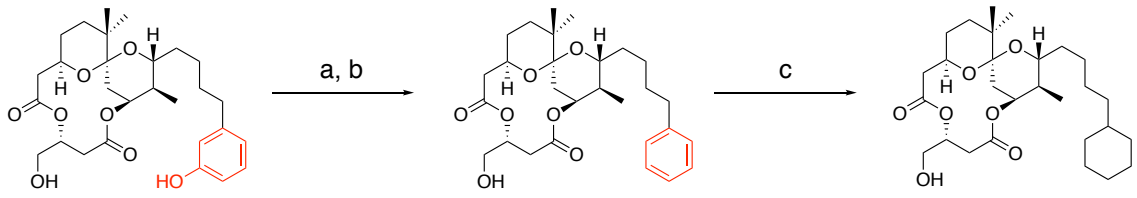

1 **15** **16**

Scheme 2. (a) *N*-phenyl-bis(trifluoromethanesulfonimide), triethylamine, DCM; (b) H_2, 10% Pd/C, *N*,*N*-diisopropylethylamine, EtOH (65% in two steps); (c) H_2, 5% Rh/C, *i*PrOH (98%)

Table 4. Values of K_i for the inhibition of [^{3}H]PDBu binding by **1**, **15**, and **16**.

K_i (nM) for PKCδ C1B		
1[a]	**15**	**16**
0.46	0.87 (0.18)[b]	3.8 (0.67)[b]

[a] Cited from ref. 39. [b] Standard deviation from four separate experiments.

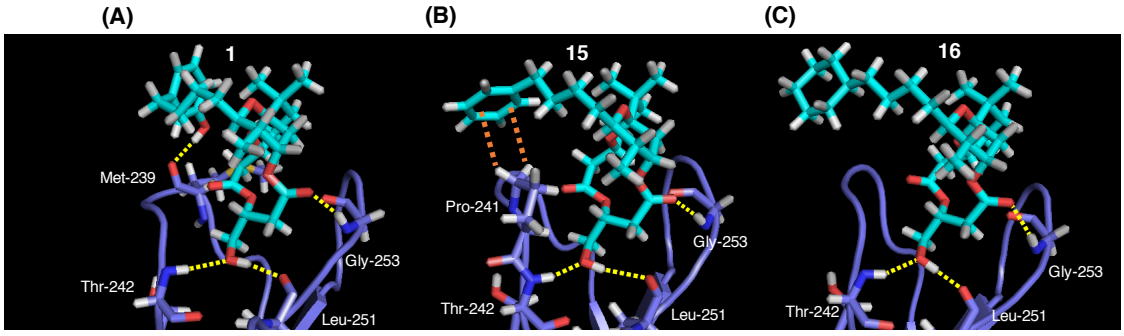

Figure 13. Structures of the PKCδ-C1B domain in complex with **1** (A), **15** (B), and **16** (C). Each compound is drawn as a stick model. δ-C1B is depicted in cartoon form, and amino acid residues that could form hydrogen bonds or be involved in CH/π interactions with the aromatic ring of each compound are represented in stick model colored purple (carbon), red (oxygen), blue (nitrogen), yellow (surfer), and white (hydrogen). Yellow and orange dashed lines represent hydrogen bonds and CH/π interactions, respectively.

The growth inhibitory activities of **15** and **16** were evaluated using a panel of 39 human cancer cell lines (JFCR39) as described in chapter 1. GI_{50} values for seven aplog-sensitive cancer cell lines are listed in Table 1 (the rest of the data are provided in Supporting Information). The anti-proliferative activity of **15** was almost equal to that of **1**. This was in agreement with a previous structure–activity study of aplog-1.[89] On the other hand, **16** showed slight weaker growth inhibitory activity than **1**, except against MKN-45. Since there is a good correlation between the binding affinity for δ-C1B and the anti-proliferative activity against aplog-sensitive cell lines as shown in chapter 1, low affinity of **16** for δ-C1B could account for its weak anti-proliferative activity.

Table 1. Growth inhibition of **1**, **15**, and **16** against aplog-sensitive cancer cell lines

		GI_{50} (log M)		
Cancer type	Cell line	**1**[a]	**15**	**16**
Breast	HBC-4	–7.48	–7.76	–7.20
	MDA-MB-231	–6.90	–5.63	–5.68
Colon	HCC2998	–6.47	–6.21	–6.08
Lung	NCI-H460	–7.07	–7.09	–6.85
	A549	–6.01	–6.12	–5.78
Stomach	St-4	–6.24	–5.93	–5.89
	MKN45	–4.97	–6.51	–6.13
Average for these seven cell lines		–6.45	–6.46	–6.23

[a] Cited from ref. 39.

Since the tumor-promoting and proinflammatory activities of phorbol esters are sensitive to the structure of their ester side chains,[90,91] **15** and **16** may exhibit adverse effects, unlike **1**. Initially, the proinflammatory activities of **15** and **16** in the mouse ear was evaluated. The ear of each ICR mouse was treated with each compound for 24 h. Proinflammatory activity was measured as an increase in the relative weight of each ear following treatment with each compound (Figure 14). In contrast to tumor-promoting TPA, **1** did not show significant proinflammatory activity even at a dose of 170 nmol. On the other hand, **15** induced inflammation at this concentration albeit weak. Moreover, **16** exhibited marked proinflammatory activity even at a dose of only 17 nmol like TPA.

The tumor-promoting activities of **15** and **16** were investigated in a two-stage carcinogenesis test on mouse skin (Figure 15). Previous study confirmed that **1** was negative for papilloma formation even in the presence of a five-fold excess of TPA in the previous experiment.[39] The skin on the back of ICR mice was treated with a single dose of 780 nmol of 7,12-dimethylbenz[a]anthracene (DMBA) and, one week later, with 8.5 nmol of **15** or **16** (10-fold excess of TPA) twice a week. In the positive control experiment using TPA (0.85 nmol), the first papilloma appeared in week 8, and all mice bore papillomas by week 14. The application of 8.5 nmol **15** did not induce any papillomas. On the other hand, 8.5 nmol of **16** significantly enhanced papilloma formation, and the percentage of tumor-bearing mice reached 50% by week 18. These results suggest that both the phenolic hydroxyl group and aromatic ring in aplogs suppressed the proinflammatory and tumor-promoting activities.

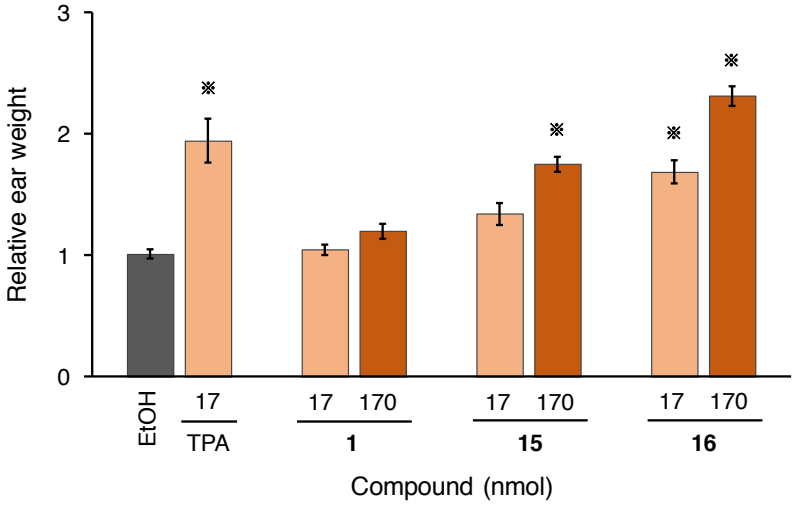

Figure 14. Change in relative weight of the mouse ear 24 h after the application of TPA, **1**, **15**, or **16**. Error bars show the standard error of four samples. ※$p < 0.01$ vs. vehicle (EtOH) group (Dunnett's test).

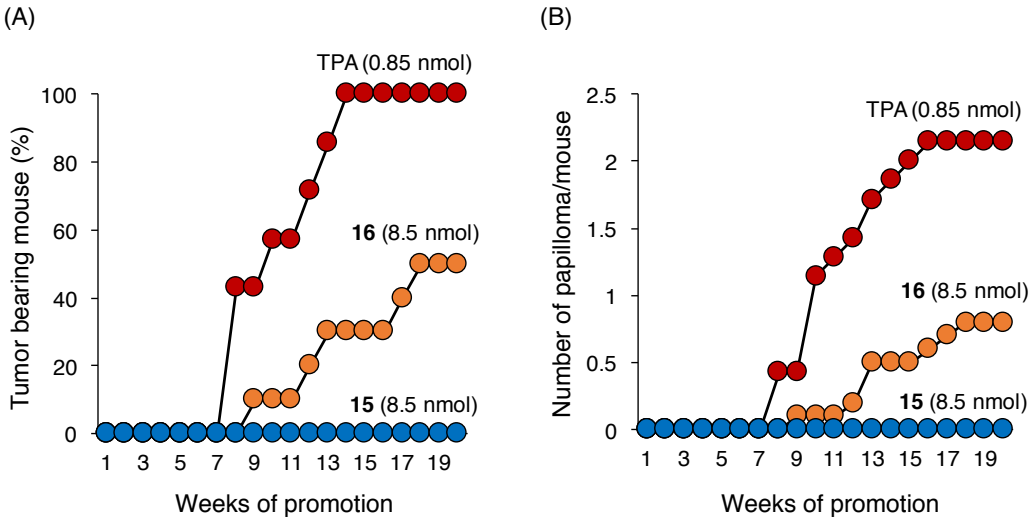

Figure 15. Tumor-promoting activity of TPA (0.85 nmol), **2** (8.5 nmol), and **3** (8.5 nmol). The back of each female six-week-old ICR mice was shaved with surgical clippers. From a week after the initiation by a single application of 780 nmol of DMBA in 0.1 mL acetone, each compound (0.85 or 8.5 nmol) in 0.1 mL acetone was applied twice a week from week 1 to week 20. TPA group consisted of seven mice, and other groups consisted of ten mice. (A) Tumor-bearing mice (%). (B) Number of papilloma per mouse.

Since the differences among phorbol esters in their tumor-promoting activities were attributed to their effect on the translocation profile of PKCδ,[91] the translocation assay in living HEK293 cells transfected with PKCδ-GFP was performed. As shown in Figure 16, stimulation by 1 μM of either **1** or **15** induced the translocation of PKCδ-GFP to the plasma membrane and the perinuclear region, possibly to the Golgi apparatus. However, stimulation by 1 μM **16** barely induced translocation of PKCδ-GFP (data not shown), reflecting low affinity for PKCδ, but a higher concentration (3 μM) of **16**, was sufficient to recruit it to the plasma membrane and near the nucleus, in a manner similar to **1** and **15**. These results indicate that the localization pattern of PKCδ is not related to the tumor-promoting activity of aplogs.

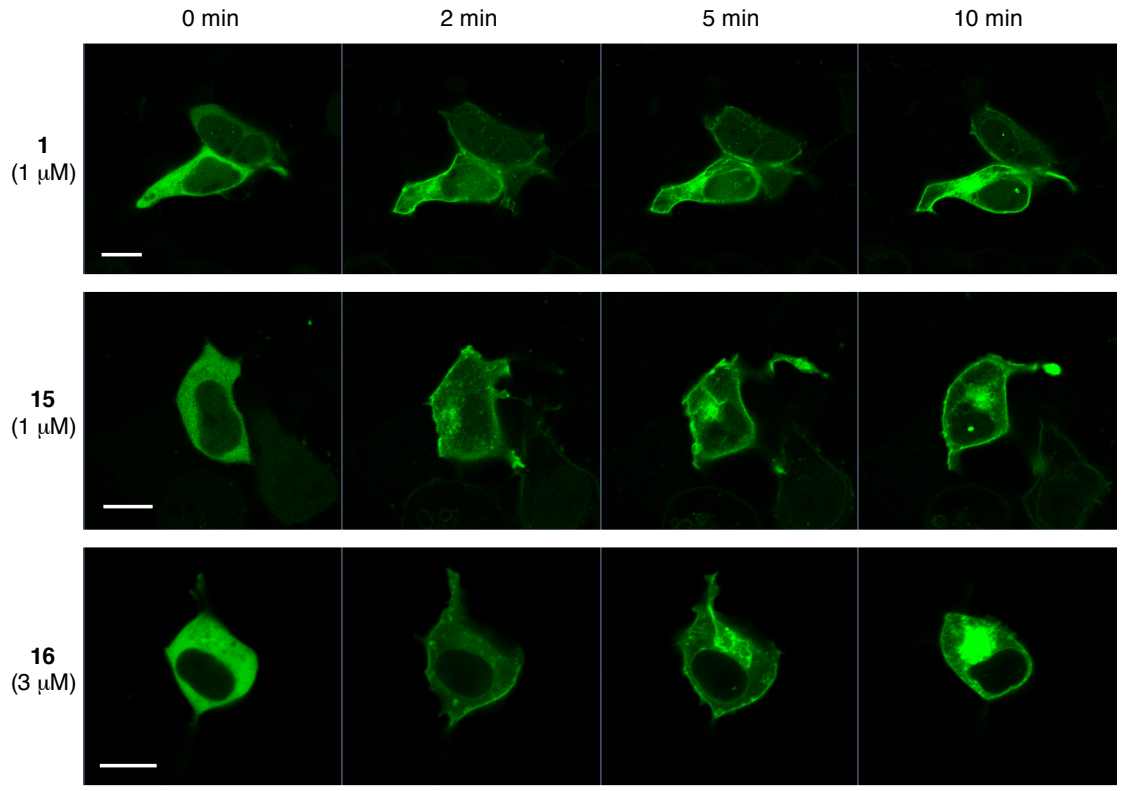

Figure 16. Translocation of PKCδ-GFP in HEK293 cells induced by **1** (1 μM), **2** (1 μM), and **3** (3 μM). Fluorescence images of HEK293 cells expressing PKCδ-GFP 0, 2, 5, and 10 min after treatment with each compound are shown. Scale bar: 10 mm.

Bryo-1 was reported to cause PKCδ-GFP to localize to the nuclear membrane and endoplasmic reticulum in HEK293 cells.[92] On the other hand, TPA caused PKCδ-GFP recruitment predominantly to the plasma membrane and the nuclear envelope,[75,76] whereas PDBu, a less hydrophobic TPA analog, promoted its accumulation in the Golgi apparatus.[93] Interestingly, translocation profile of **1** resembled that of tumor-promoting phorbol esters rather than bryo-1. Recently, Kazanietz's group demonstrated that bryo-1 prevents TPA-induced apoptosis by causing PKCδ to localize to the nuclear membrane, but that bryo-1 itself did not trigger any biological responses.[94] Keck and Blumberg also reported that bryo-1 itself exhibited only weak anti-proliferative activity, but antagonized the anti-proliferative activity of TPA.[95] In addition, most cancer clinical trials using bryo-1 have yielded disappointing results.[21,22] Therefore, tumor promoter–like PKC ligands that recruit PKCδ to the plasma membrane or the Golgi apparatus may be suitable as anti-cancer drugs. Indeed, PKCδ activation in either the plasma membrane or Golgi apparatus induces apoptosis.[94,96] Compound **1** is a novel PKC ligand that activates PKCδ in a manner similar to tumor promoters despite the absence of tumor-promoting and proinflammatory activities.

In summary, the phenolic group in the side chain of **1** maintains the affinity for C1B domain of PKCδ through hydrogen bond or CH/π interaction with Met-239 or Pro-241, resulting in potent anti-proliferative activity against aplog-sensitive cancer cell lines. In addition, the phenolic side chain could suppress side effects such as proinflammatory and tumor-promoting activities. The increase in the hydrophobicity of ester side chains of phorbol esters is generally considered to enhance tumor-promoting activity,[90,91] and tumor-promoting **16** is also more hydrophobic than **1** and **15** (calculated log P of **1**, 3.4; of **15**, 4.1; of **16**, 5.3). However, proinflammatory and tumor-promoting activities of aplogs did not merely depend on the hydrophobicity, because introduction a bromine or iodine atom onto the aromatic ring of aplog-1 and **1** did not promote these activities.[97,98] Furthermore, **1**, **15** and **16** induced the translocation of PKCδ-GFP in the manner similar to tumor-promoters though **1** and **15** were neither tumor-promoting nor proinflammatory. Recent study suggested that not only translocation sites of PKC isozymes but also depth or angle of penetration of C1 domains into the membrane could define the downstream signaling.[99] The interaction between the phenolic side chain of **1** and the amino acid residues of C1 domains may control the downstream signaling as not to promote tumorigenesis. In addition, the degradation rate of PKC isozymes may be effected by the side chain structure because the loss of PKC isozymes could enhance tumor formation.[64,65] On the other hand, ATX and DAT show tumor-promoting activity despite the presence of the phenolic group in its side chain. In the previous studies, the

hemiacetal hydroxyl group and the methoxy group of them were suggested to enhance tumor-promoting activity.[39,100] Thus, these groups may inhibit the interaction between their side chains and C1 domains or alter the penetration mode of C1 domains into the membrane by inducing conformational change or steric hindrance.

Experimental

General remarks

The following spectroscopic and analytical instruments were used: digital polarimeter, DIP-1000 (Jasco, Tokyo, Japan); ^{1}H- and ^{13}C-NMR, Avance III 500 (reference TMS, Brucker, Rheinstetten, Germany); HPLC, model 600E with a model 2487 UV detector (Waters, Milford, MA, USA); HR-ESI-qTOF-MS, Waters Xevo G2-S qTOF (Waters, Milford, MA, USA); and confocal laser scanning fluorescence microscopy, LSM700 (Carl Zeiss, Jena, Germany). HPLC was carried out on YMC-Pack SIL SL12S05-2510WT (10 mm i.d. × 250 mm, Yamamura Chemical Laboratory, Kyoto, Japan). Wakogel C-200 (silica gel, Wako Pure Chemical Laboratory, Osaka, Japan) was used for column chromatography. [^{3}H]PDBu (18.7 Ci/mmol) was custom synthesized by Perkin-Elmer Life Science Research Products (Boston, MA, USA). PKCδ-C1B peptide was synthesized as reported previously.[72] All other chemicals and regents were purchased from chemical companies and used without further purification. The purity of **15** and **16** was greater than 95% as determined by ^{1}H- and ^{13}C-NMR (Appendix). All animal use procedures were approved by Kyoto University Animal Experimentation Committee and performed according to its guidelines.

Synthesis of 15

Triethyl amine (5.5 μL, 23.8 μmol, 1.2 equiv.) and *N*-phenyl-bis(trifluoromethane-sulfonimide) (8.5 mg, 23.8 μmol, 1.2 equiv.) were added to a solution of 10-methyl-aplog-1 (**1**) (10 mg, 19.8 μmol) in DCM (150 μL) at room temperature. The reaction mixture was stirred at room temperature for 8.5 h and poured into 1 mL water. The aqueous layer was extracted four times with 2 mL EtOAc. The combined organic layers were washed with brine, dried over Na_2SO_4, filtered, and concentrated in vacuo. The residue was purified by column chromatography (silica gel, 25% EtOAc/hexane) to produce a crude mixture that consists mostly of the desired trifulate (10.5 mg). We added 25 μL *N*,*N*-diisopropylethylamine to a mixture of the trifulate (10.5 mg) and 10% Pd/C (7.9 mg) (wet support, Degussa type E101 NE/W, Sigma-Aldrich, St. Louis, MO) in 300 μL EtOH and stirred vigorously under a H_2 atmosphere at room temperature for 4 h. The mixture was filtered, and the filtrate was concentrated in vacuo. The residue was purified by column chromatography (silica gel, 25% EtOAc/hexane), and further purified by HPLC (column, YMC-Pack SIL SL-12S05-2510WT; solvent, *i*PrOH/$CHCl_3$/hexane = 2:18:80; flow rate, 3 mL/min; pressure, 660 psi; UV detector, 254 nm; retention time, 18 min) to produce **15** (6.3 mg, 12.9 μmol, 65% in two steps) as a clear oil. ^{1}H-NMR (500 MHz, $CDCl_3$, 0.0049 M; ppm) δ 0.79 (3H, d, *J* = 6.9 Hz), 0.86 (3H, s), 0.96 (3H, s), 1.29–1.38 (2H, m), 1.39–1.62 (8H, m), 1.70 (1H, m), 1.71 (1H, dd, *J* = 15.5, 4.0 Hz), 2.24 (1H, m), 2.39 (1H, dd, *J* = 13.0, 10.9 Hz), 2.49–2.55

(2H, m), 2.62 (2H, t, J = 7.7 Hz), 2.73 (1H, dd, J = 16.8, 3.4 Hz), 2.81 (1H, dd, 16.8, 11.2 Hz), 3.72 (1H, m), 3.79 (1H, ddd, J = 11.9, 5.9, 3.8 Hz), 3.87 (1H, tt, J = 10.9, 2.9 Hz), 3.94 (1H, m), 5.01 (1H, m), 5.18 (1H, m), 7.15 (1H, t, J = 1.3 Hz), 7.16–7.22 (2H, m), 7.26–7.28 (2H, m); ^{13}C-NMR (125 MHz, $CDCl_3$, 0.0049 M; ppm) δ 13.2, 21.4, 24.2, 26.0, 26.5, 27.3, 31.2, 32.3, 34.6, 36.0, 36.8, 36.9, 36.9, 42.8, 64.5, 68.3, 70.5, 71.8, 73.0, 99.9, 125.5, 128.2 (2C), 128.5 (2C), 143.1, 169.8, 171.5; IR (KBr; cm^{-1}) 3447, 2360, 1726, 1294, 1273, 1198, 1060; HR-ESI-qTOF-MS: m/z 487.2698 $[M–H]^-$ (calculated for $C_{28}H_{39}O_7$, 487.2696); $[\alpha]_D^{21.7}$ +66.3° (c = 0.13, $CHCl_3$).

Synthesis of 16

The mixture of **15** (7.1 mg, 14.5 μmol) and 5% Rh/C (4.6 mg) (wetted with 55% water, Tokyo Chemical Industry) in *i*PrOH (350 μL) was vigorously stirred under a H_2 atmosphere at room temperature for 17 h. The mixture was filtered and the filtrate was concentrated in vacuo. The residue was purified by column chromatography (silica gel, 25% EtOAc/hexane) to afford **16** (7.0 mg, 14.2 μmol, 98%) as clear oil. ^{1}H-NMR (500 MHz, $CDCl_3$, 0.0057 M; ppm) δ 0.79 (3H, d, J = 6.9 Hz), 0.83–0.92 (5H, m), 1.00 (3H, m), 1.12–1.57 (17H, m), 1.59–1.73 (6H, m), 2.25 (1H, t, J = 5.9 Hz), 2.37 (1H, dd, J = 13.0, 10.9 Hz), 2.49–2.54 (2H, m), 2.72 (1H, dd, J = 16.8, 3.5 Hz), 2.80 (1H, dd, J = 16.8, 11.2 Hz), 3.71 (1H, m), 3.79 (1H, ddd, J = 12.0, 5.9, 3.9 Hz), 3.84–3.93 (2H, m), 5.01 (1H, m), 5.17 (1H, m);
^{13}C-NMR (125 MHz, $CDCl_3$, 0.0057 M; ppm) δ 13.2, 21.4, 24.7, 26.0, 26.5 (3C), 26.6, 26.9, 27.3, 32.6, 33.5, 33.5, 34.6, 36.8, 36.9, 36.9, 37.6, 37.6, 42.7, 64.5, 68.4, 70.5, 71.8, 73.0, 99.8, 169.8, 171.5; IR (KBr; cm^{-1}) 3470, 2923, 2852, 1728, 1295, 1273, 1199, 1074, 1061; HR-ESI-qTOF-MS: m/z 493.3170 $[M–H]^-$ (calculated for $C_{28}H_{45}O_7$, 493.3165); $[\alpha]_D^{21.7}$ + 73.8° (c = 0.13, $CHCl_3$).

Inhibition of the specific binding of [^{3}H]PDBu to δ-C1B peptide

See Chapter 1.

Molecular dynamics simulation

Molecular dynamics (MD) simulations for the POPS–ligand–PKCδ-C1B ternary complex in water were carried out as described previously.[88] All MD simulations were performed using the GROMACS software package (version 5.1.4).[101] After equilibrating and relaxing the system, we performed a 30 ns NPT (constant number of atoms, pressure, and temperature) simulation without any position restraint with a 2 fs time step.

Measurements of cell growth inhibition

See Chapter 1.

Mouse ear swelling test

The author applied either a solution of each test compound in EtOH (10 μL) or EtOH as a control to the right ear of five-week-old female ICR mice (Shimizu Laboratory Supplies, Kyoto, Japan) using a micropipette. A volume of 5 μL was delivered to both the inner and outer surfaces of the ear. After 24 h, a disk (0.8 cm square) was obtained from the ear and weighed. The proinflammatory activity of each compound was determined by measuring relative ear weight, i.e., the weight of a right ear disk relative to the weight of a left ear disk. Each group consisted of four mice.

Two-stage carcinogenesis experiment

The back of each six-week-old female ICR mice (Shimizu Laboratory Supplies) was shaved with surgical clippers one day before DMBA treatment. From a week after initiation by a single dose of 780 nmol DMBA in 0.1 mL acetone, we administered 0.85 nmol of TPA in 0.1 mL acetone, 8.5 nmol of **15** in 0.1 mL acetone, or 8.5 nmol of **16** in 0.1 mL acetone to each mouse twice a week from week 1 to 20. The number of skin papilloma > 1 mm in diameter was counted every week. Each group consisted of 7–10 mice.

Translocation of PKCδ-GFP

The author transfected HEK293 cells with a plasmid encoding PKCδ-GFP using Lipofectamine® 3000. The transfected cells were cultured for 20–48 h for maximal fluorescence. Translocation of GFP-tagged PKCδ was triggered by the addition of a test compound to the culture medium (final DMSO concentration 0.05%–0.15%) to obtain the appropriate final concentration. The fluorescence of GFP was monitored by confocal laser scanning fluorescence microscopy at 488 nm excitation with a 494-nm-long pass beam splitter.

Supporting Information

I. ^{1}H and ^{13}C NMR spectra of **15** and **16**

^{1}H-1D NMR spectrum of **15** (500 MHz, $CDCl_3$, 0.0049 M)

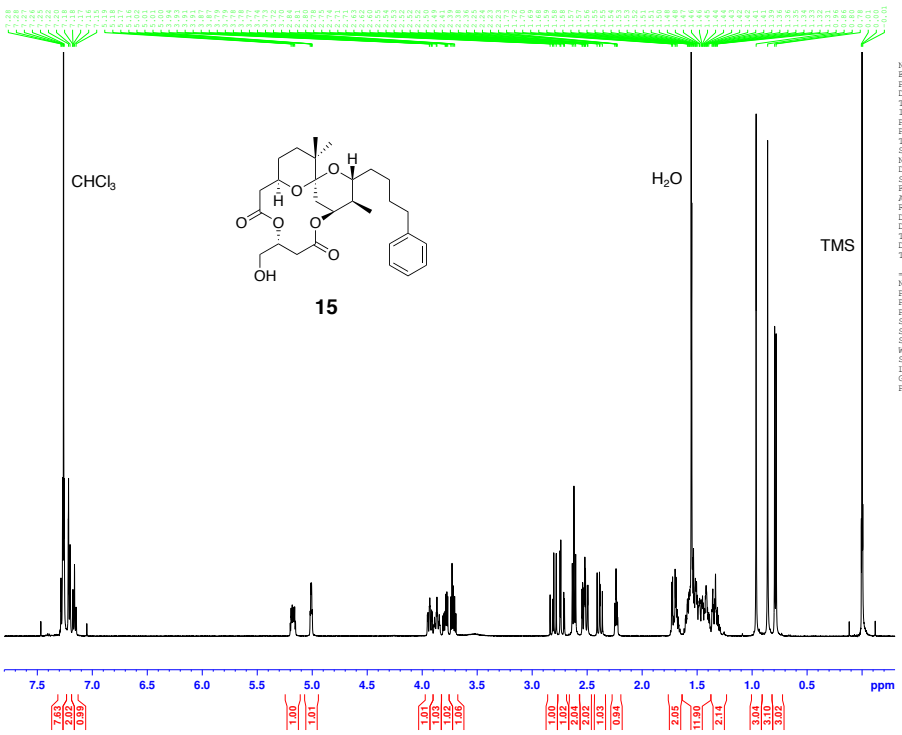

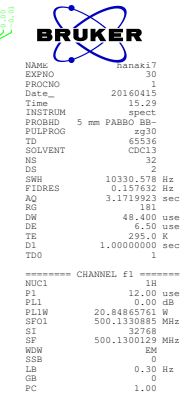

^{13}C-1D NMR spectrum of **15** (125 MHz, $CDCl_3$, 0.0049 M)

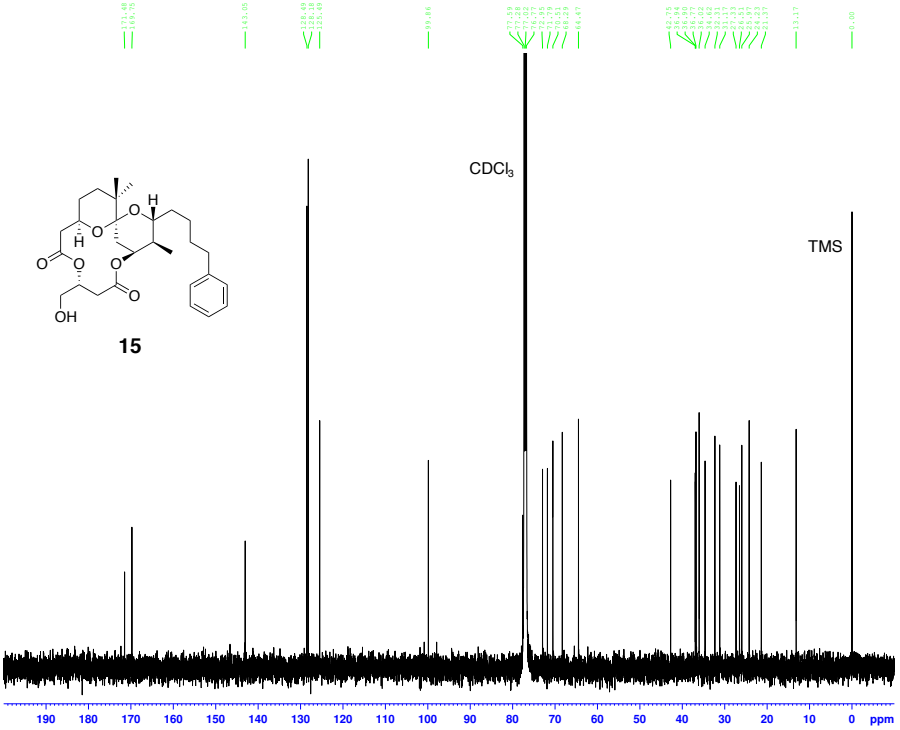

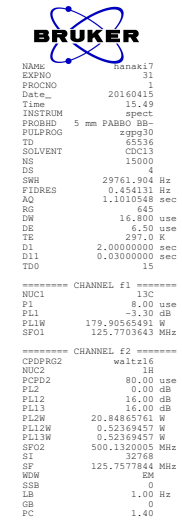

^{1}H-1D NMR spectrum of **16** (500 MHz, $CDCl_3$, 0.0057 M)

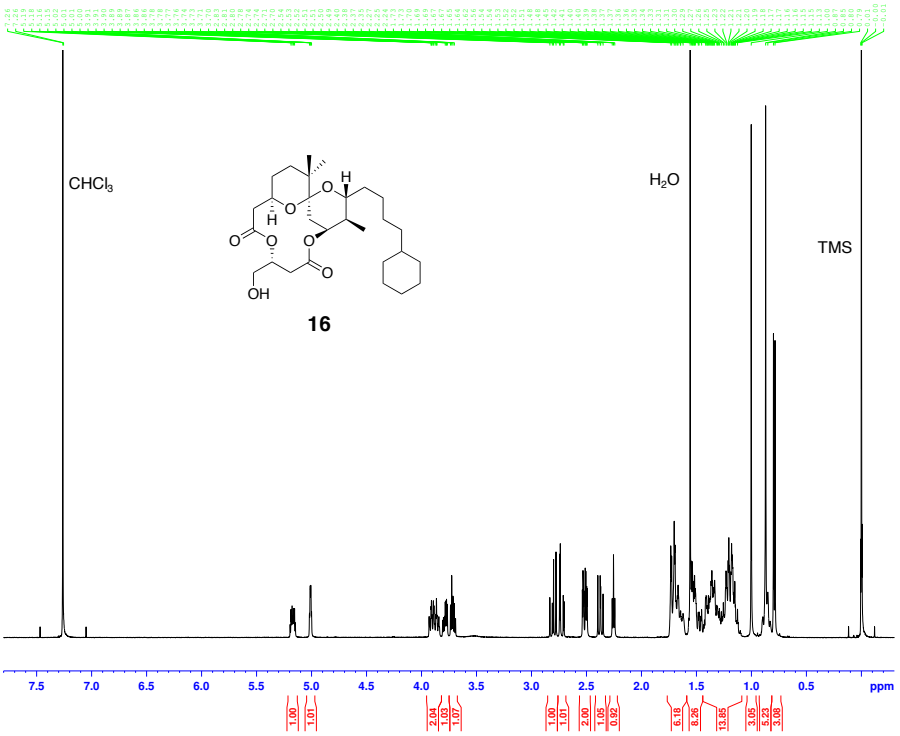

^{13}C-1D NMR spectrum of **16** (500 MHz, $CDCl_3$, 0.0057 M)

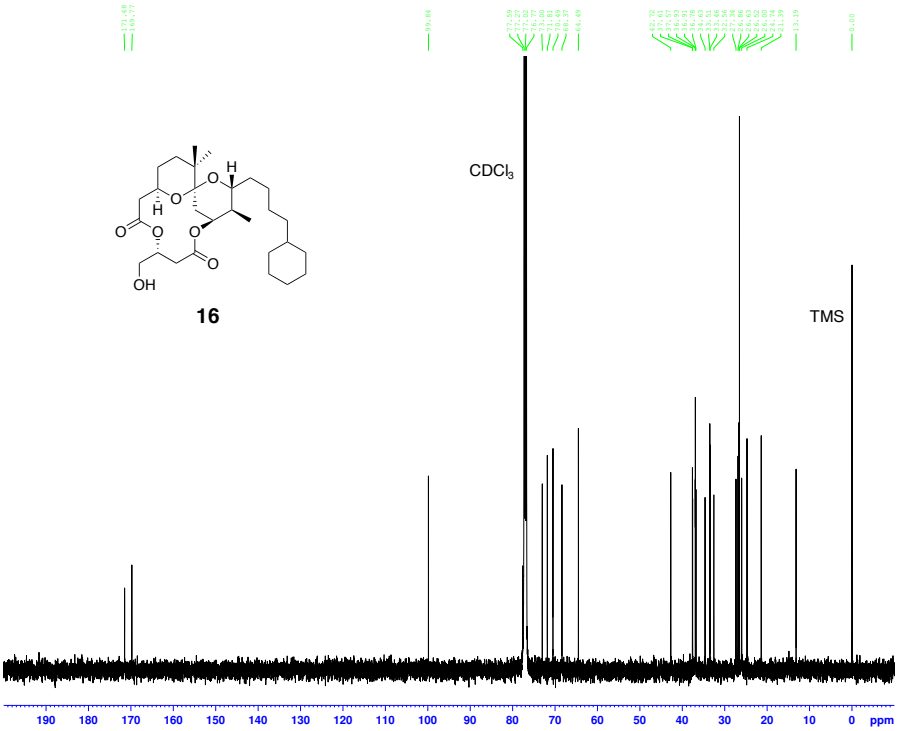

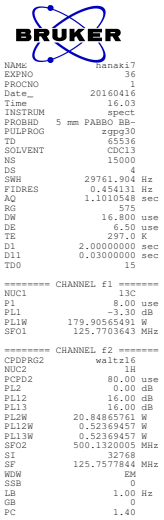

II. NOESY spectra of **1**, **15** and **16**

NOESY spectrum of **1** (500 MHz, $CDCl_3$, 0.010 M)

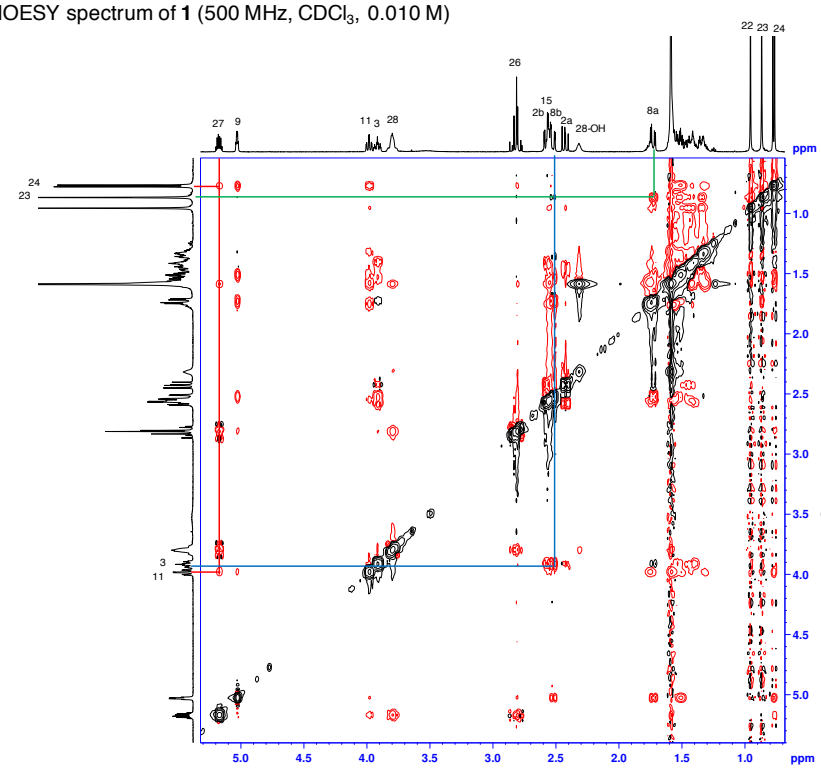

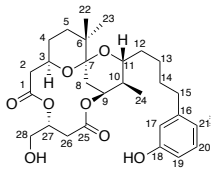

10-Methyl-aplog-1 (**1**)

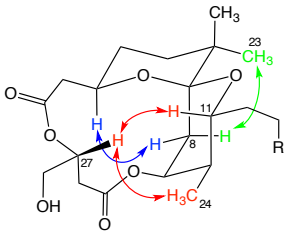

NOESY spectrum of **15** (500 MHz, $CDCl_3$, 0.0053 M)

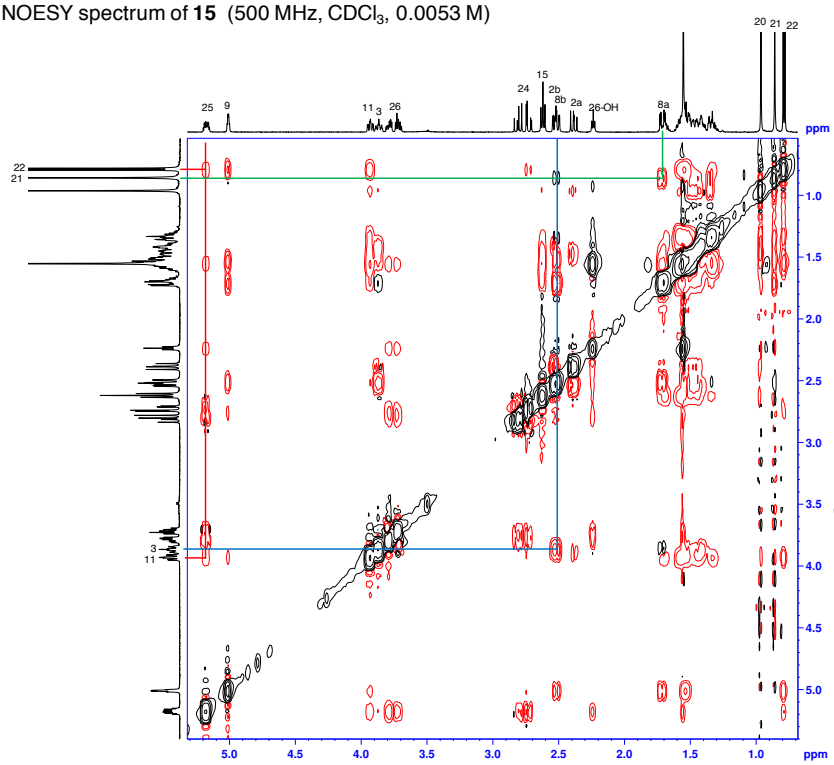

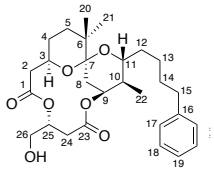

15

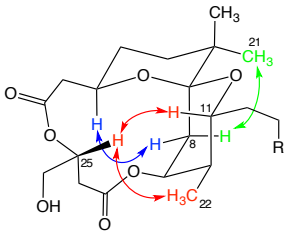

NOESY spectrum of **16** (500 MHz, $CDCl_3$, 0.0052 M)

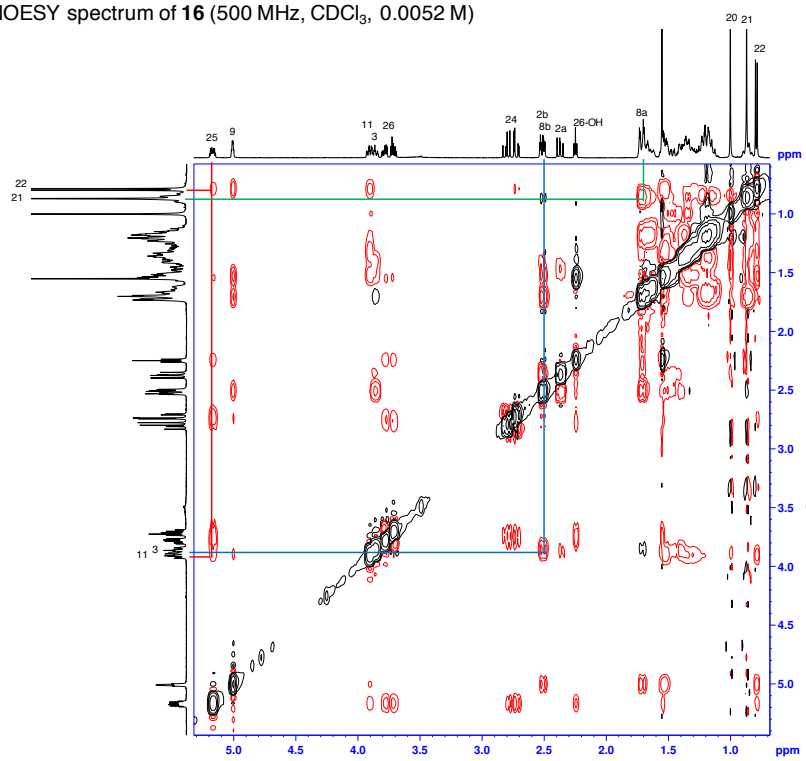

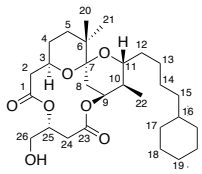

16

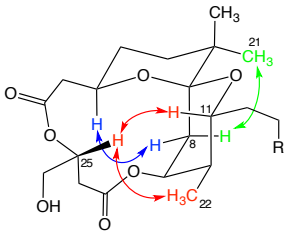

III. Growth inhibitory activities of **15** and **16** towards 39 human cancer cell lines

cancer cell lines		log GI_{50} (M)		
		1[a]	**15**	**16**
Breast	HBC-4	–7.48	–7.76	–7.20
	BSY-1	–4.91	–4.88	–4.99
	HBC-5	–4.82	–4.83	–4.90
	MCF-7	–4.84	–4.99	–5.29
	MDA-MB-231	–6.90	–5.63	–5.68
CNS	U251	–4.79	–4.76	–4.80
	SF-268	–4.83	–4.78	–4.86
	SF-295	–4.98	–4.90	–5.20
	SF-539	–4.88	–4.90	–4.91
	SNB-75	–4.92	–4.91	–4.89
	SNB-78	–6.05	–4.81	–4.79
Colon	HCC2998	–6.47	–6.21	–6.08
	KM-12	–4.82	-4.87	–4.99
	HT-29	–4.81	–4.95	–5.05
	HCT-15	–4.87	–4.78	–4.76
	HCT-116	–4.89	–5.02	–5.07
Lung	NCI-H23	–4.87	–4.75	–4.74
	NCI-H226	–6.15	–4.94	–5.02
	NCI-H522	–4.86	–4.88	–4.98
	NCI-H460	–7.07	–7.09	–6.85
	A549	–6.01	–6.12	–5.78
	DMS273	–4.88	–4.93	–5.32
	DMS114	–5.05	–4.91	–4.87
Melanoma	LOX-IMVI	–6.21	–4.76	–4.84
Ovarian	OVCAR-3	–4.88	–4.79	–4.95
	OVCAR-4	–4.77	–4.78	–4.84
	OVCAR-5	–4.92	–4.88	–4.97
	OVCAR-8	–4.75	–4.80	–4.82
	SK-OV-3	–4.88	–4.76	–4.81
Renal	RXF-631L	–4.84	–4.75	–4.84
	ACHN	–4.94	–4.90	–4.97
Stomach	St-4	–6.24	–5.93	–5.89
	MKN1	–4.87	–4.85	–4.91
	MKN-B	–4.80	–4.92	–5.29
	MKN-A	–4.82	-4.93	–4.95
	MKN45	–4.97	–6.51	–6.13
	MKN74	–4.68	–4.85	–4.85
Prostate	DU-145	–4.82	–4.84	–4.85
	PC-3	–4.94	–4.97	–4.95
MG-MID[b]		–5.24	–5.15	–5.18

[a] Kikumori, M.; Yanagita, R. C.; Tokuda, H.; Suzuki, N.; Nagai, H.; Suenaga, K.; Irie, K. *J. Med. Chem.* **2012**, *55*, 5614-5626.

[b] MG-MID: average of the log GI_{50} values of each 39 human cancer cell line.

Chapter 3

Identification of the PKC Isozymes Involved in the Anti-Proliferative and Pro-Apoptotic Activities of 10-Methyl-Aplog-1*

Introduction

As described in previous chapters, the ability to bind to PKC C1 domains is closely related to cell line-specific growth inhibition induced by 10-methyl-aplog-1 (**1**), and eight PKC isozymes and some other enzymes such as PKDs, DGKs, RasGRPs, and chimerins, which contain DAG-responsive C1 domains. To identify the targets responsible for the anti-proliferative activity of aplogs, the author determined the response to **1** of nine cancer cell lines representing common human cancers (colon, lung, prostate, and skin), quantified expression levels of each PKC isozyme in these cell lines, and confirmed the involvement of the predominant isozymes in the growth inhibition using siRNA-mediated knocking down. The mechanisms underlying the growth inhibitory activity of DAT and TPA were also discussed.

Results and Discussion

First, the nine cancer cell lines were classified based on their response to **1**. As shown in Figure 17A, **1** selectively inhibited the growth of A549, SW620, and Colo-205 cells with GI_{50} of less than 1 μM. Flow cytometry analyses clarified that treatment with 1 μM of **1** caused A549 and SW620 cells to undergo cell-cycle arrest in G1 and G2/M,

---

*The content described in this Chapter was originally published in *Biochemical and Biophysical Research Communications*. Yusuke Hanaki, Yuki Shikata, Masayuki Kikumori, Natsuki Hotta, Masaya Imoto, Kazuhiro Irie (2018) Identification of protein kinase C isozymes involved in the anti-proliferative and pro-apoptotic activities of 10-Methyl-aplog-1, a simplified analog of debromoaplysiatoxin, in several cancer cell lines. *Biochem. Biophys. Res. Commun.* **495**, 438-445. doi:10.1016/j.bbrc.2017.11.052

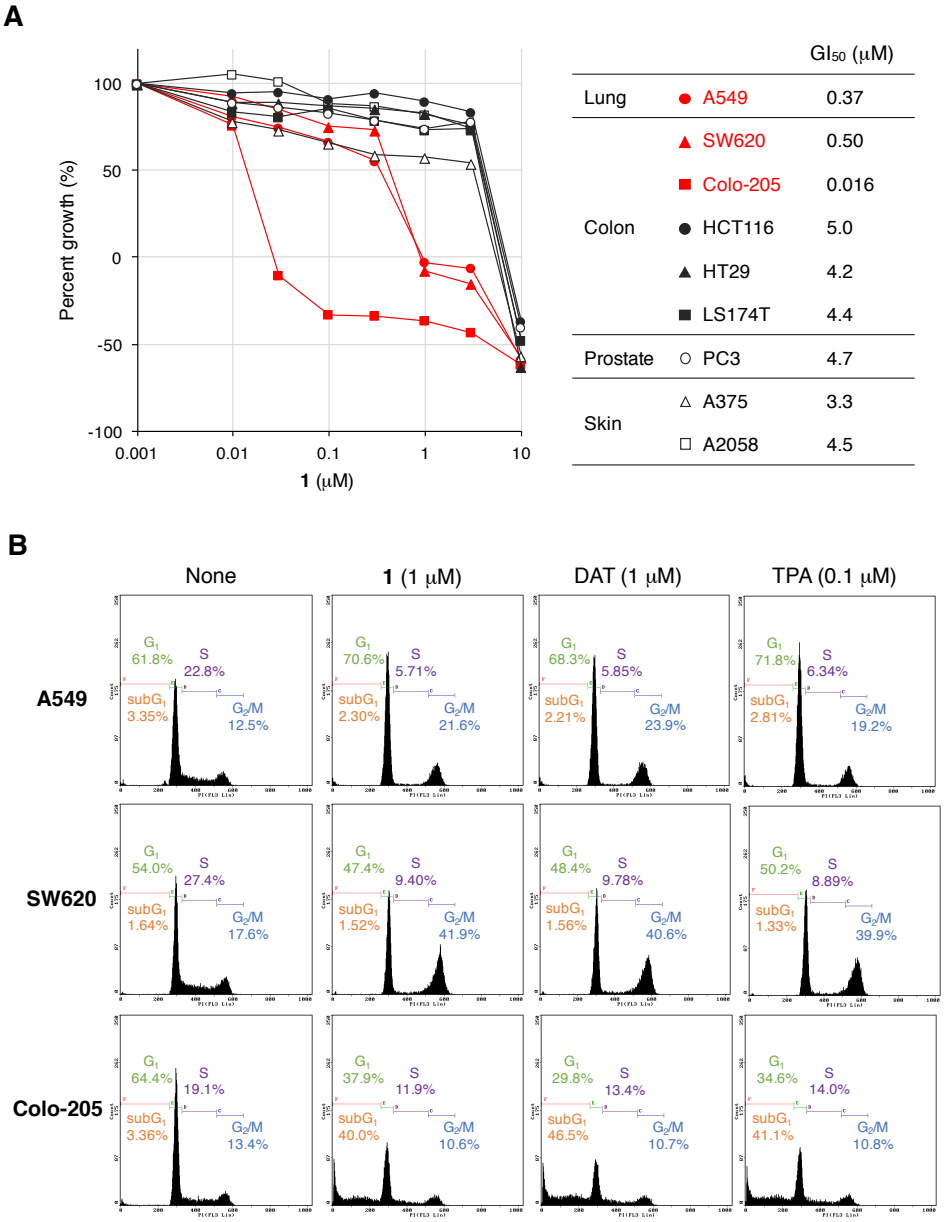

Figure 17. Growth inhibitory activity of **1** against nine cancer cell lines. (A) Compound **1** selectively inhibited the growth of A549, SW620, and Colo-205 cells. Cells were treated with the indicated concentrations of **1** for 48 h. Thereafter, cell number was determined by the MTT assay. Cell growth was expressed as a percentage relative to the control. The results were presented as the average of at least three data points. GI_{50} is the concentration required to inhibit cell growth by 50% as compared to the control. (B) **1**-, DAT-, and TPA-induced cell-cycle arrest in G1 and G2/M phase in A549 and SW620 cells, and apoptosis in Colo-205 cells. Cells were treated with each of the three PKC ligands at the indicated concentration. After 24 h, cell-cycle distributions were estimated by flow cytometry analysis following staining with propidium iodide.

while inducing apoptosis in Colo-205 cells as shown by an increase in the proportion of sub-G1 cells (Figure 17B). DAT and TPA (1 μM and 0.1 μM) also induced cell-cycle arrest and/or apoptosis in these cell lines similarly to **1**. On the other hand, such effects were not observed in other cell lines at this concentration (Supporting Information).

Next, the effects of Gö6983,[16] a PKC-selective inhibitor, on the anti-proliferative activities of **1**, DAT, and TPA was examined. Since Gö6983 itself showed weak but significant anti-proliferative activity at concentrations above 1 μM, we used concentrations below 0.5 μM. As shown Figure 18, Gö6983 nullified the growth inhibitory activity of all PKC ligands in a dose-dependent manner. These results indicate that the anti-proliferative and apoptotic activities of **1** were derived from the activation of PKC isozymes rather than the other enzymes containing PKC C1 homology domains.

To identify the PKC isozymes involved in the cell line-specific growth inhibition induced by **1**, the expression levels of conventional and novel PKC isozymes in these cancer cell lines were precisely quantified. There are some studies that have measured the relative expression levels of PKC isozymes in several cancer cell lines by western blotting.[42] However, these results are not always indicative of absolute amounts; band intensities can be affected by antibody reactivity, translation efficiency, and image exposure time. Measurements of mRNA expression using quantitative polymerase chain reaction (qPCR) is an alternative method, but often shows poor agreement with measurements of protein expression levels.[102] Therefore, absolute quantification using an automated capillary immunoassay system (The Simple Western™) was performed. Chen *et al*. have previously reported accurate and reproducible measurements of the absolute amounts of several PKC isozymes in cell lysates using this method.[102] As shown in Figure 19, PKCα and δ were predominantly expressed in these cancer cell lines, except for HT29 cells, in which only PKCδ was predominantly expressed. These results show good agreement with some reports that have shown that PKCα and δ are expressed ubiquitously, in contrast to the tissue-specific expression of other isozymes.[103,104] A previous study using conventional western blot analysis detected high levels of PKCβ and γ in lysates made from lung and colon cancer cell lines, probably due to the high reactivity of the antibodies, and these cell lines were thereby determined to express almost equal amounts of PKCα, β, γ, and δ.[47] However, our absolute quantification indicates that the PKCα and δ are expressed at much higher levels than the other isozymes in the nine cancer cell lines.

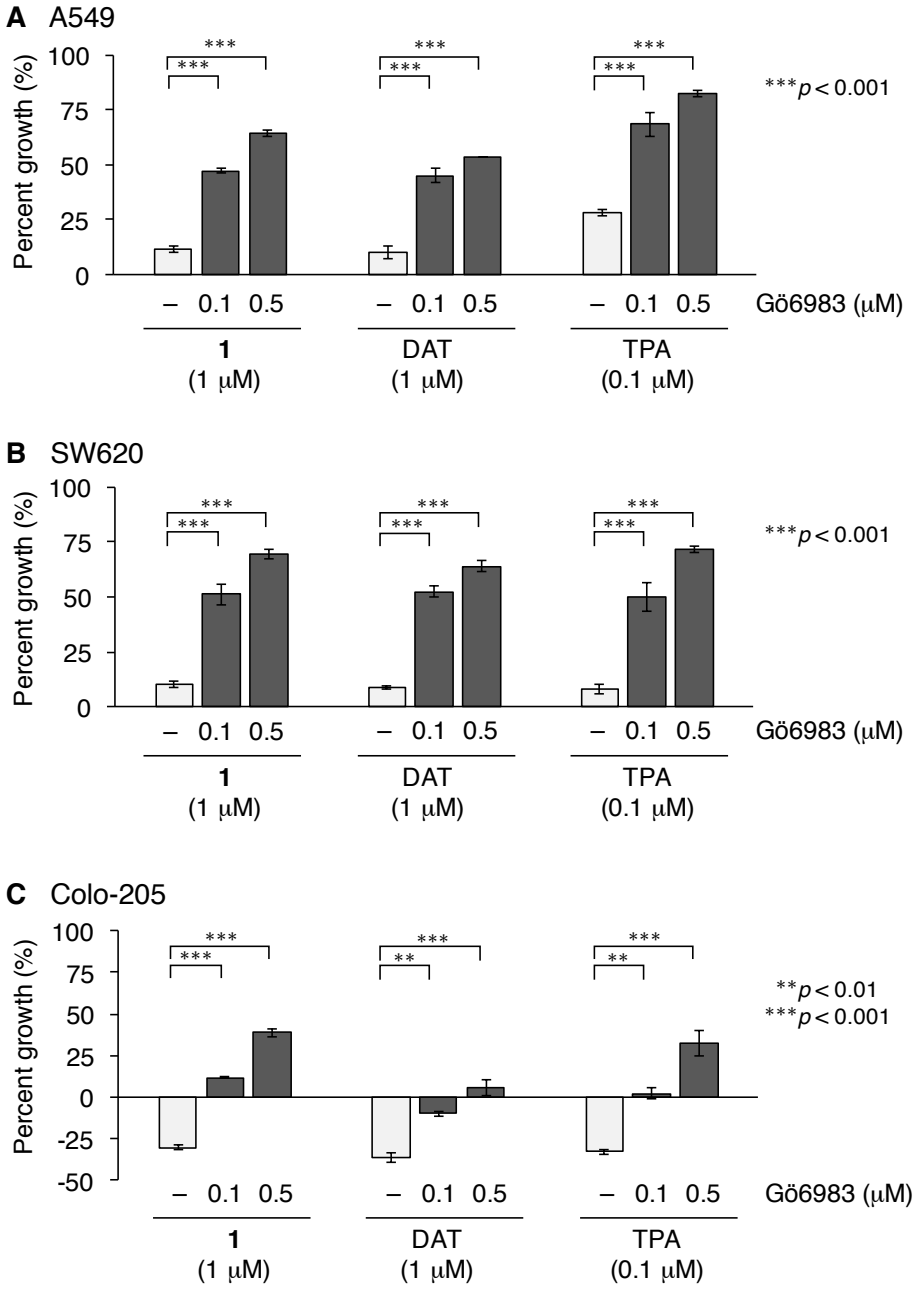

Figure 18. Effects of a PKC inhibitor 'Gö6983' on anti-proliferative and pro-apoptotic activities of PKC ligands. Gö6983 attenuated the growth inhibitory activity of **1**, DAT, and TPA against (A) A549, (B) SW620, and (C) Colo-205 cells. Cells were treated with indicated concentration of Gö6983 for 1 h before being treated with each PKC ligand for 48 h. Thereafter, the cell number was estimated with the MTT assay. Cell growth was expressed as a percentage relative to the control. Error bars represent standard error (n = 3).

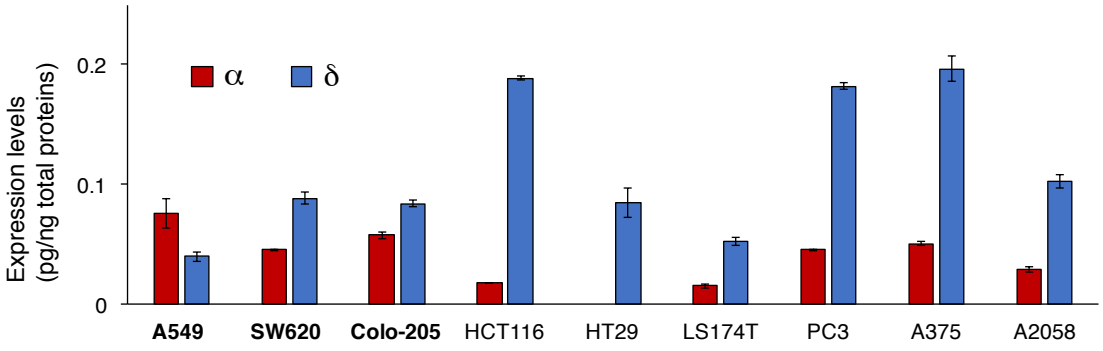

α	0.075	0.045	0.058	0.018	< 0.012	*ca.* 0.015	0.045	0.050	0.029
βI	< 0.010								
βII	< 0.0064								
γ	< 0.0032								
δ	0.040	0.088	0.084	0.189	0.084	0.052	0.182	0.196	0.102
ε	< 0.0031								*ca.* 0.0033
η	*ca.* 0.0026	< 0.0021							
θ	< 0.0062								

Figure 19. Expression levels of each PKC isozyme in nine cancer cell lines. PKCα and δ were predominantly expressed in these cell lines. The absolute amount of each PKC isozyme in cell lysates was determined using the Simple Western™ System. Error bars represent standard error from at least three independent experiments (Supporting Information). The lower limits of quantification were set based on the reactivity of each antibody.

Next, it was investigated that the effects of knocking down PKCα and δ on the anti-proliferative and pro-apoptotic activities of **1**, DAT, and TPA. In A549 cells, PKCα knockdown significantly attenuated the anti-proliferative activity of these PKC ligands, whereas the effects of PKCδ knockdown was limited (Figure 20A). In contrast, knocking down either isozyme did not influence the anti-proliferative activity in SW620 cells, but simultaneous knockdown of both isozymes significantly decreased this activity (Figure 20B). In Colo-205 cells, knocking down either isozyme had little effect on the pro-apoptotic activity, but a double knockdown significantly nullified this activity (Figure 20C). These results suggest that PKCα is mainly involved in the anti-proliferative response observed in A549 cells towards the three ligands, while both PKCα and δ play pivotal roles in the anti-proliferative and pro-apoptotic responses observed in SW620 and Colo-205 cells. On the other hand, previous study indicated that PEP005 induced apoptosis in Colo-205 cells through activation of PKCδ and downregulation of PKCα.[47] Since rottlerin inhibited PEP005-induced apoptosis, PKCδ was expected to be solely

involved in apoptosis. However, although rottlerin was initially regarded as a PKCδ-selective inhibitor, it has been revealed to reduce cellular ATP level, resulting in inhibition of other kinases and non-kinase proteins.[105] Moreover, since downregulation of PKCs always follows their activation, the actual causatives of apoptosis remained controversial. In this study, knockdown of PKCα and δ itself did not effect on the growth of A549, SW620, and Colo-205 cells. Thus, the author concluded that not degradation but activation of both PKCα and δ caused apoptosis in Colo-205 cells.

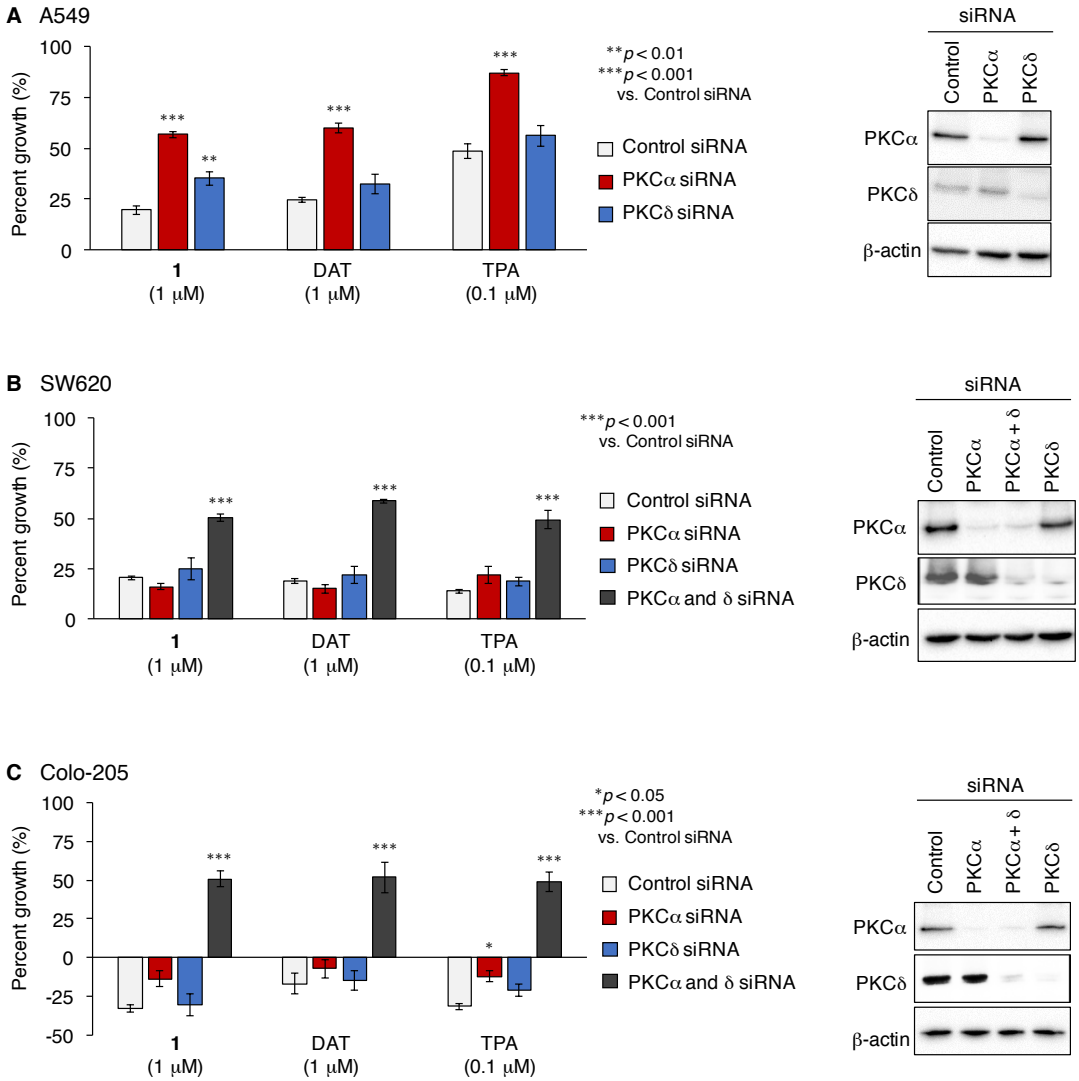

Figure 20. Effects of knocking down PKCα and δ on anti-proliferative and pro-apoptotic activities of PKC ligands. (A) A549, (B) SW620, and (C) Colo-205 cells were transfected with control or PKCα, and/or PKCδ siRNA. Transfected cells were treated with each PKC ligand for 48 h. Thereafter, cell number was estimated by the MTT assay. Cell growth was expressed as a percentage relative to the control. Error bars represent standard error (n = 3).

It is noteworthy that although structural modification or simplification of bioactive molecules often alters their mode of action or attenuated the desired activities, the mechanisms of the observed anti-proliferative and pro-apoptotic activities promoted by **1**, DAT, and TPA are quite similar. Moreover, **1** showed potent anti-proliferative activities equally to DAT but little tumor-promoting and proinflammatory effects. Thus, this simplification selectively removes the unwanted side effects without attenuating the desired anti-proliferative activities.

In summary, PKCα and δ were predominantly expressed in all cancer cell lines examined in this study, and their activation by **1**, DAT, and TPA induced cell cycle arrest or apoptosis in aplog-sensitive cell lines though the phenotypes were quite different from each other. Cell-cycle progression was inhibited in A549 and SW620 cells, while apoptosis was induced in Colo-205 cells. In addition, the anti-proliferative activity observed against A549 cells mainly depended on PKCα, while the effects on SW620 and Colo-205 cells depended on both PKCα and δ. These results suggested that PKCα and δ activation by **1** could be an effective treatment for certain cancers. Since there is no correlation between expression levels of PKC isozymes and the sensitivity to **1**, the roles of PKCα and δ in aplog-insensitive cell lines remains unknown. However, the proliferation was not stimulated by PKC ligands in any of cell line tested (Figure 17), suggesting that PKCα and δ do not contribute to cancer cell growth. Clarification of the intrinsic difference in PKC signaling between aplog-sensitive and insensitive cell lines will facilitate the establishment of the biomarker to evaluate the efficacy of **1** as an anti-cancer agent.

Experimental

Materials

DAT was purified from the cyanobacteria extracts collected in Okinawa and a red alga *Gracilaria coronopifolia* collected in Hawaii.[39] TPA was obtained from Sigma-Aldrich (St. Louis, MO). Gö6983 was obtained from Cayman Chemical Company (Ann Arbor, MI). Recombinant proteins, GST-PKCα, GST-PKCβII, GST-PKCδ, GST-PKCε, and GST-PKCθ, were obtained from Enzo Life Science (Farmingdale, NY), and GST-PKCβI, GST-PKCγ, and GST-PKCη were obtained from Abcam (Cambridge, MA). Primary antibodies were purchased from following companies: anti-PKCα from BD Bioscience (San Jose, CA), anti-PKCβI, anti-PKCβII, anti-PKCγ, anti-PKCδ, and anti-PKCη from Santa Cruz Biotechnology (Dallas, TX), anti-PKCε from Cell Signaling Technology (Danvers, MA), anti-PKCθ from Novus Biologicals (Littleton, CO), and anti-Actin from Sigma-Aldrich. Secondary antibodies, anti-mouse IgG, and anti-rabbit IgG, were obtained from ProteinSimple (Santa Clara, CA) for Simple Western™ analyses, and from GE Healthcare (Little Chalfont, UK) for conventional western blotting. Non-targeting pool siRNA and SMARTpool siRNA against PKCα and PKCδ were obtained from GE Dharmacon (Lafayette, CO).

Cell lines and cell culture

The human cancer cell lines A549, SW620, Colo-205, HCT116, HT29, LS174T, A375, and A2058 were obtained from American Type Culture Collection (Rockville, MD). PC3 cells provided by Dr. M. Kawada (Microbial Chemistry Research Center, Japan). All cell lines were maintained at 37ºC in a humidified atmosphere containing 5% CO_2 in RPMI-1640 medium supplemented with 10% fetal bovine serum.

Growth inhibition assay

Cell growth was assessed using the MTT assay. In brief, the cells were seeded in 96-well plates and cultured for 24 h. Thereafter, they were treated with various concentrations of 10-Me-Aplog-1 for an additional 48 h. The cells were subsequently treated with 0.5 mg/mL MTT (Sigma-Aldrich) for 4 h at 37ºC, and lysed with DMSO (Wako Pure Chemical Industries, Osaka, Japan). Absorbance at 595 nm was measured for the control well (C) and the test well (T) along with that for the test well at time 0 (T_0) using a Multiskan FC (Thermo Scientific, Waltham, MA). Cell growth inhibition (percent growth) by each compound was calculated as $100[(T - T_0)/(C - T_0)]$ when $T > T_0$, and $100[(T - T_0)/T_0]$ when $T < T_0$.

Cell-cycle analysis

The percentage of cells in different cell-cycle phases was measured by flow cytometry following staining with propidium iodide (PI, Wako Pure Chemical Industries). In brief, cells were seeded in 6-well plates, and after 24 h of culture they were treated with each compound for an additional 24 h. Following treatment, cells were harvested and fixed with 70% ice-cold ethanol at 4ºC, followed by treatment with 10 μg/mL RNase A (Wako Pure Chemical Industries) for 20 min at 37ºC. RNase-treated cells were subsequently stained with 50 μg/mL PI. PI fluorescence was measured by EPICS ALTRA (Beckman Coulter, Brea, CA).

Quantification of PKC isozymes

Expression levels for each PKC isozyme were determined using the Simple Western™ System (ProteinSimple) according to an earlier report[85] and the manufacturer's instructions. Cells were lysed in RIPA buffer (ProteinSimple) containing phosphatase and protease inhibitors. Protein concentration was measured for each lysate using Bradford's method with γ-globulin as a standard. Cell lysates were mixed with each GST-tagged recombinant PKC isozyme, sample buffer, fluorescent molecular weight markers, and 40 mM dithiothreitol, before being heated at 90ºC for 5 min. The resulting samples, primary antibodies, secondary antibodies, luminol-peroxide mix, and antibody diluent were dispensed into the assay plate. Separation electrophoresis and immunodetection were performed automatically. Signal intensities were measured using Compass Software (ProteinSimple).

RNA interference

Control siRNA or siRNA against each PKC isozyme was introduced into each cancer cell line using Lipofectamine RNAiMax (Invitrogen, Carlsbad, CA) according to manufacturer's protocol. Twenty-four hours after transfection, cells were harvested and re-seeded in white 96-well plates for the growth inhibition assay as described above, and in 6-well plates for western blotting.

Western blotting

Cells were harvested and lysed in RIPA buffer [25 mM HEPES pH 7.8, 1.5% Triton X-100, 1% sodium deoxycholate, 0.1% SDS, 0.5 M NaCl, 5 mM EDTA, 50 mM NaF, 0.1 mM Na_3VO_4 and cOmplete™ Protease Inhibitor Cocktail Tablets (Roche, Germany)] by sonication. The resulting lysates were centrifuged at 13,000 rpm for 15 min to remove insoluble fragments. Equal amounts of total protein were subsequently subjected to SDS-polyacrylamide gel electrophoresis before being transferred on to a PVDF membrane (Millipore, Billerica, MA). The membrane was probed with the indicated antibodies. The chemiluminescence signal was detected using an Immobilon Western kit (Millipore) and ChemiDoc™ XRS+ System (Bio-Rad, Hercules, CA).

Supporting Information

I. Effects of **1** on the cell-cycle of HCT116, HT29, LS174T, PC3, A375, and A2058 cells.

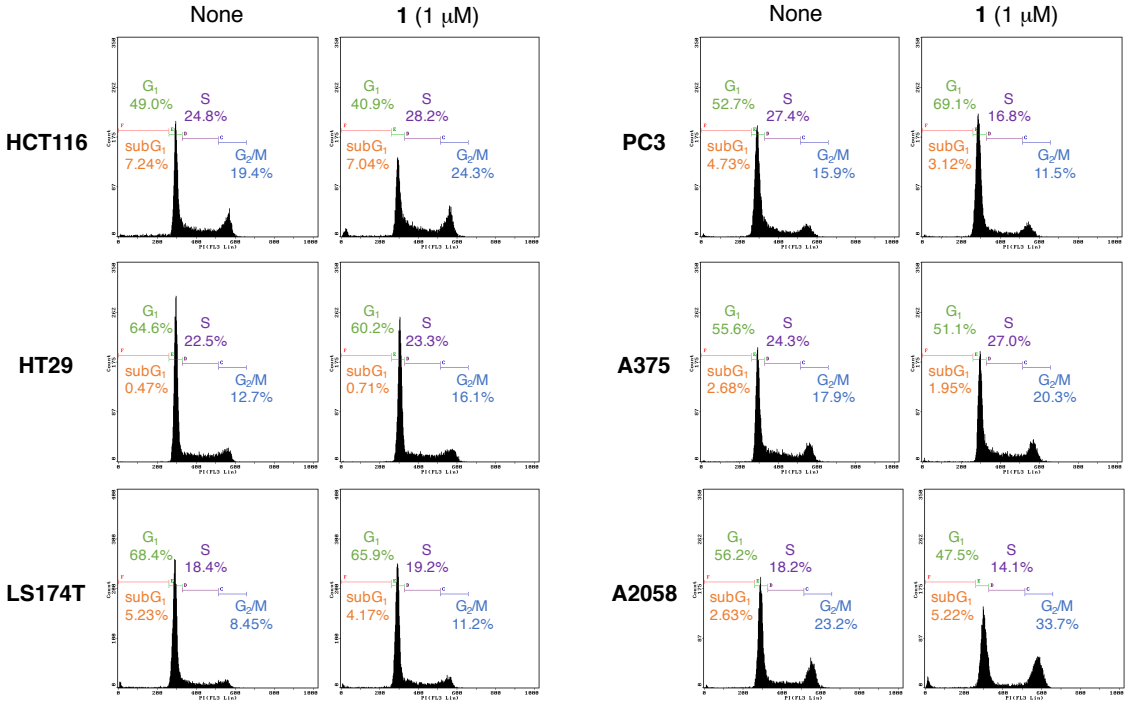

II. Quantification of PKC isozymes in lysates of 9 cancer cell lines.

Expression levels (pg/ng total protein)		A549	SW620	Colo-205	HCT116	HT29	LS174T	PC3	A375	A2058
α	Run1	0.094	0.045	0.050	0.019	< 0.012	0.019	0.046	0.048	0.028
	Run2	0.080	0.046	0.057	0.018	< 0.012	0.015	0.046	0.053	0.026
	Run3	0.052	0.045	0.064	0.018		ca. 0.012	0.044	0.050	0.033
	Run4			0.059						
	Average	0.075	0.045	0.058	0.018	< 0.012	ca. 0.015	0.045	0.050	0.029
δ	Run1	0.032	0.079	0.076	0.185	0.064	0.054	0.181	0.217	0.094
	Run2	0.043	0.097	0.088	0.189	0.106	0.045	0.177	0.184	0.114
	Run3	0.044	0.089	0.078	0.192	0.083	0.058	0.187	0.188	0.099
	Run4			0.084						
	Average	0.040	0.088	0.082	0.189	0.084	0.052	0.182	0.196	0.102
βI	Run1	< 0.010								
βII	Run1	< 0.0064								
γ	Run1	< 0.0032								
ε	Run1	< 0.0031								ca. 0.0033
η	Run1	ca. 0.0026	< 0.0021							
θ	Run1	< 0.0062								

Summary and Conclusion

Naturally-occurring tumor-promoters bind to and activate both conventional and novel PKC isozymes, and inhibited the growth of several cancer cell lines, but their potent tumor-promoting and proinflammatory activities have hampered their clinical use. Bryo-1, a non tumor-promoting PKC ligand, was spotlighted as a promising anti-cancer agent. However, clinical trials using bryo-1 had given rather disappointing results probably due to its weak anti-proliferative activity.

Aplog-1 and 10-methyl-aplog-1 (**1**) are simplified analogs of tumor-promoting DAT. They showed significant anti-proliferative activity against several cancer cell lines without tumor-promoting and proinflammatory activities. However, the mechanisms of their unique biological activities remain unclear. The author first synthesized new derivatives (**2**–**4**) of aplog-1 at position 27 that differed in the ability to bind to the C1 domains of PKC isozymes. Since a good correlation was observed between anti-proliferative activity and affinity for δ-C1B, PKC isozymes and other enzymes that contain PKC C1 homology domains were proposed to be involved in the cell line-specific growth inhibitory activity of aplogs.

On the other hand, the phenolic group on the side chain of **1** was not essential for binding to the C1 domain, but could make an additional hydrogen bond and/or CH/π interaction with amino acid residues of the C1 domains. These interactions may be related to the suppression of tumor-promoting and proinflammatory activities because **16**, whose phenolic group was replaced with a cyclohexyl group, cleary exhibited these side effects. Generally, non tumor-promoting PKC ligands localized PKCδ to the nuclear membrane, while tumor-promoters recruited it to the plasma membrane. However, **1**, **15**, and **16** induced its translocation to the plasma membrane regardless of their tumor-promoting activity. Therefore, the phenolic side chain of **1** may not tune the translocation sites of PKC, but instead, control the interaction mode between PKC C1 domains and plasma membrane, resulting in limited side effects.

The above results led the author to investigate the further role of each PKC isozyme in the anti-proliferative activity of **1**. Absolute quantification of PKC isozyme levels in nine cancer cell lines followed by RNAi-mediated knockdown experiments revealed that PKCα and δ are involved in the cell-cycle arrest and entry into apoptosis by aplog-sensitive cancer cell lines induced by **1**, DAT, and TPA. Previous PKC ligands without tumor-promoting activity were reported to activate PKC isozymes in a different manner from tumor-promoters and to show only weak anti-proliferative activity, but **1** significantly inhibited the growth of aplog-sensitive cell lines in a manner similar to the

tumor-promoting DAT and TPA despite the lack of tumor-promoting and proinflammatory activities. On the other hand, since the phenotypes were quite different among cell lines, the anti-proliferative mechanisms of PKC ligands could depend on cancer cell types. Although the roles of PKCα and δ in aplog-insensitive cell lines remain unclear, proliferation was not stimulated by PKC ligands in any of cell line tested, suggesting that PKCα and δ do not contribute to cancer cell growth. Therefore, the activation of PKCα and δ by **1** may be an effective anti-cancer treatment for particular cancers with few adverse effects. These findings suggested that structural simplification and optimization of pleiotropic PKC ligands are efficient strategies for generating new anti-cancer compounds.

Acknowledgments

This work was carried out in the Laboratory of Organic Chemistry in Life Science, Division of Food Science and Biotechnology, Graduate School of Agriculture, Kyoto University, from 2011 to 2013 and 2015 to 2018.

First of all, the author would like to express his special thanks to Dr. Kazuhiro Irie, Professor of Kyoto University, for his practical advice, valuable discussion, and continuous encouragement. This study could not have been completed without his guidance. The author would also like to offer his sincere thanks to Dr. Kazuma Murakami, Associate Professor of Kyoto University, for his warm encouragement and insightful suggestions throughout the graduate research.

The author is grateful to Dr. Masaya Imoto, Professor of Keio University, Dr. Etsu Tashiro, Lecturer of Keio University, and Dr. Yuki Shikata of Keio University for their valuable propositions and indispensable contributions to this study. The author is also grateful to Dr. Shingo Dan, Ms. Mutsumi Okamura, and Ms. Mao Noguchi at the Japanese Foundation for Cancer Research for their help with cell growth inhibition assay and constructive guidance. The author thanks Dr. Naoaki Saito, Professor of Kobe University and Dr. Naoko Adachi, Assistant Professor of Kobe University for their assistant with the PKC-translocation assay, supplying the anti-PKC antibodies and valuable advice on this study. The author also thanks Dr. Ryo C. Yanagita, Associate Professor of Kagawa University, for the computational analysis and his practical suggestions. The author expresses gratitude to Dr. Hiroshi Nagai, Professor of Tokyo University of Marine Science and Technology, and Dr. Kiyotake Suenaga, Professor of Keio University, for supplying debromoaplysiatoxin. The author is obliged to Dr. Masaya Nagao, Professor of Kyoto University, and Dr. Taiho Kambe, Associate Professor of Kyoto University, for the use of their chemiluminescence imaging systems and warm encouragement.

The author is indebted to Dr. Akira Murakami, Professor of University of Hyogo, for his encouragement and valuable comments. The author feels gratitude to Mr. Harukuni Tokuda, Researcher of Kyoto University, for his assistance with the indispensable biological assays and many kindnesses. The author expresses his heartfelt gratitude to Dr. Masayuki Kikumori of Kyoto University for his encouragement, continuous help and accurate guidance, which lay the foundation for this study. The author also expresses gratitude to Ms. Sayo Ueno and Ms. Natsuki Hotta of Kyoto University for their significant contribution to this study, and to all members of the Laboratory of Organic Chemistry in Life Science for their considerable help and encouragement.

The research was supported in part by a Grant-in-aid for the Promotion of Science for Young Scientists Grant from The Ministry of Education, Culture, Sports, Science and Technology, Japan.

Finally, the author would like to express his deepest gratitude to his family, Koji Hanaki, the late Natsumi Hanaki, and Dr. Mizuho Hanaki, for their understanding, continuous support, sincere encouragement, and deep affection during the long-time study at Kyoto University.

References

1. Nishizuka, Y. (1995) Protein kinase C and lipid signaling for sustained cellular responses. *FASEB J.* **9**, 484-496.
2. Takai, Y., Kishimoto, A., Inoue, M., and Nishizuka, Y. (1977) Studies on a cyclic nucleotide-independent protein kinase and its proenzyme in mammalian tissues. I. Purification and characterization of an active enzyme from bovine cerebellum. *J. Biol. Chem.* ***252***, 7603-7609.
3. Inoue, M., Kishimoto, A., Takai, Y., and Nishizuka, Y. (1977) Studies on a cyclic nucleotide-independent protein kinase and its proenzyme in mammalian tissues. II. Proenzyme and its activation by calcium-dependent protease from rat brain. *J. Biol. Chem.* **252**, 7610-7616.
4. Takai, Y., Kishimoto, A., Iwasa, Y., Kawahara, Y., Mori, T., and Nishizuka, Y. (1979) Calcium-dependent activation of a multifunctional protein kinase by membrane phospholipids. *J. Biol. Chem.* **254**, 3692-3695.
5. Takai, Y., Kishimoto, A., Kikkawa, U., Mori, T., and Nishizuka, Y. (1979) Unsaturated diacylglycerol as a possible messenger for the activation of calcium-activated, phospholipid-dependent protein kinase system. *Biochem. Biophys. Res. Commun.* **91**, 1218-1224.
6. Hokin, M. R., and Hokin, L. E. (1953) Enzyme secretion and the incorporation of P32 into phospholipides of pancreas slices. *J. Biol. Chem.* **203**, 967-977.
7. Michell, R. H. (1975). Inositol phospholipids and cell surface receptor function. *Biochim. Biophys. Acta* **415**, 81-147.
8. Newton, A. C. (2001) Protein kinase C: structural and spatial regulation by phosphorylation, cofactors, and macromolecular interactions. *Chem. Rev.* **101**, 2353-2364.
9. Giorgione, J. R., Lin, J. H., McCammon, J. A., and Newton, A. C. (2006) Increased membrane affinity of the C1 domain of protein kinase Cδ compensates for the lack of involvement of its C2 domain in membrane recruitment. *J. Biol. Chem.* **281**, 1660-1669.
10. Lamark, T., Perander, M., Outzen, H., Kristiansen, K., Øvervatn, A., Michaelsen, E., Bjørkøy, G., and Johansen, T. (2003) Interaction codes within the family of mammalian Phox and Bem1p domain-containing proteins. *J. Biol. Chem.* **278**, 34568-34581.
11. Castagna, M., Takai, Y., Kaibuchi, K., Sano, K., Kikkawa, U., and Nishizuka, Y. (1982) Direct activation of calcium-activated, phospholipid-dependent protein kinase by tumor-promoting phorbol esters. *J. Biol. Chem.* **257**, 7847-7851.
12. Fujiki, H., and Sugimura, T. (1987) New classes of tumor promoters: teleocidin, aplysiatoxin, and palytoxin. *Adv. Cancer Res.* **49**, 223-264.
13. Tamaoki, T., Nomoto, H., Takahashi, I., Kato, Y., Morimoto, M., and Tomita, F. (1986) Staurosporine, a potent inhibitor of phospholipid/Ca++dependent protein kinase. *Biochem. Biophys. Res. Commun.* **135**, 397-402.
14. Rüegg, U. T., and Gillian, B. (1989) Staurosporine, K-252 and UCN-01: potent but nonspecific inhibitors of protein kinases. *Trends Pharmacol. Sci.* **10**, 218-220.

15. Martiny-Baron, G., Kazanietz, M. G., Mischak, H., Blumberg, P. M., Kochs, G., Hug, H., Marmé, D. and Schächtele, C. H. (1993) Selective inhibition of protein kinase C isozymes by the indolocarbazole Gö 6976. *J. Biol. Chem.* **268**, 9194-9197.
16. Gschwendt, M., Dieterich, S., Rennecke, J., Kittstein, W., Mueller, H. J., and Johannes, F. J. (1996) Inhibition of protein kinase Cμ by various inhibitors. Inhibition from protein kinase c isoenzymes. *FEBS Lett.* **392**, 77-80.
17. Faul, M. M., Gillig, J. R., Jirousek, M. R., Ballas, L. M., Schotten, T., Kahl, A., and Mohr, M. (2003) Acyclic N-(azacycloalkyl) bisindolylmaleimides: isozyme selective inhibitors of PKCβ. *Bioorg. Med. Chem. Lett.* **13**, 1857-1859.
18. Seynaeve, C. M., Kazanietz, M. G., Blumberg, P. M., Sausville, E. A., and Worland, P. J. (1994) Differential inhibition of protein kinase C isozymes by UCN-01, a staurosporine analogue. *Mol. Pharmacol.* **45**, 1207-1214.
19. Wilkinson, S. E., Parker, P. J., and Nixon, J. S. (1993) Isoenzyme specificity of bisindolylmaleimides, selective inhibitors of protein kinase C. *Biochem. J.* **294**, 335-337.
20. Nemunaitis, J., Holmlund, J. T., Kraynak, M., Richards, D., Bruce, J., Ognoskie, N., Kwoh, T. J., Geary, R., Dorr, A., Von Hoff, D., and Eckhardt, S. G. (1999) Phase I evaluation of ISIS 3521, an antisense oligodeoxynucleotide to protein kinase C-alpha, in patients with advanced cancer. *J. Clin. Oncol.* **17**, 3586-3595.
21. Zhang, L. L., Cao, F. F., Wang, Y., Meng, F. L., Zhang, Y., Zhong, D. S., and Zhou, Q. H. (2015) The protein kinase C (PKC) inhibitors combined with chemotherapy in the treatment of advanced non-small cell lung cancer: meta-analysis of randomized controlled trials. *Clin. Transl. Oncol.* **17**, 371-377.
22. Pettit, G. R., Herald, C. L., Doubek, D. L., Herald, D. L., Arnold, E., and Clardy, J. (1982) Isolation and structure of bryostatin 1. *J. Am. Chem. Soc.* **104**, 6846-6848.
23. Lorenzo, P. S., and Dennis, P. A. (2003). Modulating protein kinase C (PKC) to increase the efficacy of chemotherapy: stepping into darkness. *Drug Resist. Update* **6**, 329-339.
24. Kollár, P., Rajchard, J., Balounová, Z., and Pazourek, J. (2014) Marine natural products: bryostatins in preclinical and clinical studies. *Pharm. Biol.* **52**, 237-242.
25. Lebwohl, M., Swanson, N., Anderson, L. L., Melgaard, A., Xu, Z., and Berman, B. (2012) Ingenol mebutate gel for actinic keratosis. *N. Engl. J. Med.* **366**, 1010-1019.
26. Fidler, B., and Goldberg, T. (2014). Ingenol mebutate gel (picato): a novel agent for the treatment of actinic keratoses. *P&T* **39**, 40-46.
27. Trost, B. M., and Dong, G. (2008) Total synthesis of bryostatin 16 using atom-economical and chemoselective approaches. *Nature* **456**, 485-488.
28. Keck, G. E., Poudel, Y. B., Cummins, T. J., Rudra, A., and Covel, J. A. (2010) Total synthesis of bryostatin 1. *J. Am. Chem. Soc.* **133**, 744-747.
29. Manaviazar, S., and Hale, K. J. (2011) Total synthesis of bryostatin 1: A short route. *Angew. Chem. Int. Ed.* **50**, 8786-8789.
30. Lu, Y., Woo, S. K., and Krische, M. J. (2011) Total synthesis of bryostatin 7 via C–C bond-forming hydrogenation. *J. Am. Chem. Soc.* **133**, 13876-13879.
31. Wender, P. A., Baryza, J. L., Brenner, S. E., DeChristopher, B. A., Loy, B. A., Schrier, A. J., and Verma, V. A. (2011) Design, synthesis, and evaluation of potent bryostatin analogs that modulate PKC translocation selectivity. *Proc. Natl. Acad. Sci. USA* **108**, 6721-6726.

32. Wender, P. A., Hardman, C. T., Ho, S., Jeffreys, M. S., Maclaren, J. K., Quiroz, R. V., Ryckbosch, S. M., Shimizu, A. J., Sloane, J. L. and Stevens, M. C. (2017) Scalable synthesis of bryostatin 1 and analogs, adjuvant leads against latent HIV. *Science* **358**, 218-223.
33. Winkler, J. D., Rouse, M. B., Greaney, M. F., Harrison, S. J., and Jeon, Y. T. (2002) The first total synthesis of (±)-ingenol. *J. Am. Chem. Soc.* **124**, 9726-9728.
34. Tanino, K., Onuki, K., Asano, K., Miyashita, M., Nakamura, T., Takahashi, Y., and Kuwajima, I. (2003) Total synthesis of ingenol. *J. Am. Chem. Soc.* **125**, 1498-1500.
35. Jørgensen, L., McKerrall, S. J., Kuttruff, C. A., Ungeheuer, F., Felding, J., and Baran, P. S. (2013) 14-step synthesis of (+)-ingenol from (+)-3-carene. *Science* **341**, 878-882.
36. Szállási, Z., Krsmanovic, L., and Blumberg, P. M. (1993) Nonpromoting 12-deoxyphorbol 13-esters inhibit phorbol 12-myristate 13-acetate induced tumor promotion in CD-1 mouse skin. *Cancer Res.* **53**, 2507-2512.
37. Shimomura, K., Mullinix, M. G., Kakunaga, T., Fujiki, H., and Sugimura, T. (1983) Bromine residue at hydrophilic region influences biological activity of aplysiatoxin, a tumor promoter. *Science* **222**, 1242-1244.
38. Nakagawa, Y., Yanagita, R. C., Hamada, N., Murakami, A., Takahashi, H., Saito, N., Nagai, H., and Irie, K. (2009) A simple analogue of tumor-promoting aplysiatoxin is an antineoplastic agent rather than a tumor promoter: development of a synthetically accessible protein kinase C activator with bryostatin-like activity. *J. Am. Chem. Soc.* **131**, 7573-7579.
39. Kikumori, M., Yanagita, R. C., Tokuda, H., Suzuki, N., Nagai, H., Suenaga, K., and Irie, K. (2012) Structure–activity studies on the spiroketal moiety of a simplified analogue of debromoaplysiatoxin with antiproliferative activity. *J. Med. Chem.* **55**, 5614-5626.
40. Kikumori, M., Yanagita, R. C., and Irie, K. (2014) Improved and large-scale synthesis of 10-methyl-aplog-1, a potential lead for an anticancer drug. *Tetrahedron* **70**, 9776-9782.
41. Emoto, Y., Manome, Y., Meinhardt, G., Kisaki, H., Kharbanda, S., Robertson, M., Ghayur, T., Wong, W. W., Kamen, R., and Weichselbaum, R. (1995) Proteolytic activation of protein kinase C delta by an ICE-like protease in apoptotic cells. *EMBO J.* **14**, 6148.
42. Basu, A. (2003) Involvement of protein kinase C-δ in DNA damage-induced apoptosis. *J. Cell. Mol. Med.* **7**, 341-350.
43. Basu, A., Lu, D., Sun, B., Moor, A. N., Akkaraju, G. R., and Huang, J. (2002) Proteolytic activation of protein kinase C-ε by caspase-mediated processing and transduction of antiapoptotic signals. *J. Biol. Chem.* **277**, 41850-41856.
44. Smith, L., Zhi, W., and Smith, J. B. (2003) Caspase processing activates atypical protein kinase C ζ by relieving autoinhibition and destabilizes the protein. *Biochem. J.* **375**, 663-671.
45. Szállási, Z., Denning, M. F., Smith, C. B., Dlugosz, A. A., Yuspa, S. H., Pettit, G. R., and Blumberg, P. M. (1994) Bryostatin 1 protects protein kinase C-delta from down-regulation in mouse keratinocytes in parallel with its inhibition of phorbol ester-induced differentiation. *Mol. Pharmacol.* **46**, 840-850.
46. Wang, Q. J., Bhattacharyya, D., Garfield, S., Nacro, K., Marquez, V. E., and Blumberg, P. M. (1999) Differential localization of protein kinase C δ by phorbol esters and related compounds using a fusion protein with green fluorescent protein. *J. Bio. Chem.* **274**, 37233-37239.

47. Serova, M., Ghoul, A., Benhadji, K. A., Faivre, S., Le Tourneau, C., Cvitkovic, E., Lokiec, F., Lord, J., Ogbourne, S. M., Calvo, F., and Raymond, E. (2008). Effects of protein kinase C modulation by PEP005, a novel ingenol angelate, on mitogen-activated protein kinase and phosphatidylinositol 3-kinase signaling in cancer cells. *Mol. Cancer Ther.* **7**, 915-922.
48. Yoshida, K., Liu, H., and Miki, Y. (2006). Protein kinase C δ regulates Ser46 phosphorylation of p53 tumor suppressor in the apoptotic response to DNA damage. *J. Biol. Chem.* **281**, 5734-5740.
49. Lasfer, M., Davenne, L., Vadrot, N., Alexia, C., Sadji-Ouatas, Z., Bringuier, A. F., Pessayre, D. and Reyl-Desmars, F. (2006) Protein kinase PKC delta and c-Abl are required for mitochondrial apoptosis induction by genotoxic stress in the absence of p53, p73 and Fas receptor. *FEBS Lett.* **580**, 2547-2552.
50. Cross, T., Griffiths, G., Deacon, E., Sallis, R., Gough, M., Watters, D., and Lord, J. M. (2000) PKC-d is an apoptotic lamin kinase. *Oncogene* **19**, 2331-2337.
51. Shanmugam, M., Krett, N. L., Maizels, E. T., Murad, F. M., Rosen, S. T., and Hunzicker-Dunn, M. (2001) A role for protein kinase C δ in the differential sensitivity of MCF-7 and MDA-MB 231 human breast cancer cells to phorbol ester-induced growth arrest and p21 WAFI/CIP1 induction. *Cancer Lett.* **172**, 43-53.
52. Ashton, A. W., Watanabe, G., Albanese, C., Harrington, E. O., Ware, J. A., and Pestell, R. G. (1999) Protein kinase Cδ inhibition of S-phase transition in capillary endothelial cells involves the cyclin-dependent kinase inhibitor p27Kip1. *J. Biol. Chem.* **274**, 20805-20811.
53. Fukumoto, S., Nishizawa, Y., Hosoi, M., Koyama, H., Yamakawa, K., Ohno, S., and Morii, H. (1997) Protein kinase C δ inhibits the proliferation of vascular smooth muscle cells by suppressing G1 cyclin expression. *J. Biol. Chem.* **272**, 13816-13822.
54. Grossoni, V. C., Falbo, K. B., Kazanietz, M. G., de Kier Joffé, E. D. B., and Urtreger, A. J. (2007) Protein kinase C δ enhances proliferation and survival of murine mammary cells. *Mol. Carcinog.* **46**, 381-390.
55. Xia, S., Chen, Z., Forman, L. W., and Faller, D. V. (2009). PKCδ survival signaling in cells containing an activated p21 Ras protein requires PDK1. *Cell. Signal.* **21**, 502-508.
56. Poli, A., Mongiorgi, S., Cocco, L., and Follo, M. Y. (2014) Protein kinase C involvement in cell cycle modulation.
57. Cooke, M., Magimaidas, A., Casado-Medrano, V., and Kazanietz, M. G. (2017) Protein kinase C in cancer: The top five unanswered questions. *Mol. Carcinog.* **56**, 1531-1542.
58. Nakagawa, M., Oliva, J. L., Kothapalli, D., Fournier, A., Assoian, R. K., and Kazanietz, M. G. (2005) Phorbol ester-induced G1 phase arrest selectively mediated by protein kinase Cδ-dependent induction of p21. *J. Biol. Chem.* **280**, 33926-33934.
59. Oliva, J. L., Caino, M. C., Senderowicz, A. M., and Kazanietz, M. G. (2008) S-phase-specific activation of PKCα induces senescence in non-small cell lung cancer cells. *J. Biol. Chem.* **283**, 5466-5476.
60. Santiago-Walker, A. E., Fikaris, A. J., Kao, G. D., Brown, E. J., Kazanietz, M. G., and Meinkoth, J. L. (2005) Protein kinase C δ stimulates apoptosis by initiating G1 phase cell cycle progression and S phase arrest. *J.Biol. Chem.* **280**, 32107-32114.

61. Kitamura, K., Mizuno, K., Etoh, A., Akita, Y., Miyamoto, A., Nakayama, K. I., and Ohno, S. (2003) The second phase activation of protein kinase C δ at late G1 is required for DNA synthesis in serum-induced cell cycle progression. *Genes Cells* **8**, 311-324.
62. Gao, T., Brognard, J., and Newton, A. C. (2008) The phosphatase PHLPP controls the cellular levels of protein kinase C. *J. Biol. Chem.* **283**, 6300-6311.
63. Antal, C. E., and Newton, A. C. (2014) Tuning the signalling output of protein kinase C. *Biochem. Soc. Trans.* **42**, 1477-1483.
64. Newton, A. C., and Brognard, J. (2017) Reversing the Paradigm: Protein Kinase C as a Tumor Suppressor. *Trends Pharmacol. Sci.* **38**, 438-447.
65. Antal, C. E., Hudson, A. M., Kang, E., Zanca, C., Wirth, C., Stephenson, N. L., Trotter, E. W., Gallegos, L. L., Miller, C. J., Furnari, F. B., Hunter, T., Brognard, J., and Newton, A. C. (2015) Cancer-associated protein kinase C mutations reveal kinase's role as tumor suppressor. *Cell* **160**, 489-502.
66. Yoshizawa, S., Fujiki, H., Suguri, H., Suganuma, M., Nakayasu, M., Matsushima, R., and Sugimura, T. (1990). Tumor-promoting activity of staurosporine, a protein kinase inhibitor on mouse skin. *Cancer Res.* **50,** 4974-4978.
67. Nakamura, H., Kishi, Y., Pajares, M. A., and Rando, R. R. (1989) Structural basis of protein kinase C activation by tumor promoters. *Proc. Natl. Acad. Sci. USA* **86**, 9672-9676.
68. Kishi, Y., and Rando, R. R. (1998) Structural basis of protein kinase C activation by tumor promoters. *Accounts Chem. Res.* **31**, 163-172.
69. Mitsunobu, O. (1981) The use of diethyl azodicarboxylate and triphenylphosphine in synthesis and transformation of natural products. *Synthesis* **1**, 1-28.
70. Nicolaou, K. C., Fylaktakidou, K. C., Monenschein, H., Li, Y., Weyershausen, B., Mitchell, H. J., Wei, H. X., Guntupalli, P., Hepworth, D., and Sugita, K. (2003) Total synthesis of apoptolidin: construction of enantiomerically pure fragments. *J. Am. Chem. Soc.* **125**, 15433-15442.
71. Inanaga, J., Hirata, K., Saeki, H., Katsuki, T., and Yamaguchi, M. (1979) A rapid esterification by means of mixed anhydride and its application to large-ring lactonization. *Bull. Chem. Soc. Jpn.* **52**, 1989-1993.
72. Irie, K., Oie, K., Nakahara, A., Yanai, Y., Ohigashi, H., Wender, P. A., Fukuda, H., Konishi, H., and Kikkawa, U. (1998) Molecular basis for protein kinase C isozyme-selective binding: the synthesis, folding, and phorbol ester binding of the cysteine-rich domains of all protein kinase C isozymes. *J. Am. Chem. Soc.* **120**, 9159-9167.
73. Sharkey, N. A., and Blumberg, P. M. (1985) Highly lipophilic phorbol esters as inhibitors of specific [3H] phorbol 12, 13-dibutyrate binding. *Cancer Res.* **45**, 19-24.
74. Shindo, M., Irie, K., Nakahara, A., Ohigashi, H., Konishi, H., Kikkawa, U., Fukuda, H., and Wender, P. A. (2001) Toward the identification of selective modulators of protein kinase C (PKC) isozymes: establishment of a binding assay for PKC isozymes using synthetic C1 peptide receptors and identification of the critical residues involved in the phorbol ester binding. *Bioorg. Med. Chem.* **9**, 2073-2081.
75. Masuda, A., Irie, K., Nakagawa, Y., and Ohigashi, H. (2002) Binding selectivity of conformationally restricted analogues of (−)-indolactam-V to the C1 domains of protein kinase C isozymes. *Biosci. Biotechnol. Biochem.* **66**, 1615-1617.

76. Irie, K., Nakagawa, Y., and Ohigashi, H. (2004) Indolactam and benzolactam compounds as new medicinal leads with binding selectivity for C1 domains od protein kinase C isozymes. *Curr. Pharm. Des.* **10**, 1371-1385.
77. Fujiki, H., Tanaka, Y., Miyake, R., Kikkawa, U., Nishizuka, Y., and Sugimura, T. (1984) Activation of calcium-activated, phospholipid-dependent protein kinase (protein kinase C) by new classes of tumor promoters: teleocidin and debromoaplysiatoxin. *Biochem. Biophys. Res. Commun.* **120**, 339-343.
78. Zur Hausen, H., Bornkamm, G. W., Schmidt, R., and Hecker, E. (1979) Tumor initiators and promoters in the induction of Epstein—Barr virus. *Proc. Natl. Acad. Sci. USA* **76**, 782-785.
79. Ito, Y., Yanase, S., Fujita, J., Harayama, T., Takashima, M., and Imanaka, H. (1981) A short-term in vitro assay for promoter substances using human lymphoblastoid cells latently infected with Epstein-Barr virus. *Cancer Lett.* **13**, 29-37.
80. Suganuma, M., Fujiki, H., Tahira, T., Cheuk, C., Moore, R. E., and Sugimura, T. (1984) Estimation of tumor promoting activity and structure-function relationships of aplysiatoxins. *Carcinogenesis* **5**, 315-318.
81. Yamori, T., Matsunaga, A., Sato, S., Yamazaki, K., Komi, A., Ishizu, K., Mita, I., Edatsugi, H., Matsuba, Y., Takezawa, K., Nakanishi, O., Kohno, H., Nakajima, Y., Komatsu, H., Andoh, T., and Tsuruo, T. (1999) Potent antitumor activity of MS-247, a novel DNA minor groove binder, evaluated by an in vitro and in vivo human cancer cell line panel. *Cancer Res.* **59**, 4042-4049.
82. Nakatsu, N., Nakamura, T., Yamazaki, K., Sadahiro, S., Makuuchi, H., Kanno, J., and Yamori, T. (2007) Evaluation of action mechanisms of toxic chemicals using JFCR39, a panel of human cancer cell lines. *Mol. Pharmacol.* **72**, 1171-1180.
83. Kazanietz, M. G. (2002) Novel "nonkinase" phorbol ester receptors: the C1 domain connection. *Mol. Pharmacol.* **61**, 759-767.
84. Wender, P. A., De Brabander, J., Harran, P. G., Jimenez, J. M., Koehler, M. F., Lippa, B., .Park, C. M., and Shiozaki, M. (1998) Synthesis of the first members of a new class of biologically active bryostatin analogues. *J. Am. Chem. Soc.* **120**, 4534-4535.
85. Monks, A., Scudiero, D., Skehan, P., Shoemaker, R., Paull, K., Vistica, D., Hose, C., Langley, J., Cronise, P., Vaigro-Wolff, A., Gray-Goodrich, M., Cabpbell, H., Mayo, J., and Boyd, M. (1991) Feasibility of a high-flux anticancer drug screen using a diverse panel of cultured human tumor cell lines. *J. Natl. Cancer Inst.* **83**, 757-766.
86. Skehan, P., Storeng, R., Scudiero, D., Monks, A., McMahon, J., Vistica, D., Warren, J. T., Bokesch, H., Kenney, S., and Boyd, M. R. (1990) New colorimetric cytotoxicity assay for anticancer-drug screening. *J. Natl. Cancer Inst.* **82**, 1107-1112.
87. Maegawa, T., Akashi, A., Yaguchi, K., Iwasaki, Y., Shigetsura, M., Monguchi, Y., and Sajiki, H. (2009) Efficient and practical arene hydrogenation by heterogeneous catalysts under mild conditions. *Chem. Eur. J.* **15**, 6953-6963.
88. Ashida, Y., Yanagita, R. C., Takahashi, C., Kawanami, Y., and Irie, K. (2016) Binding mode prediction of aplysiatoxin, a potent agonist of protein kinase C, through molecular simulation and structure–activity study on simplified analogs of the receptor-recognition domain. *Bioorg. Med. Chem.* **24**, 4218-4227.

89. Yanagita, R. C., Kamachi, H., Tanaka, K., Murakami, A., Nakagawa, Y., Tokuda, H., Nagai, H., and Irie, K. (2010) Role of the phenolic hydroxyl group in the biological activities of simplified analogue of aplysiatoxin with antiproliferative activity. *Bioorg. Med. Chem. Lett.* **20**, 6064-6066.
90. Baird, W. M., and Boutwell, R. K. (1971) Tumor-promoting activity of phorbol and four diesters of phorbol in mouse skin. *Cancer Res.* **31**, 1074-1079.
91. Wang, Q. J., Fang, T. W., Fenick, D., Garfield, S., Bienfait, B., Marquez, V. E., and Blumberg, P. M. (2000) The lipophilicity of phorbol esters as a critical factor in determining the pattern of translocation of protein kinase Cδ fused to green fluorescent protein. *J. Biol. Chem.* **275**, 12136-12146.
92. Hui, X., Reither, G., Kaestner, L., and Lipp, P. (2014) Targeted activation of conventional and novel protein kinases C through differential translocation patterns. *Mol. Cell. Biol.* **34**, 2370-2381.
93. Kang, M., and Walker, J. W. (2005) Protein kinase Cδ and ε mediate positive inotropy in adult ventricular myocytes. *J. Mol. Cell. Cardiol.* **38**, 753-764.
94. Von Burstin, V. A., Xiao, L., and Kazanietz, M. G. (2010) Bryostatin 1 inhibits phorbol ester-induced apoptosis in prostate cancer cells by differentially modulating protein kinase C (PKC) δ translocation and preventing PKCδ-mediated release of tumor necrosis factor-α. *Mol. Pharmacol.* **78**, 325-332.
95. Keck, G. E., Poudel, Y. B., Rudra, A., Stephens, J. C., Kedei, N., Lewin, N. E., and Blumberg, P. M. (2012) Role of the C 8 gem-dimethyl group of bryostatin 1 on its unique pattern of biological activity. *Bioorg. Med. Chem. Lett.* **22**, 4084-4088.
96. Kajimoto, T., Shirai, Y., Sakai, N., Yamamoto, T., Matsuzaki, H., Kikkawa, U., and Saito, N. (2004) Ceramide-induced apoptosis by translocation, phosphorylation, and activation of protein kinase Cδ in the Golgi complex. *J. Biol. Chem.* **279**, 12668-12676.
97. Kamachi, H., Tanaka, K., Yanagita, R. C., Murakami, A., Murakami, K., Tokuda, H., Suzuki, N., Nakagawa, Y., and Irie, K. (2013) Structure–activity studies on the side chain of a simplified analog of aplysiatoxin (aplog-1) with anti-proliferative activity. *Bioorg. Med. Chem.* **21**, 2695-2702.
98. Kikumori, M., Yanagita, R. C., Tokuda, H., Suenaga, K., Nagai, H., and Irie, K. (2016) Structural optimization of 10-methyl-aplog-1, a simplified analog of debromoaplysiatoxin, as an anticancer lead. *Biosci. Biotechnol. Biochem.* **80**, 221-231.
99. Ryckbosch, S. M., Wender, P. A., and Pande, V. S. (2017) Molecular dynamics simulations reveal ligand-controlled positioning of a peripheral protein complex in membranes. *Nature Commun.* **8**, 6.
100. Yanagita, R. C., Kamachi, H., Kikumori, M., Tokuda, H., Suzuki, N., Suenaga, K., Nagai, H., and Irie, K. (2013) Effects of the methoxy group in the side chain of debromoaplysiatoxin on its tumor-promoting and anti-proliferative activities. *Bioorg. Med. Chem. Lett.* **23**, 4319-4323.
101. Van Der Spoel, D., Lindahl, E., Hess, B., Groenhof, G., Mark, A. E., and Berendsen, H. J. (2005) GROMACS: fast, flexible, and free. *J. Comput. Chem.* **26**, 1701-1718.
102. Chen, J. Q., Heldman, M. R., Herrmann, M. A., Kedei, N., Woo, W., Blumberg, P. M., and Goldsmith, P. K. (2013) Absolute quantitation of endogenous proteins with precision and

accuracy using a capillary Western system. *Anal. Biochem.* **442**, 97-103.
103. Wetsel, W. C., Khan, W. A., Merchenthaler, I., Rivera, H., Halpern, A. E., Phung, H. M., Negro-Vilar, Y. A., and Hannun, Y. A. (1992) Tissue and cellular distribution of the extended family of protein kinase C isoenzymes. *J. Cell Biol.* **117**, 121-133.
104. Liu, W. S., and Heckman, C. A. (1998) The sevenfold way of PKC regulation. *Cell. Signal.* **10**, 529-542.
105. Soltoff, S. P. (2007) Rottlerin: an inappropriate and ineffective inhibitor of PKCδ. *Trends Pharmacol. Sci.* **28**, 453-458.

List of Publications

Original Papers

1) Yusuke Hanaki, Masayuki Kikumori, Sayo Ueno, Harukuni Tokuda, Nobutaka Suzuki, Kazuhiro Irie (2013) Structure-activity studies at position 27 of aplog-1, a simplified analog of debromoaplysiatoxin with anti-proliferative activity. *Tetrahedron* **69**, 7636-7645.
2) Yusuke Hanaki, Masayuki Kikumori, Harukuni Tokuda, Mutsumi Okamura, Shingo Dan, Naoko Adachi, Naoaki Saito, and Kazuhiro Irie (2017) Loss of the phenolic hydroxyl group and aromaticity from the side chain of anti-proliferative 10-Methyl-aplog-1, a simplified analog of aplysiatoxin, enhances its tumor-promoting and proinflammatory activities. *Molecules* **22**, 631.
3) Yusuke Hanaki, Yuki Shikata, Masayuki Kikumori, Natsuki Hotta, Masaya Imoto, Kazuhiro Irie (2018) Identification of protein kinase C isozymes involved in the anti-proliferative and pro-apoptotic activities of 10-Methyl-aplog-1, a simplified analog of debromoaplysiatoxin, in several cancer cell lines. *Biochem. Biophys. Res. Commmun.* **495**, 438-445.

Related papers

4) Yusuke Hanaki, Ryo C. Yanagita, Takahiro Sugahara, Misako Aida, Harukuni Tokuda, Nobutaka Suzuki, Kazuhiro Irie (2015) Synthesis and biological activities of the amide derivative of aplog-1, a simplified analog of aplysiatoxin with anti-proliferative and cytotoxic activities. *Biosci. Biotechnol. Biochem.* **79**, 888-895.